Development of a Novel Thermal Management Technology of Tablet Computers using Phase Change Materials

by

Tousif Ahmed

Submitted in partial fulfillment of the requirements
for the degree of Master of Applied Science

at

Dalhousie University
Halifax, Nova Scotia
August 2016

To my parents – those who never said 'NO' to me.

Table of Contents

List of Tables

List of Figures

Abstract

Tablet computers (PCs) are continuously moving toward light, thin, and small shape factors to achieve an eye appealing design while providing extreme mobility. The increased integration of electronic components with high power density, small size, and compact layout is leading to alarming operating temperatures of tablet PCs. Overheating greatly reduces the service life of components, resulting in failure of components, and thus reducing system reliability. Therefore, the thermal management of tablet PCs is becoming increasingly important. This research focuses on developing an inexpensive and practical solution for thermal management of tablet PCs using phase change materials (PCMs) encapsulated in aluminized laminate film. The performance of the tablet PC with PCM thermal energy storage (TES) unit for both continuous as well as intermittent operation was investigated. The application of latent heat storage from PCM melting provided good thermal performance during transient operation while sensible heat storage in PCMs and heat spreading in aluminized laminate film provided very favorable steady-state thermal performance of the tablet PC. Findings of this research confirm that the implementation of PCM–based TES unit is a viable option for thermal management of very compact electronic systems such as tablet PCs.

List of Abbreviations and Symbols Used

Abbreviations

ABS	Acrylonitrile Butadiene Styrene, a common plastic polymer
ANOVA	Analysis of Variance
CNC	Computer Numerical Control
CR	Corrosion Ratio
DSC	Differential Scanning Calorimetry
GPU	Graphics Processing Unit
GSM	Global System for Mobile communications
HCI	Human-Computer Interaction
HDPE	High Density Polyethylene
IR	InfraRed
LED	Light Emitting Diode
LHS	Latent Heat Storage
MPCM	Microencapsulated Phase Change Material
NUC	Non-uniformity Correction
OS	Operating System
PCB	Printed Circuit Board
PCM	Phase Change Material
PDA	Personal Digital Assistant
PPMS	Physical Property Measurement System
QFP	Quad Flat Plate
SoC	System on a Chip
TES	Thermal Energy Storage

Symbols

A	Specimen area (cm^2)
$Ah_{battery}$	Ampere-hour rating of the battery (A-hr)
a_m	PCM melt fraction
$C_{p,l}$	Heat Capacity of Liquid (J/g·K)
$C_{p,s}$	Heat Capacity of Solid (J/g·K)
Gr_L	Grashof Number
k_s	Thermal Conductivity of the Solid (W/m·K)
L	Characteristic length of the tablet PC (m)
Nu	Nusselt Number
P	Power Density of Heater (W/in^2)
Q	Quantity of heat stored (kJ)
Q'	Total Input Power of the Heater(W)
q''	Input Power Density of the Heater(W/in^2)
Ste	Stefan Number
T_f	Final Temperature (°C)
T_{Heater}	Heater Temperature (°C)
T_i	Initial Temperature (°C)
T_{onset}	Onset of melting Temperature (ºC)
T_s	Surface temperature of the tablet PC (°C)
T_∞	Ambient temperature (°C)
$t_{operation}$	Duration of operation (minutes)
T_{PCM}	PCM Temperature (°C)
V	Supplied Voltage (V)
$V_{battery}$	Operating voltage of the battery (V)
V_R	Rated Voltage of Heater (V)
$\Delta_{fus}H$	Latent Heat of Fusion (J/g)
$\Delta_{trs}H$	Transition Enthalpy Change (J/g)
$\Delta_{trs}V$	Change in volume due to phase change (cc)
Δm	Change in mass (mg)
Pr	Prandtl Number
Ra_L	Rayleigh Number
Δt	Duration of test (yr.)
υ	Kinematic Viscosity (m^2/s)

Acknowledgements

Foremost, I would like to thank my supervisor, Professor Dr. Dominic Groulx, director of the Laboratory of Applied Multiphase Thermal Engineering (LAMTE). I have been incredibly fortunate to have an advisor who gave me the liberty to explore on my own, and at the same time the direction to recover when my steps were stumbled. He has been supportive since the first day I started working at LAMTE. My learning from Dominic was not only confined to my research. I strongly believe my experience at LAMTE will be an asset for the next step of my life, most importantly, as I have decided to follow in his footsteps to become a researcher too. Thanks Dominic, for being such a remarkable mentor.

I also would like to thank Dr. Mary Anne White and Dr. Clifton Johnston, my thesis committee members, for their constructive review and insightful comments on my thesis.

I would like to gratefully acknowledge Intel Corporation for the financial and technical support which made this work possible, along with the Natural Sciences and Engineering Research Council of Canada (NSERC), the Nova Scotia Government (Graduate Scholarship program) and the Canadian Foundation for Innovation (CFI) for further laboratory financial assistance.

Special thanks go to Dr. Samer Kahwaji and Dr. Mary Anne White for conducting outstanding research on phase change materials (PCMs) at MAW's Lab and providing this research with supporting data.

I was very lucky to have the opportunity to work with some very bright and enthusiastic minds. I would like to thank Ryan P. Scott for helping me to set-up the experimental part of my research. I also thankfully acknowledge the contributions of Dr. Aminul Islam, Mahmud Hasan, Dr. Maha Bhouri, Mohammed Azad, Tahrim Alam, those who helped me to shape this thesis properly.

Thanks to all of my Lab and office mates: Ali, Ben, Florent, Laura, Louis, Moe, Dane, Trent, and not to mention those Facebook friends who spoiled the new season of *Game of Thrones* for me. I did not watch a single episode of season 6 and that, ironically, saved tons of my working hours!

Finally, I am grateful to Almighty for giving me the strength and determination to carry on this tough but rewarding phase of my life.

Tousif Ahmed

Halifax, August 2016

Chapter 1

Introduction

In recent years, tablet computers (PCs) have gained much popularity over laptop computers due to their processing power similar to an entry level laptop computer and their smaller form factor. Additionally, tablet PCs have longer battery life and larger screens compared to smartphones which facilitates doing regular computing work on a more portable platform by tablet PC's users. In 2015, almost 144 million people owned a tablet PC in the USA alone (Statista.com, 2012). It is expected to have 303 million units of tablet PC shipped only in 2018, which is 78% more than the expected shipment of laptop computers in the same year (Statista.com, 2016). Nowadays, tablet PCs are being populated with more and more features and functionalities in very compact packages (*i.e.* typical thickness 6 to 10 mm), such as 4K displays and large memories. These 4K displays require enormous computational and graphical processing power, which additionally, result in high-power consumption. The skin temperature of today's tablet PCs can reach up to 60 °C while consuming power up to 12 W (Courtney, 2015).

High power consumption and high heat generation in tablet PCs have negative impacts on the long-term reliability and the thermal comfort of tablet PC users. Different studies (Greenspan *et al.*, 2003; Patapoutian *et al.*, 2003; Story, 2006) suggest that holding a tablet PC with a back surface temperature exceeding 42 to 45 °C can lead to severe user discomfort. Besides, Joule heating of electronic components in tablet PCs (*i.e.* relays, resistors, transistors, etc.) causes accelerated degradation, and hence reduces the life-span of the device (McPherson, 2010). For instance, the reliability of an electronic device can be reduced by 4% due to only 1 °C increase in the device's operating temperature limit (varies from device to device) (Cheng *et al.*, 2012), and an increase of 10 to 20 °C may double its failure rate (Mithal, 1996). Statistics show that more than 55% of electronic

device failures are related to high-temperature (Yeh, 1995). Also, lithium-ion batteries, the most common power source of tablet PCs, suffer from a hazardous process called 'thermal runaway'. It is triggered by high heat which leads to an increase in reaction rate, and therefore, even more heat generated, starting a hazardous cycle of heat generation (Lin *et al.*, 2013). In the most extreme cases, 'thermal runaway' can result in an explosion causing physical harm to the user. Amon *et al.* (1994) presented a design of a wearable computer system encompassing all four disciplines: Electronics, Mechanical, HCI (human-computer interaction), and Software. They found it very challenging to develop a design having a small size and offering high reliability due to cooling issues. All these facts have made tablet PC's manufacturers most concerned about the thermal management of tablet PCs.

Achievement of a satisfactory thermal management system of tablet PCs is dependent upon a few factors, which commonly include the available space in the device. Characterization and optimization of the performance of fan heatsink modules by Lin and Chou (2004) and Loh *et al.* (2001) are mainly focused on large scale applications, with little effort focused on scales suitable to portable electronic devices such as tablet PCs. Unlike traditional active cooling in desktop computers which allow relatively large scale heat sinks and fans, typical tablet PCs do not have sufficient space for the installation of a robust active thermal solution. Moreover, the divergence of Moore's law (Moore, 1998), offering twice the computational power at least every two years, and the improvement in battery technologies, which did not even double over the last decade, are forcing researchers to change their approaches for cooling tablet PCs to ways that do not use any battery power. As a result, cooling of tablet PCs is becoming more and more challenging.

In recent years, phase change materials (PCMs) have attracted much attention as an alternative passive cooling technique for portable electronics (Alawadhi and Amon, 2003; Tan and Tso, 2004; Kandasamy *et al.*, 2007; Tan *et al.*, 2009; Fok *et al.*, 2010; Saha and Dutta, 2010; Wang and Yang, 2011; Novikov *et al.*, 2014; Sponagle and Groulx, 2015). Advantages of PCM-based systems include high latent heat of fusion, small volume change during phase change, non-toxic, inexpensive, and do not require any moving part and external power source which provides unaltered standby time of tablet PCs. Usually,

PCMs in a PCM-based thermal energy storage (TES) system absorb and store heat during transient heating (charging phase). When the electronic device is idle, melted PCMs disperse heat to the surrounding and re-solidify (discharging phase). Temperature rise of tablet PCs can be delayed until PCMs are fully melted, as PCMs melt at a constant temperature. Thermal management of tablet PCs through practical means of PCM-based TES units has not been achieved so far, due to encapsulation issues. Indeed, the convenience of the PCM encapsulation technique was marred by PCM leakage and contact materials corrosion problems (Farrell *et al.*, 2006). Moreover, the most common problem with past PCM-based TES units is their large physical dimensions, which are not suitable for very thin tablet PCs.

In this study, a new kind of PCM-based TES unit using aluminized laminate film (nylon/Al/polypropylene) is presented. The average thickness is only 1/16″ (2 mm) which makes this kind of TES unit a good fit for today's thin tablet PCs. This thesis works toward implementing thin PCM-based TES units in an experimental setup having representative physical and thermal behaviour of a real tablet PC. Moreover, the present price of this solution is less than $10, and can be expected to be even less if produced commercially. Hence, this thermal management solution would not affect the base price of tablet PCs.

1.1 Objectives

The main objective of this thesis is to develop a thermal management system for tablet PCs using PCMs.

To achieve this goal, first a thermal analysis of actual tablet PCs was made in order to understand their thermal behaviour under different usage loads and to develop an experimental tablet PC producing thermal behaviour comparable to actual tablet PCs. The thermal response of the experimental tablet PC was investigated under both continuous and intermittent operation.

Once this previous task was complete, the specific objectives of the research are summarized as follows:

- To determine the temperature management effectiveness of PCM-based TES units at different angular orientations by observing the effect of inclination on the melting of PCMs as well as on the thermal response of the experimental tablet PC.

- To observe the effect of varying power input levels on the melting of PCMs as well as on the thermal response of the experimental tablet PC and thus determine the effectiveness of PCM-basted TES units at different usage load of the tablet PC.

- To determine the performance of different size of PCM-based TES units by observing the effect of varying size of TES units on the melting of PCMs as well as on the thermal response of the experimental tablet PC.

- To determine the effectiveness of smaller component-wise PCM-based TES units by observing the effect of varying latent heat storage capacity as well as the effect of localized cooling of particular components on the overall thermal response of the tablet PC.

- To draw a conclusive decision on the viability of using PCM-based TES units for the thermal management of tablet PCs based on the results obtained from different objectives of this research.

Chapter 2

Literature Review

This chapter provides brief reviews on thermal behaviour study of portable electronics, research on PCMs' thermo-physical properties, and experiments on PCM based TES systems. This section also points out some of the research gaps needed to be filled by the current research to develop a practical PCM TES based thermal management system for tablet PCs.

2.1 Thermal Analysis of Portable Electronics

Tablet PCs have unique thermal characteristics because of their high-power density and the limited freedom for thermal management enhancement found therein. Typical tablet PCs run on Intel Atom or ARM Cortex processors as these processors are powered by lower power compared to desktop PC grade processors. Due to low power consumption, average chip temperature of tablet PCs can be as low as 33 °C during regular operating mode (Siddiqui, 2015). Focusing on this matter and to maintain an overall thin profile, tablet PCs do not have any added heatsinks or fans for active cooling. Hence, tablet PCs can be described as '*devices without heat sink*' (Grimes *et al.*, 2010). Generally, tablet PC manufacturers use heat spreaders to distribute heat from the chip to low temperature regions of the tablet. This method can effectively maintain a comfortable skin temperature (below 45 °C) unless tablet PCs are subjected to heavy usage loads such as gaming and high-definition video playback. During heavy usage, the skin temperature can be as high as 60 °C which results in severe users' discomfort. As a result, analyzing and understanding the thermal behaviour of tablet PCs is an important step in developing a novel thermal management system for tablet PCs. Several studies have been done to cover

this aspect and to introduce proper techniques for investigating the thermal behaviour of portable electronic devices (*i.e.* tablet PCs).

Luo *et al.* (2008) developed a thermal resistance network to analyze mobile handheld systems based on their experiments and numerical simulations. Power input level was varied from 0.5 W to 2.2 W. The excess temperature over ambient air was found to be approximately proportional to the power consumption of the heater. However, their thermal resistance network was oversimplified as each component was modeled as one block with a single uniform temperature value. Xie *et al.* (2014) presented a computer program called 'Therminator' to develop a compact thermal model for given device specifications. Case study results of the program showed that the performance of the device is linearly related to its skin temperature. Their results were compared with a commercial CFD code and it was found that 'Therminator' had an accuracy of ±0.5 °C. Gurrum *et al.* (2012) determined the thermal properties of different device components through several CFD trials. They found that thermal pads (gap fillers) are useful in decreasing the chip temperature, but they lead to an increase in skin temperature. A comprehensive thermal study was performed by Carroll and Heiser (2010) to measure the power consumption of different components of a smartphone. It was found that, in the suspended (locked) mode, the Global System for Mobile Communications (GSM) module consumed the greatest amount of power and hence contributed the greatest amount of heat. On the other hand, during the idle mode (no particular application usage but the display turned on), most of the power is consumed by the graphics processing unit (GPU). Pals and Newman (1995) studied the thermal behaviour of Li/Polymer battery during the discharging phase and found that the temperature in the cell increases more quickly due to the decrease of overpotentials in the beginning of the discharging phase. Moreover, increased current supply from the battery also results in higher heat generation.

Since the introduction of Android, iOS, and Windows operating systems (OS) in portable devices, hardware acceleration has increased dramatically in a very compact package. As a result, most of the literature results mentioned above are nearly obsolete, as those are based on previous generations of portable smart devices. As a result, thermal analysis of

contemporary devices is necessary to understand power consumption, heat generation, heat spreading at different operating conditions and usage loads.

2.2 Phase Change Materials (PCMs)

In the last two decades, prospective areas of PCM-based TES application expanded drastically. Various applications of PCM-based TES units can be found in the open literature (Zalba *et al.*, 2003; Sharma *et al.*, 2009; Agyenim *et al.*, 2010; Groulx *et al.*, 2014), which include thermal storage for solar energy (Telkes, 1947; Kamimoto *et al.*, 1986; Li *et al.*, 1991), space temperature control (Feldman *et al.*, 1986; Hawes *et al.*, 1993), thermal protection of food and beverages (Chalco-Sandoval *et al.*; Espeau *et al.*, 1997), vehicle thermal comfort (Socaciu *et al.*, 2016), thermal management of electronic devices (Hodes *et al.*, 2002; Alawadhi and Amon, 2003; Fok *et al.*, 2010; Baby and Balaji, 2012), to name a few. In the following sections, research on different aspects of developing standalone PCM-based thermal management systems are discussed.

2.2.1 Selection

Selection of PCMs requires extensive studies based on the application area (Zalba *et al.*, 2003), economic viability (Zhao and Zhang, 2011; Oró *et al.*, 2012), kinetic, chemical, and thermo-physical properties (Cabeza, 2008; Sharma *et al.*, 2009; Cabeza *et al.*, 2011), and so on. A generalized classification of PCMs is presented in Fig. 2-1.

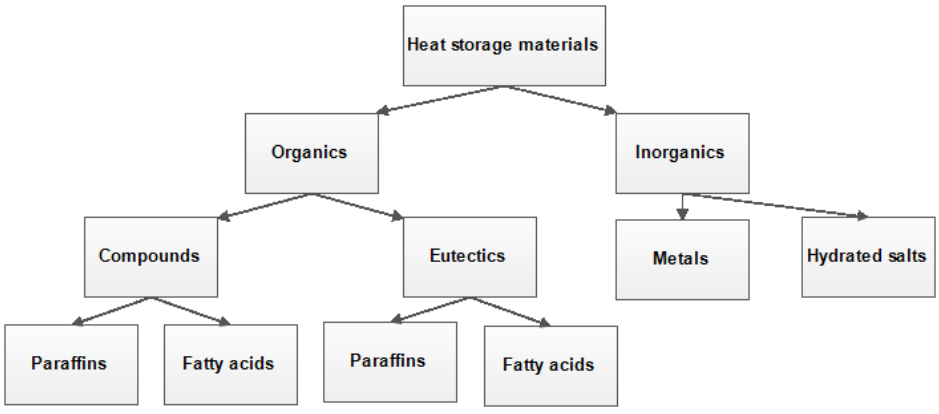

Figure 2-1 Types of Phase Change Materials.

In research conducted by Lane (1980), 20,000 PCM compounds were selected for the study and about 200 materials were identified as most promising, including organic, inorganic compounds, and eutectic mixtures. The total number of selected PCMs were then shrunk down to 40 for laboratory inspections. Most of the selected PCMs were discarded due to incongruent melting (non-uniform melting with phase separation), slow crystallization, and chemical instability. Desirable properties of PCMs for different applications can be found in various studies (Sharma *et al.*, 2009; Oró *et al.*, 2012; Ge *et al.*, 2013). For low energy storage applications, PCMs require to have the following properties:

- Desired melting point temperature matching the application;
- High latent heat of melting per unit volume for high latent heat storage;
- High specific heat in order to provide significant sensible heat storage;
- Negligible volume changes on phase change and low vapor pressure at operating temperature (*i.e.* non-volatile);
- High nucleation rate to avoid supercooling of liquid phase during solidification;
- Excellent consistency of the properties even after numerous phase change transitions;
- Non-toxic, non-flammable, and non-explosive behaviour;
- Non-corrosive to the encapsulation material;
- Inexpensive and easily available for an overall inexpensive system.

A high transition enthalpy change ($\Delta_{fus}H$) was also mentioned as a useful property by Groulx *et al.* (2014) for electronic cooling applications. They mentioned $\Delta_{fus}H \geq 200$ J/g as an ideal value. A more subtle factor to consider for a PCM is the hysteresis associated with the phase transition, *i.e.*, the difference in T_{onset} on heating compared with cooling. Minimal hysteresis is required in applications where heat is to be recovered immediately

on cooling. Some PCMs have low hysteresis as an intrinsic property. PCMs with high hysteresis require nucleation agents or mechanical activation to attain low hysteresis.

2.2.2 Thermo-physical Properties of PCMs: A Generic Review

Most PCMs have different melting temperatures, and therefore, are suitable for different applications (building temperature control, solar thermal storage, electronic cooling, etc.). Having only the required melting temperature or latent heat of fusion does not make a PCM ideal for a specific application. In addition to the melting temperature and the latent heat of fusion, there are still many other important properties to be considered for a proper design of PCM TES system, as pointed out in section 2.2.1. Inorganic compounds provide almost double the volumetric energy storage density (250-400 J/cc) compared to organic compounds (128-200 J/cc) (Sharma *et al.*, 2009). Hence, it is absolutely necessary to study thermophysical properties of different PCMs due to the difference of thermal and chemical behaviour, which may affect the design of PCM-based TES system performance.

2.2.2.1 Organic Phase Change Materials

Organic PCM compounds are usually classified as paraffins and non-paraffins (including fatty acids, esters). These compounds have congruent melting, self-nucleation, and non-corrosive properties.

Paraffins. Abhat (1983) defined paraffin as alkanes having 14-40 carbon atoms and melting point between 6 and 80 °C. Due to being safe, chemically stable, inexpensive, and non-corrosive, paraffins gained much attentions in PCM-based electronic cooling research (Krishnan *et al.*, 2005). Furthermore, they have remarkable self-nucleation properties (Abhat *et al.*, 1981). However, paraffin shows some undesirable properties such as: (i) low thermal conductivity, and (ii) moderate flammability. Studying thermo-physical properties, Sharma *et al.* (2009) categorized PCMs into three groups according to their application promise: Group I – most promising, Group II – promising, and Group III – less promising. Most paraffins were placed in Group I and Group II. Also, *n*-eicosane, the most

common paraffin used in PCM-based TES applications, was mention as most promising by the same authors.

Non-paraffins. Fatty acids are the most commonly used PCMs in non-paraffin family. Fatty acids have comparable latent heat of fusion to that of paraffin. These types of PCMs have a melting point between 17 and 70 °C which is not continuous throughout. Abhat (1983) reported that fatty acids also tend to avoid supercooling. Laboratory of Applied Multiphase Thermal Engineering (LAMTE) and Mary Anne White's (MAW's) Lab at Dalhousie University reported excellent performance of dodecanoic acid as PCM for application requiring melting temperature between 40 to 45 °C range (Desgrosseilliers *et al.*, 2011; Murray *et al.*, 2011; Liu *et al.*, 2012). Only major drawback reported by Abhat (1983) was their cost, which is 2 to 2.5 times greater than that of paraffin. Physical properties of some common fatty acids compiled by Abhat (1983) are presented in Table 2-1.

Esters are another kind of non-paraffin PCMs which have started to make strong appearance in the PCM market. Their low price to performance ratio characteristics compared to paraffins is one of the main reason behind this. Esters are commonly called fatty acid esters or vegetable-based PCMs. Esters have melting temperature from - 90°C to 150°C with latent heats between 150 and 220 kJ/kg (Sutterlin, 2014). Additionally, the safety and environmental benefits of using esters are superior to those of paraffins. Usually, esters degrade in six months or less when discarded in a landfill, whereas paraffins remain undegraded for decades.

Thermo-physical properties of some common organic PCMs were compared with literature values after measuring the properties of those PCMs by differential scanning calorimetry (DSC) in MAW's Lab at Dalhousie University and the obtained results are summarized in Table 2-2.

Table 2-1 Thermo-physical Properties of some fatty acids Abhat *et al.* (1981).

PCM	T_{onset} (°C)	ΔH_{fus}		ρ (g/cc)	C_p (kJ/kg-K)	k (W/m-K)
		kJ/kg	J/cc			
Octanoic acid	16.5	149	128	1.033	-	0.148
Decanoic acid	31.5	153	136	0.886	-	0.149
Dodecanoic acid	42 – 44	178	155	0.870	1.6	0.147
Tetradecanoic acid	54	187	158	0.844	1.6 (Solid), 2.7 (liquid)	-
Hexadecanoic acid	63	187	159	0.847	-	0.165
Octadecanoic acid	70	203	191	0.941	2.35	0.172

Table 2-2 Thermo-physical properties of some common organic PCMs tested and compared at MAW's Laboratory in Dalhousie university.

PCM	PCM Type	T_{onset} (°C) **MAW's Lab**	T_{onset} (°C) literature	ΔH_{fus} (kJ/kg) **MAW's Lab**	ΔH_{fus} (kJ/kg) literature	ΔH_{fus} (J/cm^3) **MAW's Lab**	ΔH_{fus} (J/cm^3) literature
Nonadecane	Paraffin	31.8	31.7*	181	170*	139	137
Decanoic (capric) acid	Fatty acid	32	31.5**	145	152-163^	128	133-144
Eicosane	Paraffin	37.5	36.6*	246	247*	192	195
Dodecanoic acid	Fatty acid	43.3	41-49$^{+\%}$	184	177-212^	160	153-186
Docosane	Paraffin	43.8	42.95 - 43.6*	234	154-157*	180	122
Paraffin Wax SA327212	Paraffin	55.0	58-62	171	--	142	--
Paraffin Wax SA411663	Paraffin	61.1	≥ 65	197	--	164	--
Stearic acid	Fatty acid	54.3	60-70$^{\%}$	161	187-214*	137	158-182
Tetradecanoic acid	Fatty acid	54.7	49-58$^{\%}$	186	183-205	156	154-176
Octadecanol	Alcohol	55.8	55.2-56.3$^{@}$	218	145-246$^{@}$	177	118-200
PT-37	Ester	36.3	37^{X}	206	210^{X}	173	193^{X}
Hexadecanoic acid	Fatty acid	60.5	55-64$^{\%}$	179	163-204^{+}	152	138-173

*Dirand *et al.* (2002)
**Abhat (1983)
^Sharma *et al.* (2009)
$^{+}$Adriaanse *et al.* (1964)
$^{\%}$Abhat *et al.* (1981)
^{X}Entropy Solutions (2014)
$^{@}$ van Miltenburg and Oonk (2005)

2.2.2.2 Inorganic Phase Change Materials

Inorganic phase change materials can be classified as salt-hydrates and metallic. Metallic PCMs have very limited applications in practice due to the fact that the resulting systems are typically dense. However, being metals, these PCMs provide high thermal conductivity and no heat transfer enhancement technique is required. Ge *et al.* (2013) illustrated some recent developments in metallic PCM-based TES systems. They mentioned high thermal conductivity, large volumetric enthalpy of fusion, and long-term stability after millions of thermal cycling, as promising properties of metallic PCMs. Physical properties of some metallic PCMs are presented in Table 2-3.

Table 2-3 Physical properties of some metal PCMs (Wee *et al.*, 1998; Sharma *et al.*, 2009; Haiyan LI, 2011).

Metal PCM	T_{onset} (ºC)	ΔH_{fus} (kJ/kg)
Gallium-Antimony eutectic	29.8	-
Gallium	30.0	80.3
Cerrolow eutectic	58	90.9
Bi–Cd–In eutectic	61	25
Cerrobend eutectic	70	32.5
Bi–Pb–In eutectic	70	29
Bi–In eutectic	72	25
Bi–Pb–tin eutectic	96	-
Bi–Pb eutectic	125	-
Cesium	28.65	16.4

Salt hydrates. The introduction of salt-hydrate as PCMs for solar house heating dates back as early as 1947 (Telkes, 1947). These PCMs have chemical formula $M{\cdot}nH_2O$, where M signifies the inorganic compound. Table 2-4 presents the thermo-physical properties of some common salt-hydrate PCMs. One of the major problems of salt hydrate PCMs reported by Abhat (1983) is the incongruent melting. This is characterized by the phenomenon called decomposition where the solid phase separates from the compound and sediments at the bottom of the vessel. Supercooling is also observed in salt-hydrate PCMs due to poor nucleating properties.

Table 2-4 Thermo-physical properties of some common salt hydrate PCMs Abhat (1983).

PCM	T_{onset} (°C)	ΔH_{fus}		C_p (kJ/kg-K)	k (W/m-K)	Ref
		(kJ/kg)	(J/cm^3)			
$KF.4H_2O$	18.5	231	336	1.84 (Solid) 2.39 (Liquid)	-	Schroder (1980)
$CaCl_2.6H_2O$	29.7	171	256	1.45 (Solid)	-	Abhat *et al.* (1981)
$Na_2SO_4.10H_2O$	32.4	254	377	1.93 (Solid)	0.544	Abhat *et al.* (1981)
$Na_2HPO_4.12H_2O$	35.0	281	405	1.70 (Solid) 1.90 (Liquid)	0.514 (32°C) 0.476 (49°C)	Hale *et al.* (1971)
$Zn(NO_3)_2.6H_2O$	36.4	147	304	1.34 (Solid) 2.26 (Liquid)	-	Abhat *et al.* (1981)
$Na_2S_2O_3.5H_2O$	48.0	201	322	1.46 (Solid) 2.39 (Liquid)	-	Abhat *et al.* (1981)

Telkes (1952) suggested using nucleating agents having the same crystal structures as the parent substance, and Lorsch *et al.* (1975) recommended using "cold finger" in the PCM to avoid supercooling. Though salt-hydrate PCMs have some drawbacks, greater overall density of the salt provides high volumetric heat storage density.

2.2.3 Long Term Stability of PCMs

One of the most severe tests that PCMs must pass is the thermal stability with numerous cycles of repeated melting and solidification for long term system design. Abhat (1983) suggested at least 1000-2000 phase change transition tests of PCMs for developing long term PCM-based thermal storage systems. Usually, change of melting temperature and change of heat of fusion are the deciding factors of thermal stability of a PCM in the thermal cycling test. Additionally, Abhat (1983) suggested measuring the temporal variation of temperature as well as temporal variation of the heat transfer rate within the PCM during charging and discharging phase. PureTemp, a prominent PCM manufacturer, specifies that the tolerable degree of deviation for the purity of a PCM can be up to ~2% from the initial measurement (Entropy Solutions, 2015). An automated thermal cycling facility (Fig. 2-3) was built at the LAMTE at Dalhousie University (Kheirabadi and Groulx, 2014) which facilitated the observation of changes in PCMs' thermo-physical properties after several phase change transition cycling.

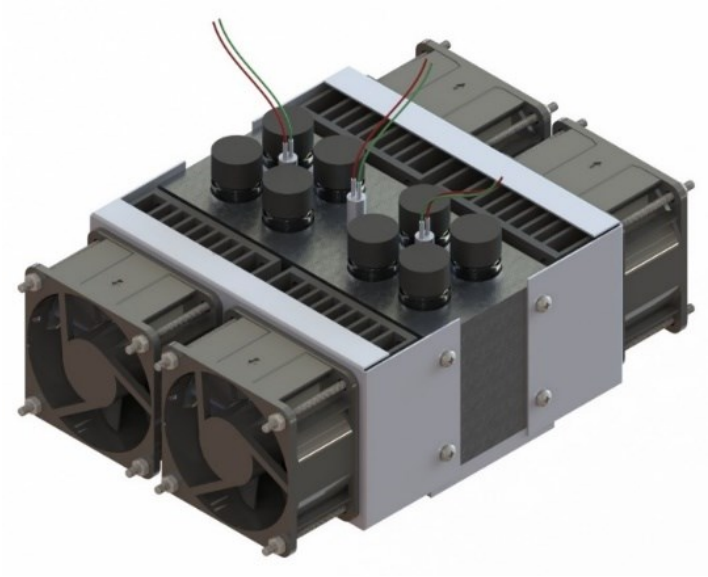

Figure 2-2 The Automated Thermal Cycler (Kheirabadi and Groulx, 2014).

Desgrosseilliers *et al.* (2013b) reported an analysis of dodecanoic acid up to 500 phase transition cycles. Negligible changes of T_{onset} and $\Delta_{trs}H$ were reported after performing analysis of variance (ANOVA) at 95% confidence interval of the DSC data. Variations of T_{onset} and $\Delta_{trs}H$ were within 1.5 °C and 3.6% of the documented value respectively. Changes in volume ($\Delta_{trs}V$) and hysteresis were in an acceptable range which indicate that dodecanoic acid has very good long-term stability after several phase transition cycling. For limited thermal cycling (120 cycles), Abhat *et al.* (1981) also mentioned that paraffins and dodecanoic acid (lauric acid) do not show any sign of degradation. After performing DSC analysis of *n*-eicosane up to 4000 phase change transition cycle in MAW's Lab at Dalhousie University, no noticeable changes in $\Delta_{trs}H$ and T_{onset} were found; as can be seen in Fig. 2-4. In case of PT-37, PureTemp mentioned that PT-37 has a stable latent heat of fusion over the course of 10,000 phase transition cycles (Entropy Solutions, 2014).

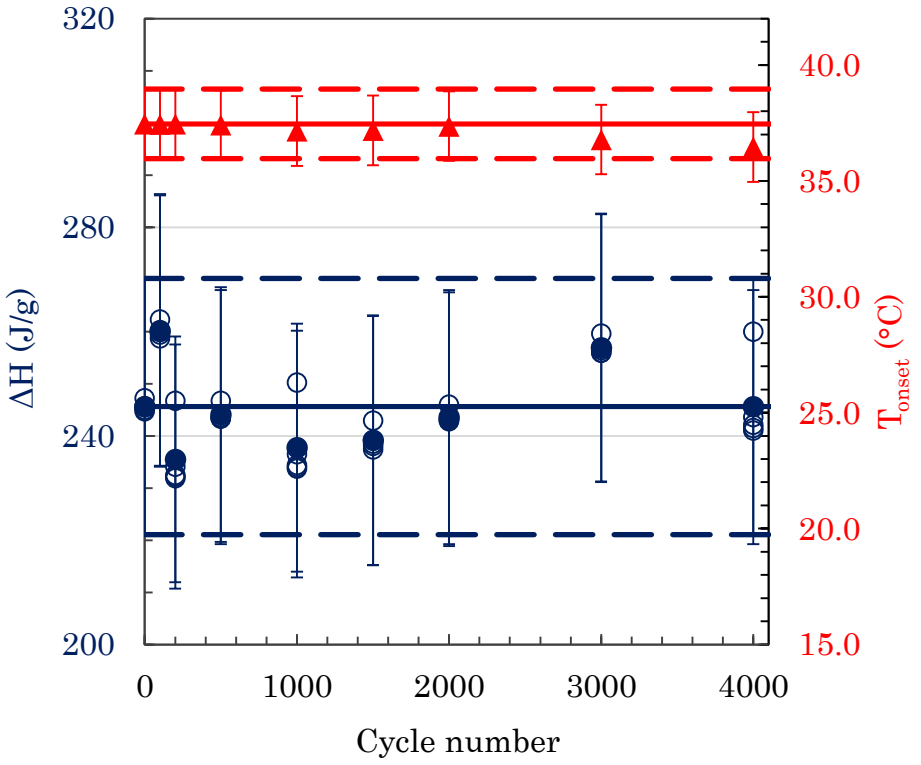

Figure 2-3 DSC obtained values of T_{onset} and $\Delta_{trs}H$ for *n*-eicosane up to 4000 phase change transition cycles[1] (used with permission from Dr. White and Dr. Kahwaji).

Up to 1500 thermal cycles were done for stearic acid, acetamide, and paraffin wax by Sharma *et al.* (1999) and Sharma *et al.* (2002). Latent heat variation of 0 to 23%, –1 to +14% and –12 to +2% were observed for stearic acid, acetamide, and paraffin wax respectively for 300 cycles. The same authors concluded that acetamide and stearic acid show good stability after 300 and 1500 thermal cycles. Studies by Sari (2003a, b) showed that changes from 0.07 °C to 7.87 °C in melting temperature and from 1% to 27.7% in latent heat of fusion can occur in case of stearic acid, palmitic acid, myristic acid, and dodecanoic acids (lauric acid) after different numbers of phase transition cycles (up to 1200). These stability tests show slight deviation in the change of latent heat and melting temperature compared to some results found in MAW's lab at Dalhousie University. Usually, PCM manufacturers offer wide ranges of PCMs having different percentage of purity. Hence, the variation in thermal cycling tests with same PCM might be attributed to

[1] All PCM research was conducted by Dr. Samer Kahwaji in MAW's Lab under the supervision of Dr. Mary Anne White.

the differences in chemical purity and aging of PCMs used. Wada *et al.* (1984) observed decreasing heat storage capacity of hydrated sodium acetate during thermal cycling. They also studied the effect of the thickening agent on the latent heat capacity of three different samples. Same authors reported that thickening agent improves the latent heat significantly even after 500 thermal cycles.

2.2.4 Encapsulation Materials and Techniques

Low thermal conductivity is one of the major bottlenecks for PCMs which limits their usage in practice (Zalba *et al.*, 2003; Sarı and Karaipekli, 2007; Sharma *et al.*, 2009). However, the thermal conductivity of the Latent Heat Storage (LHS) system can be increased by containerization, commonly called encapsulation, and by increasing surface area for heat transfer (*i.e.* using finned TES unit) (Amin *et al.*, 2014). Encapsulation also facilitates protecting the PCM from environmental factors (*e.g.* humidity) (Lane, 1985), increasing compatibility with sensitive system components. Encapsulation can be classified based on the level of size (Lane, 1980) as: macro-encapsulation (macro-PCM), micro-encapsulation (micro-PCM), and nano-encapsulation (nano-PCM). In his work, Lane (1985) emphasized the correct selection of PCM encapsulation materials for viable commercial implementation. He suggested that mechanical durability and integrity, good heat transfer, chemical compatibility, and vapor impermeability (Lane, 1980; Lane, 1985) are the primary aspects to be considered for the selection of PCM encapsulation materials. Cost and ease of manufacture are also important for an economically feasible system (Lane *et al.*, 1978). In addition, a LHS system using encapsulated PCMs also provides structural stability, easy handling (Regin *et al.*, 2008), high thermal conductivity, and sufficient surface area for enhanced heat transfer (Lane, 1985; Zhang *et al.*, 2010). Macro-encapsulation of PCMs was the main mode of PCM containerization in this study due to an inexpensive and easy way of manufacturing and no apparent drawbacks compared to microencapsulation, such as increased supercooling tendencies and more difficult heat transfer (Lane, 1985). In this section, a brief discussion on different macro-encapsulations is presented.

Werner (1987) performed experiments on TES systems using PCM (a mixture of 90% myristic and 10% dodecanoic acid) encapsulated in polypropylene, polyethylene, and polyamide. No chemical reaction was found between the PCM and polyamide. However, paraffin shows diffusion with polypropylene and polyethylene. The author also reported that encapsulation of organic PCMs is more difficult than inorganic PCMs due to the similar chemical structure of organic PCMs and encapsulation materials. In an attempt to cool an electronic device, Tan and Tso (2004) used an aluminum block with four rectangular cavities filled with PCM (*n*-eicosane). Fok *et al.* (2010) investigated the use of finned aluminum T6-6061 block as PCM (*n*-eicosane) encapsulation, which is an extended work of Tan and Tso (2004). They used three different aluminum blocks as PCM encapsulation with different sizes (minimum thickness was 21 mm) and different number of fins. Kandasamy *et al.* (2007) also used an experimental model with PCM (paraffin wax) filled rectangular aluminum enclosure (14 mm thick) at different heat input levels and angular orientation. In another study, Kandasamy *et al.* (2008) used three different aluminum heatsinks with fins (minimum thickness being 10 mm) filled with PCM (paraffin wax) and tested the performance of the system. These aluminum-based encapsulations were able to reduce the peak temperature of model electronic devices under study due to high thermal conductivity of aluminum heatsink as well as substantial latent heat storage in PCMs. But, the substantial size of the aluminum-based encapsulations is one of their inherent drawbacks in the thermal management applications of very thin tablet PCs. Hence, with a tablet PC's thickness in the order of 10 mm, it is very difficult to implement such aluminum-based encapsulations in practice. Moreover, these studies do not cover any optimization and stability (chemical, physical, etc.) analysis of the system.

Unconventional encapsulation methods such as stencil printing and 'dam and fill', as can be seen in Fig. 2-5, used by Novikov *et al.* (2014), have very high prospects in tablet PC cooling applications. In the stencil printing method, 1:1 mixture of grounded PCM and acrylic resin, a carrier, was produced using the same technique presented by Bremerkamp *et al.* (2012). A standard conformal coating (binder material) is usually used to make a homogenous mixture with pulverised silica gel (or PCM). The low viscosity of binder allows a high content of silica gel addition and with that a construction of an open porous coating. This method was originally proposed by Yeung *et al.* (2003). In the case of 'dam

and fill' encapsulation, a dam of acrylic resin was built around the heating element and then filled with PCMs. Significant delay in the transient temperature rise (50% longer operation time before reaching 120 °C) was observed with 100% erythritol in the 'dam and fill' encapsulation. After 300 minutes of heating, as high as 25 °C temperature reduction with the baseline condition (165 °C) was noted. Bremerkamp *et al.* (2012) utilized the hydration and dehydration process[2] of silica gel instead of using an actual PCM for electronic cooling. Conformal coating of acrylic resin was used to secure the circuit from moisture absorbed by silica gel. As TES materials reside in contact with the electronic components, very rigorous insulation (coating of resin) of the whole circuit is necessary for this type of encapsulation. This in turns reduces the reliability of the system. Moreover, further metallurgical, chemical and physical stability studies of the encapsulation material (*i.e.* resin) are also necessary to apply this method readily in tablet PC cooling.

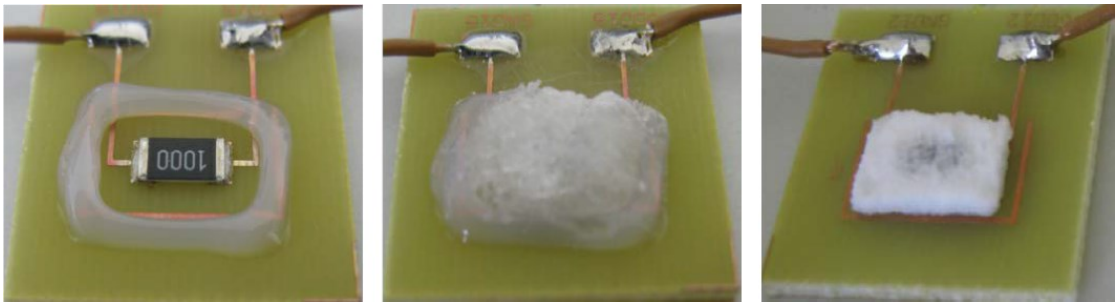

Figure 2-4 Applying dam (left) and PCM as fill material (middle), stencil printed PCM (right) (Novikov *et al.*, 2014) © IEEE 2014.

A few researchers (Lane, 1980; Schultz, 2007; Desgrosseilliers *et al.*, 2012; Desgrosseilliers, 2012; Desgrosseilliers *et al.*, 2013a, 2014) used conventional packaging aluminized laminates as prospective encapsulation materials in their studies. A stack of metal foil and thermoplastic laminate (*i.e.* nylon/Al/polypropylene) are commonly used for food and electronic packaging material (Lane *et al.*, 1978; Stessel, 1996; Elopak, 2009; recyclecartons.ca, 2011; TetraPak, 2011). In addition to good shape conformability and excellent barrier properties, this material has gained much attention due to its very thin feature, which facilitates encapsulation of PCMs suitable for today's compact tablet PC cooling. Laminate film encapsulation also provides chemical toughness and low cost of

[2] can be considered similar to vaporization and condensation; suggested by Ruthven (1984)

the system. Lane (Lane *et al.*, 1978; Lane, 1980; Lane, 1985) mentioned laminate films as the most inexpensive PCM encapsulation method. The laminate material was found very promising for salt hydrate PCMs. However, he mentioned that the performance of the laminate material is poor for organic PCMs, as the heat sealed seam was attacked by organic PCMs at high operating temperatures (Lane, 1980). Furbo and Schultz (2007) presented a work where they used sodium formate trihydrate ($NaCOOH{\cdot}3H_2O$) encapsulated in 0.113 mm thick laminated pouches having 9.0 μm thin aluminum foil. Lane (1985) did not consider heat transfer enhancement in the laminate pouch, since the heat transfer medium was air and PCMs under consideration did not show any supercooling. In addition, Furbo and Schultz (2007) only considered flexibility and self-stability of the laminate film as selection criteria. Potential heat transfer benefits of using laminate films were presented by Desgrosseilliers *et al.* (Desgrosseilliers, 2012; Desgrosseilliers *et al.*, 2013a, 2014) for salt hydrate PCMs. They presented two-region (heated region and fin region) fin model Desgrosseilliers *et al.* (2013a) for finite heat source and non-uniform heating. In their two-region fin model, Desgrosseilliers *et al.* (2014) confirmed that overall heat transfer of the system is dominated by the large thermal conductivity of the metal (Al) layer.

Due to the thermo-chemical reaction between PCMs and encapsulation materials, corrosion has become a major issue in the design of PCM-based TES systems. Immersion corrosion tests for some common metals in contact with salt hydrate PCMs were studied by Cabeza, *et al.* (Cabeza *et al.*, 2001a, 2001b; Cabeza *et al.*, 2002). They tested the PCMs within a temperature range of 32 to 36 °C and 48 to 58 °C. Although the tests were conducted for a short period of time (2 weeks), in the study (Cabeza *et al.*, 2001a) aluminum was found to be the worst for containing certain salt hydrate PCMs (zinc nitrate hexahydrate, sodium hydrogen phosphate dodecahydrate, and calcium chloride hexahydrate). In another study (Cabeza *et al.*, 2002), with relatively long-term experiments (10 weeks), Cabeza recommended using aluminum and stainless steel for sodium acetate trihydrate ($CH_3COONa{\cdot}3H_2O$) and sodium thiosulfate pentahydrate ($Na_2S_2O_3{\cdot}5H_2O$) PCMs. Copper and brass were not recommended for sodium thiosulfate pentahydrate ($Na_2S_2O_3{\cdot}5H_2O$) due to severe corrosion rate. Sodium acetate trihydrate ($CH_3COONa{\cdot}3H_2O$) showed mild corrosion with copper and brass. Hence, appropriate

caution was suggested when using sodium acetate trihydrate ($CH_3COONa \cdot 3H_2O$) with brass or copper.

Commonly, most studies use the term corrosion rate (CR) to measure the suitability of encapsulation materials for a certain period of PCM storage. Usually, the corrosion rate is calculated using weight loss method (Schweitzer, 2009) from the change in mass (Δm), specimen area (A), and duration of test (Δt). The formula is generally written as:

$$\text{CR} = \frac{\Delta m}{A \cdot \Delta t} \text{ (mg/cm}^2\text{yr)} \tag{2.1}$$

Recommended storage duration of PCMs in encapsulation materials based on corrosion rate can be found in Table 2-5.

Table 2-5 Guide for corrosion weight loss used in the industry.

CR (mg/cm^{2}yr)	Recommendation (Ghali *et al.*, 2007)
>1000	Completely destroyed within days
100 – 999	Not recommended for service greater than a month
50 – 99	Not recommended for service greater than a year
10 – 49	Caution recommended, based on the specific application
0.3 – 9.9	Recommended for long term service
< 0.2	Recommended for long term service; no corrosion, other than as a result of surface cleaning, was evidenced

In 12 weeks of study, Ferrer *et al.* (2015) mentioned that PT-23, an ester based PCM similar to PT-37, does not show signs of corrosion on any metal under study (aluminum, SS 316, SS 304, carbon steel, and copper). They observed corrosion rate of 0 – 1 mg/cm^{2}yr with some specimens which they attributed to the process of surface cleaning instead of corrosion of materials. After 12 weeks of immersion test in MAW's Lab with *n*-eicosane and PT-37, delamination of aluminized laminate foil was mentioned because of mass gain over time as can be seen in Fig. 2-6[3]. It can be seen that after 12 weeks of testing, corrosion rate was below 50 mg/cm^{2}yr for both *n*-eicosane and PT-37. Delamination of the laminate film was observed, since adhesive layers of the laminate film came off due to absorption of PCMs into the laminate films. However, no corrosion of aluminum layer was mentioned. In typical encapsulations, PCMs only come in contact with the polypropylene

[3] Conducted by Dr. Samer Kahwaji at MAW's Lab under the supervision of Dr. Mary Anne White.

layers with no chance of attacking the adhesive layer on both sides of the aluminum layer. This is in contrary to the immersion test where the whole specimen is immersed in liquid PCMs. Hence, for a long-term encapsulation of PT-37 and *n*-eicosane, it can be assumed that usage of aluminized laminate film will not pose any problem.

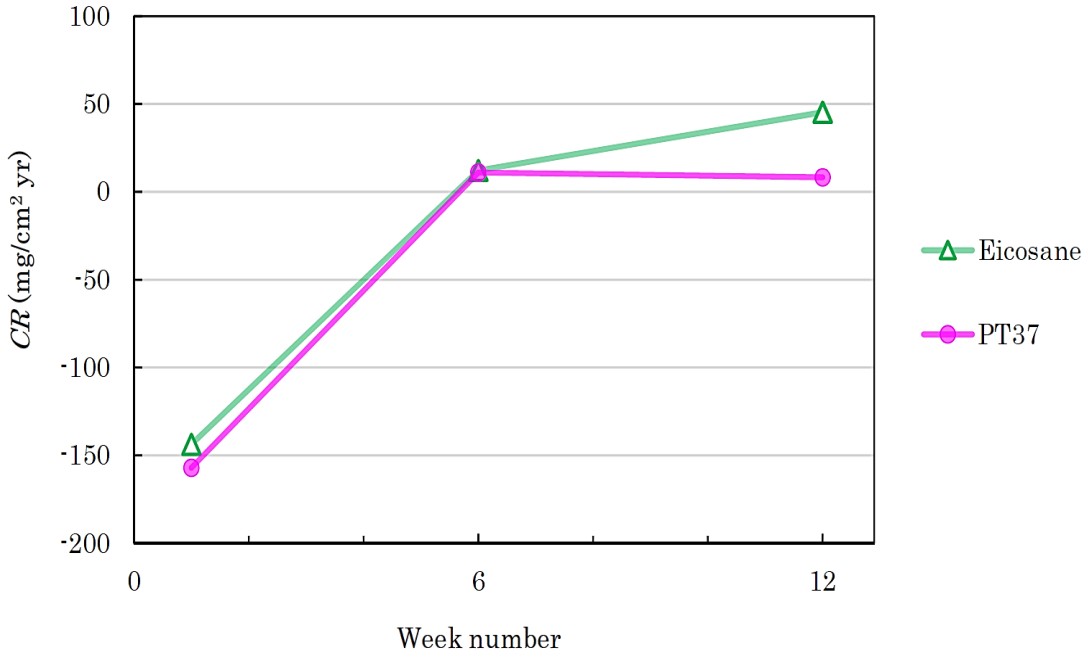

Figure 2-5 Corrosion rate of aluminized laminate film with *n*-eicosane and PT-37 (used with permission from Dr. White and Dr. Kahwaji).

Table 2-6 provides the summary of different encapsulation methods studied by different researchers.

Table 2-6 Summary of encapsulation materials research

Sl. No.	PCM(s)	Type	Material(s)/ Dimensions	Remarks from the study	Ref.
1.	Various	Macro	Aluminized laminate film	Not suitable for organic PCMs; heat sealed seam was attacked by organic PCMs	Lane (1980)
2.	$NaCOOH \cdot 3H_2O$	Macro	Aluminized laminate film	-	Furbo and Schultz (2007)
3.	Salt Hydrates	Macro	Aluminized laminate film	Provided good encapsulation for salt hydrate PCMs. The thermal conductivity of the metal layer was dominant. Good overall thermal conductivity of the encapsulation.	(Desgrosseilliers *et al.*, 2012; Desgrosseilliers, 2012; Desgrosseilliers *et al.*, 2013a)
4.	*n*-eicosane PT-37	Macro	Aluminized laminate film	The film may delaminate. But, no corrosion of Al layer.	***
5.	*n*-eicosane	Macro	Aluminum; 85×72×21 mm 91×72×21 mm	Increased thermal conductivity with finned encapsulation. No remarks on chemical stability of encapsulation materials	Fok *et al.* (2010)
6.	Paraffin wax	Macro	Aluminum; 132×80×14 mm	Same	Kandasamy *et al.* (2007)
7.	Paraffin wax	Macro	Aluminum; 16×14×12.5 mm 31×31×10 mm 30×30×18 mm	Same	Kandasamy *et al.* (2008)
8.	Silica Gel (hydration and dehydration)	Macro	Mixture of silica gel with acrylic resin	Increased thermal conductivity of the overall system. No metallurgical remarks on the encapsulation material	Bremerkamp *et al.* (2012)
9.	Astorphase 125; Erythritol; $MgCl_2.6H_2O$	Macro	Dam and fill; Stencil Printing	Same	Novikov *et al.* (2014)
10.	$Zn(NO_3)_2.6H_2O$	Macro	Aluminum, Steel, Brass, Copper, Stainless Steel	Rapid corrosion of Al and steel slower corrosion of Brass and Cu	Cabeza *et al.* (2001a)
	$Na2HPO4.12H_2O$			Aluminum badly corroded. Brass, copper, and SS were corrosion resistant.	
	$CaCl_2.6H_2O$			Pitting in Aluminum. Brass and copper were found corrosion resistant.	
11.	$CH_3COONa \cdot 3H_2O$	Macro	Same	Aluminum, steel, SS recommended. Brass and copper recommended for short-term.	Cabeza *et al.* (2002)

*** Materials research in MAW's Lab at Dalhousie University.

2.3 Experimental Research on PCM-based TES systems

Investigations on the use of PCM-based TES systems, including PCM hybrid heat sinks in the temperature control of electronic devices have been conducted by several researchers. This section presents some of that research and is divided into two sub-sections: (i) classical experimental analysis of PCM-based systems, and (ii) application of PCM-based TES units in portable electronic cooling. Classical experimental studies on PCM melting are necessary to understand the basic melting and solidification phenomena of PCMs under different operating conditions (*i.e.* inclination, power input, wall temperature, etc.). Additionally, those studies can be considered as the basis for setting standard ways to investigate PCM-based TES units installed into a tablet PC.

Classical experimental analysis of PCM-based systems. Shokouhmand and Kamkari (2013) experimentally investigated the basic melting process of dodecanoic acid in a rectangular TES unit. They mentioned that initially conduction is the dominant process of heat transfer, which shifts to convection after a sufficient amount of time. After analyzing the obtained Nusselt number (Nu), they pointed out four stages of heat transfer throughout the melting process: conduction, transition, strong convection, and vanishing convection. In another study (Kamkari *et al.*, 2014), they investigated the effect of system inclination on the melting process of dodecanoic acid. A remarkable decrease in melting time was reported when the inclination angle was decreased. This was attributed to the rise of vortical and chaotic flow[4] arrangements in the liquid PCMs. This resulted in, an average of 35% and 53% faster melting for 45^{o} and 0^{o} (horizontal) inclination respectively. Also, more than twice the heat transfer enhancement ratio was achieved for 0^{o} inclination compared to that of the vertical enclosure. Conclusions of these previous studies were confirmed by Lu *et al.* (2014). They reported that minimum thermal resistance of the heatsink was found for 60° and 75° inclinations.

[4] Mainly observed in convection dominated phase change process and not discernable in conduction dominated heat transfer.

Application of PCM-based TES units in portable electronic cooling. Alawadhi and Amon (2003) examined a physical model to mimic a portable wearable device, a very simple system having a polymer (epoxy) made body and a heater which simulates the system on a chip (SoC) of electronic devices. Good thermal response of the system was achieved by PCM-based TES units while PCMs were melting. An increased Stefan number (Ste), a dimensionless number which is defined as the ratio of sensible heat to latent heat ($C_p\Delta T/\Delta_{fus}H$), resulted in a linear increase in PCM melting. Their experimental work established the feasibility of the concept of cooling electronic devices using PCM-based TES units. But, due to drastic increase in the compactness of portable electronic devices, application of such PCM-based TES units is limited to the cooling of stationary electronic devices such as desktop computers instead of modern tablet PCs.

Kandasamy *et al.* (2007) investigated the phase change process of paraffin wax at different power levels and angular orientations of the PCM enclosure. They reported no significant effects of inclination on heat source peak temperature during thermal management of electronics using paraffin wax. Hodes *et al.* (2002) presented transient thermal management of an experimental ABS (Acrylonitrile Butadiene Styrene) handset using tricosane and Thermasorb-122, a microencapsulated PCM having a melting temperature of 48 °C and a heat of fusion of 160 kJ/kg. Only 9.5 g of tricosane provided 5 times longer operation before reaching the 'too hot' (62 °C) set-point temperature for 3 W power supply. In a similar study, Tan *et al.* (2009) measured the thermal performance of a PCM cooled mobile phone with different usage loads and orientations of the experimental device by means of a PCM-based TES unit (21 mm thickness). They were able to reduce by 6.4 °C peak surface temperature of the setup for both frequent usage condition and heavy usage condition. In an earlier study, they made an experimental setup with embedded PCM (*n*-eicosane) in a cavity to investigate the cooling of personal digital assistants (PDAs) (Tan and Tso, 2004). However, their experimental model consisted of an aluminum block, heat transferring block, and heaters which do not represent a real-life PDA. On the contrary, Kandasamy *et al.* (2008) used a FR4 sheet, plastic quad flat package (QFP) with copper lead for a standardized setup (JESD51-2A, 2008) which has a better representation of electronic devices. They also used heat spreader for better heat dissipation to the heatsink. Since aluminum is a very good conductor of heat, even without PCM, aluminum heat sinks

facilitated substantial reduction of thermal resistance as well as the temperature of the Quad Flat Plate (QFP) package. However, due to isothermal energy storage during phase change, better transient response was obtained with PCM hybrid heatsinks. Moreover, increasing power input levels increased the system transient cooling performance due to the increased buoyancy effect. The use of PCMs resulted in 10 °C lower skin temperature compared to the skin temperature with an empty heatsink for 4 W heat input during unsteady operation. After 30 minutes of operation the junction temperature did not reach the peak value (90 °C) but in case of the baseline operation (no PCM – no heatsink), it took only 6 minutes to reach the peak junction temperature. Tomizawa *et al.* (2016) investigated the thermal response of a mobile device equipped with a microencapsulated PCM (MPCM) sheet. Although their experimental model had dimensions encountered in a tablet PCs, the construction (both materials and components) does to employ the true intricacy of a real table PC. MPCM sheet was able to delay the saturation time of both heater and skin temperature. The delay was almost 5 minutes for the heater and 7 minutes for the skin. However, their study showed that using only PCM performs even better. PCMs provided 16% and 24% additional delay for the heater and skin respectively before reaching the saturation temperature compared to the MPCM sheet.

2.4 Summary

The review of the aforementioned research illustrates that the use of PCM-based TES units for portable electronic device (*i.e.* tablet PC) cooling is a viable option. The combination of those studies can answer common questions associated with PCM melting-solidification phenomenon and performance of electronic devices cooled by PCM-based TES units. Though present PCM-based TES systems might be used successfully for cooling stationary electronic devices (desktop computers, etc.), those studies fail to address the following points, which are necessary for their implementation into a real tablet PC:

- Study of an experimental model intricate enough to mimic tablet PCs very closely; both physically (dimensions and materials) and thermally.

- Development of a thin encapsulation capable of fitting into a real-life tablet PC having close to 10 mm of overall thickness.

Moreover, the study of the stability of PCM encapsulation material to ensure long-term reliability of the system is also necessary, which are still unaddressed in those studies.

Chapter 3

Thermal Analysis of Tablet PCs

The objective of this analysis was to determine the transient thermal response of two popular tablet computers: Dell Venue 8 Pro (Windows OS) and Samsung Galaxy Note 8 (Android OS). The results of the thermal analysis were used to build a simplified circuit board which was integrated in the experimental setup to produce thermal behaviour pattern similar to a real tablet PC. Only one tablet PC was selected to be used as a substrate of the experimental setup based on the comparison of the thermal responses of both tablet PCs during different tests.

Both tablet PCs were tested under two different types of applications to mimic regular usage load and heavy usage load by using Skype and two stress test applications: HeavyLoad (Jam-Software, 2014) for Windows OS and StabilityTest (Wise, 2015) for Android OS. The display was turned off for all stress tests. As a result, heat generation from the LED strip was omitted in the entire study. Figure 3-1 shows the IR images of both display (front) side and back side of the two tablet PCs after 60 minutes of stress testing. It is evident that the Dell tablet had worse thermal response compared to the Samsung tablet. The maximum temperature of the back cover was 55 °C and 43 °C for the Dell and Samsung tablet PC respectively. Type – T thermocouples were also attached on the back cover to observe external thermal behaviours of the two studied tablet PCs. The positions of the thermocouples were determined by studying the IR images of the back cover. Thermocouples were attached to the area with the highest temperature has observed on the IR image. External thermal response recorded by thermocouples can be seen from Fig. 3-2 for both regular usage load (skype video calling) and heavy usage load (stress test). It is interesting to note that the Windows (Dell) tablet had higher idle temperatures than the Android (Samsung) tablet PC in both cases. This was expected since the Windows

(Dell) tablet PC was running on Windows OS which is not properly optimized for tablet PC platforms and usually takes greater computational power compared to Android OS.

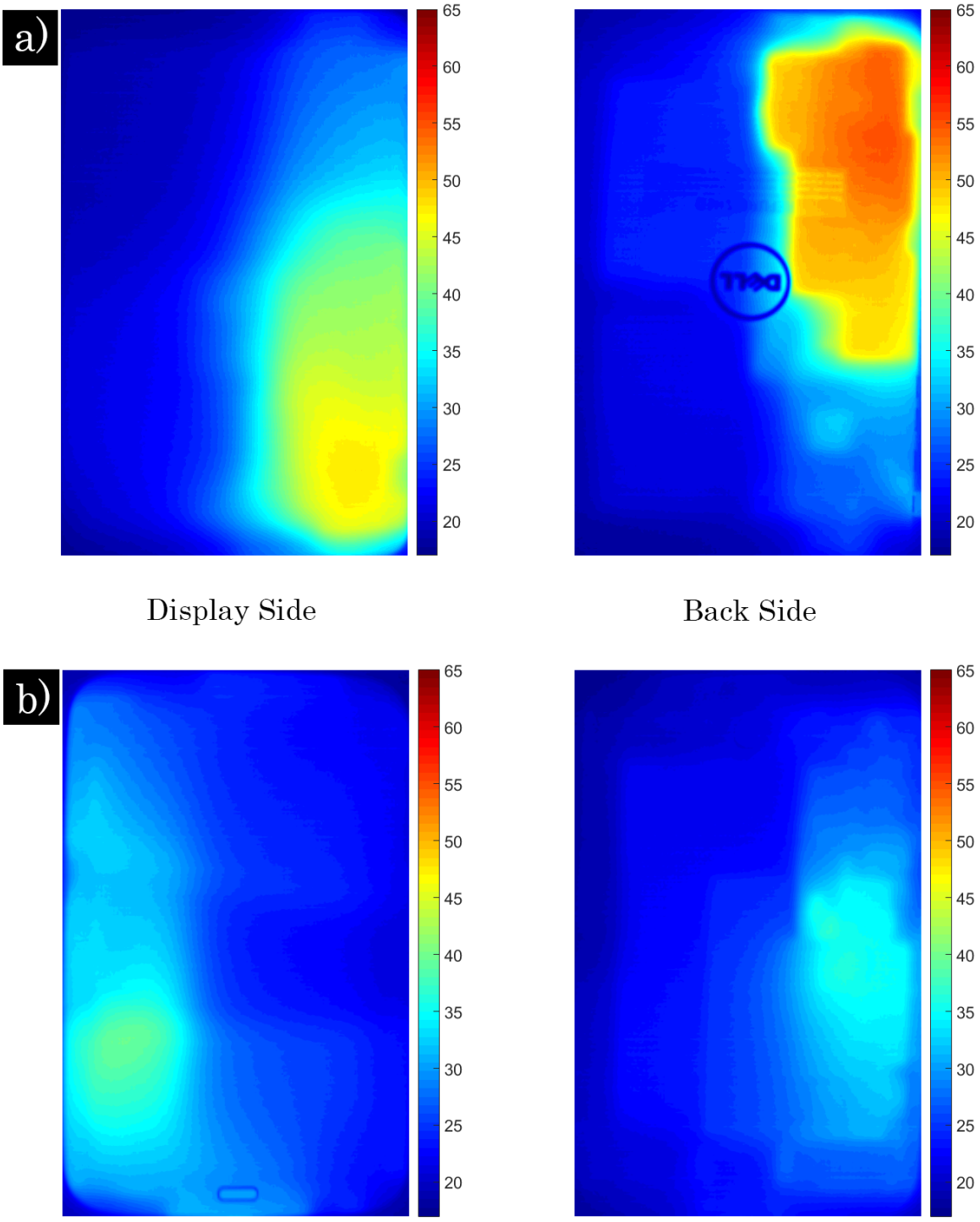

Figure 3-1 IR images showing the thermal response of the commercial tablet PCs after 60 minutes of stress tests: a) Dell Venue 8 Pro, b) Samsung Galaxy Note 8.

The sudden temperature decrease after 8 minutes on the Windows (Dell) tablet PC might have occurred due to a temperature control program called 'thermal throttling' which can be found very commonly in today's computer chips. Additional thermal analysis data with different operations and thermal response of internal components during the stress test can be found in Appendix A. Based on thermal analysis results, the Windows (Dell) tablet was set as the baseline tablet PC, as it had worse temperature response in most tests compared to the Android (Samsung) tablet PC.

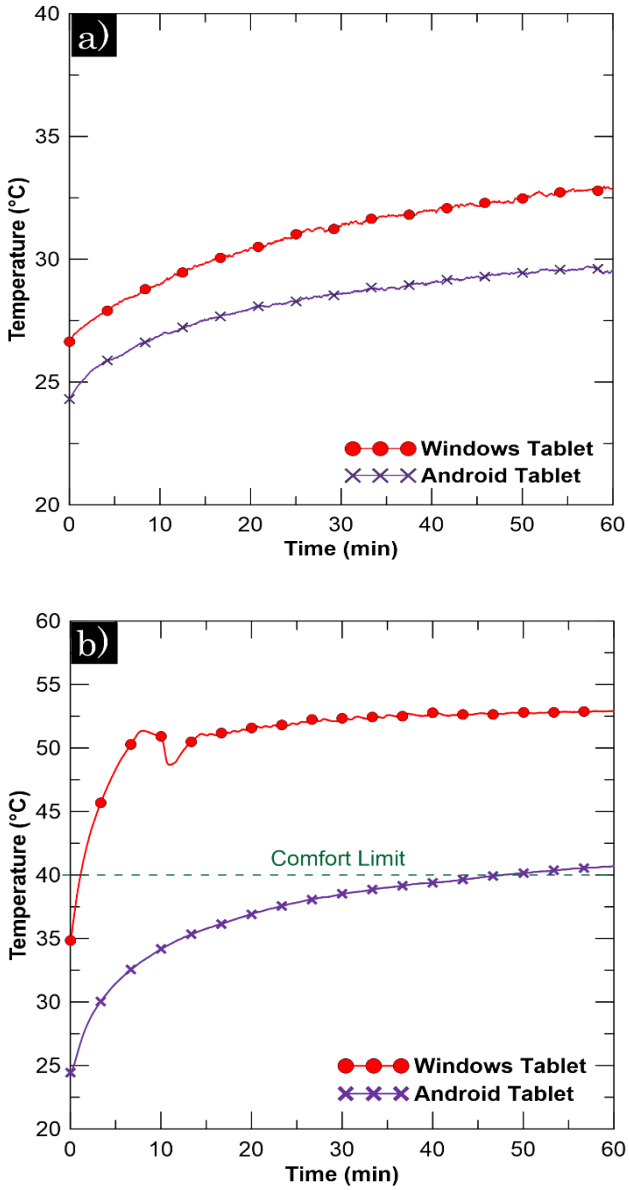

Figure 3-2 Thermal response of working tablet PCs under 60 minutes of: a) skype video calling and b) stress test.

Figure 3-3 shows the thermal response of the internal components of both tablet PCs after 60 minutes of stress test. Discrete high temperature blocks in the IR images signify that the chip was the main contributor to the heat generation in tablet PCs. During the stress test, chips on both tablet PC ran at as high as 70 °C. As very compact internal design allows negligible air gaps, conduction can be considered as the main mode of heat transfer from the chip to other internal components. As a result, development of a simplified circuit board was possible with only one heater attached on a FR4 board (with similar thermal conductivity of an original circuit board) to get a close approximation of the real case.

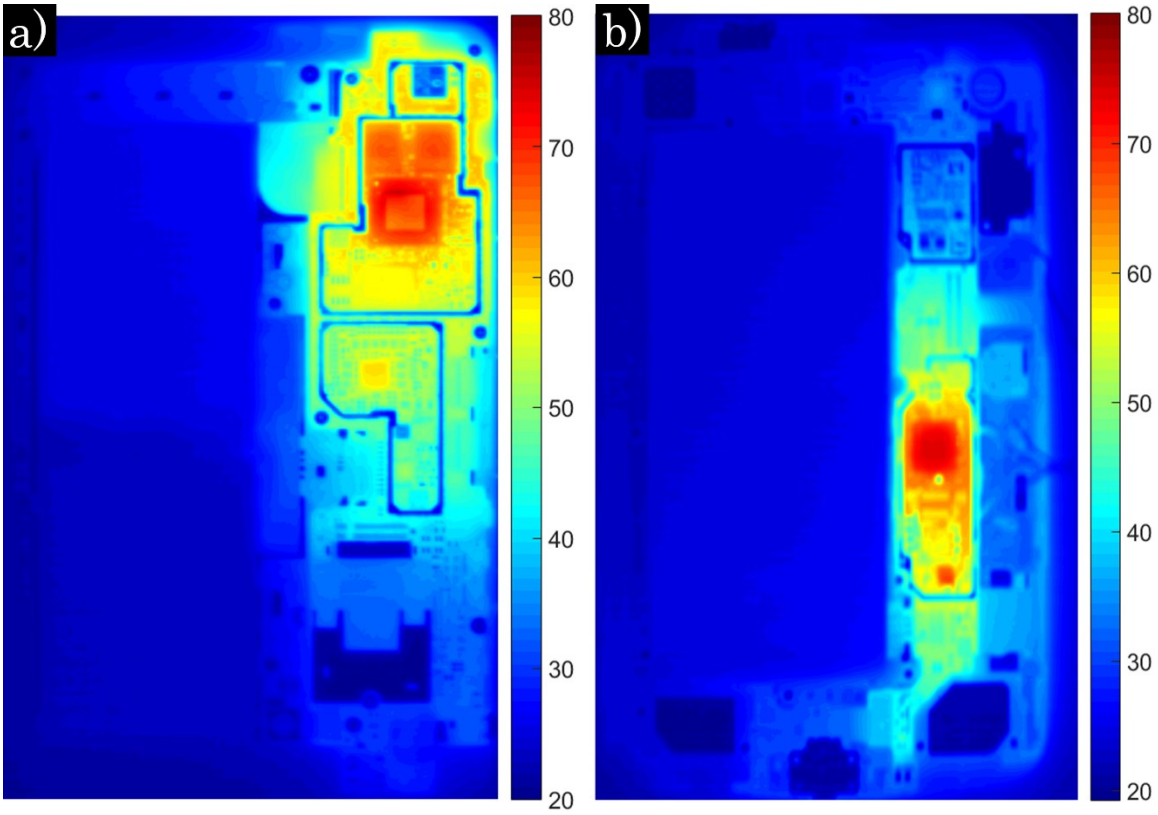

Figure 3-3 IR image of the internal components in tablet PCs after 60 minutes of stress test: a) Windows (Dell) tablet PC b) Android (Samsung) tablet PC.

To mimic heat generation from tablet PCs, it is important to know how much power is consumed during a certain operation. Power consumed during different tests are listed in Table 3-1. Observation of powers consumption is also necessary because the amount of heat generated is related to the consumption of power for a definite operation. It is evident that during the stress test, more power was consumed leading to higher heat generation.

Total power dissipations of a portable electronic device can be computed by the following formula:

$$P = \frac{V_{\text{battery}} Ah_{\text{battery}}}{t_{\text{operation}}} = \frac{\text{Battery Wattage rating (Wh)}}{t_{\text{operation}}} \quad (3.1)$$

where, $V_{battery}$ is the rated voltage of the battery, $Ah_{battery}$ is the ampere-hour rating of the battery, and $t_{operation}$ is the duration of the test.

Table 3-1 Overall power consumption of both tablet PCs for different operations.

Tablet PCs	Tests	Initial Charge (%)	Final Charge (%)	Battery Wattage Rating (Wh)	Duration of Test (hrs)	Power Consumed (W)	Back Cover Temperature after 60 minutes (°C)
Samsung Tablet	Cont. Skype Video Call	100	68	17.25	1.67	3.3	28
	Continuous stress test	78	32	17.25	1.8	4.4	41
Dell Tablet	Cont. Skype Video Call	99.5	68.8	18	1.67	3.3	33
	Continuous stress test	95	47.2	18	1.8	5.0	53

3.1 Summary

As expected, the thermal response of both tablet PCs showed that heat generation is directly related to the power consumption. The Windows (Dell) tablet was found to have worse thermal response compared to the Android (Samsung) tablet for same mode of operations. Thermal response of internal components revealed that the chip is the main heat generating component. A simplified mock circuit board is proposed to be used in the experimental setup based on the thermal analysis of internal components of the tablet PCs.

Chapter 4

Experimental Setup and Procedures

This chapter presents the detailed description of procedures and methodologies used to characterize PCMs, build the experimental setup, and conduct each experiments. It is divided into the following sub-sections: (i) selection of PCMs and experimental procedures for measuring their thermo-physical properties, (ii) details of the apparatus, hardware, and experimental procedures used to collect data, and (iii) sources of uncertainties in experimental results.

4.1 Selection and Characterization of PCMs[5]

The main selection criterion of PCMs for this study was their melting temperature. Sponagle and Groulx (2015) showed numerically that PCMs with melting temperatures of 43.3 and 55.8 °C did not completely melt under the conditions expected during the use of tablet PCs, and hence did not provide significant latent heat storage in the TES system. Better results were obtained for PCMs with melting temperature of 32 °C. Indeed, it was found that such PCMs can provide an efficient thermal management of the tablet PC by reaching a fully-melted state after 30 minutes of operation. Based on that numerical study, two PCMs were selected: *n*-eicosane and PT-37 (a commercial PCM manufactured by PureTemp) with melting temperatures of 35.6 and 36.3 °C, respectively. The physical appearance of these PCMs can be seen in Fig. 4-1. PCMs with higher melting temperatures

[5] Conducted at MAW's Lab in Dalhousie University under the supervision of Dr. Mary Anne White. This portion of work was done by Dr. Samer Kahwaji, a co-author of a paper presented at the ASME 2016 summer heat transfer conference (Ahmed *et al.*, 2016).

were selected because the average outdoor temperature during summer (May – August) in North America is 30 °C[6] which is very close to the suggested melting temperature (32 °C) of PCM used in the numerical study. As a result, PCMs with a melting temperature of 32 °C may melt early simply being exposed to the environmental temperature and thus defying the thermal management advantages of the system during the tablet PC operation.

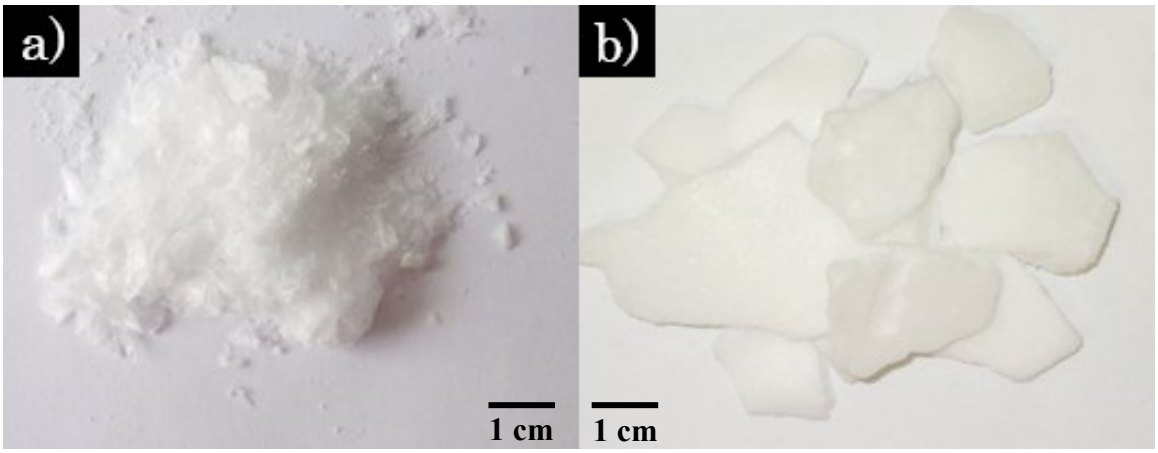

Figure 4-1 Appearance of PCMs: a) n-eicosane and b) PT-37 (used with permission from Dr. White and Dr. Kahwaji).

Typical tablet PCs have a life span of 5 years under normal handling (Taylor, 2015). As the usage load varies very widely in a tablet PC so is the amount of heat generated, PCMs may undergo several phase transition every day. As a result, to ensure long term reliability and effective performance of PCM-based thermal management systems, selected PCMs should have consistent thermo-physical properties after many phase change transition and should be chemically non-reactive to its encapsulation. Usually, 10,000 phase transition cycling test is recommended for 20 yr long system design considering only one phase transition daily (Abhat, 1983). Based on this, in the case of using PCMs in tablet PCs and portable electronic device cooling applications, a total number of 10,000 to 20,000 thermal cycles (considering 4 - 8 phase transition cycles daily) can be recommended.

Research on PT-37 and *n*-eicosane have shown that both PCMs have good chemical stability under many repeated melting-solidification cycles (Section 2.2.3). PT-37 and *n*-eicosane were found to be stable after 10,000 and 4,000 cycles of operation respectively

[6] See http://www.usclimatedata.com/ for more information.

which comply with the required long term system design. Moreover, corrosion of aluminized laminate films, the prospective encapsulation material used in the current research, was found to be negligible with these PCMs (section 2.2.4).

Selection of reasonably priced PCMs is another important factor to produce low cost PCM-based thermal management systems. The material cost depends considerably on the classification of the PCMs (*i.e.*, organic, inorganic, or biomaterial). Usually salt hydrate PCMs have 18% higher price than paraffins and fatty acids (Lane, 1980). Being by-products from oil refineries, commercial paraffins are relatively less expensive; a recent price of paraffin wax is \$0.85−\$0.91/lb (Jan Kosny, 2013). The price of paraffins and most other PCMs increases with purity. Pure paraffin wax (>99%) has a higher price tag than technical grade paraffins (90% - 95%) (James C. Mulligan, 2002). For instance, the cost of *n*-eicosane used in the current study is \$200/lb for a laboratory grade sample with 99% purity[7]. However, the price of technical grade *n*-eicosane can be as low as \$4.3/lb (Jan Kosny, 2013). The price of PCMs can be further reduced if they are ordered in bulk amount (*i.e.* 1000 lbs or more) for mass production of PCM-based thermal management systems. Current *n*-eicosane price drops by 41.4% if ordered by 100 g basis instead of 25 g basis[7]. Similarly, the recommended selling price of PT-37 is \$20/lb for samples which reduces to \$5/lb if more than 1000 lbs is ordered. These price ranges of PCMs can be considered competitive enough for commercial manufacturing of PCM-based TES units for thermal management of tablet PCs.

The characterization study of *n*-eicosane and PT-37 in MAW's lab at Dalhousie University[8] determined the latent heat of fusion ($\Delta_{fus}H$), specific heat (C_p) of both solid and liquid phase, onset of the melting temperature (T_{onset}), and thermal conductivity of the solid phase (k_s). $\Delta_{fus}H$ and T_{onset} of *n*-eicosane and PT-37 were measured using a DSC - TA Instruments Q200. All measurements were performed in a He gas atmosphere, with a He flow rate of 25 mL/min. The heating and cooling rates were 10 K/min for $\Delta_{fus}H$ determination and 2 K/min for T_{onset}, as recommended by Johnson and White (2014) for accurate ΔH and temperature measurements. The uncertainty of this DSC system is

[7] See https://www.alfa.com/en/catalog/A13853/ for more information.
[8] Conducted by Dr. Samer Kahwaji from Chemistry Department at Dalhousie University.

typically of ±10% and ±1.5 °C for $\Delta_{fus}H$ and T_{onset} respectively. The latent heat of fusion, $\Delta_{fus}H$ and the melting temperature, T_{onset} were determined from the DSC thermograms shown in Fig. 4-2 and the resulting values are presented in Table 4-1.

The DSC was also used to measure the heat capacities of the solid ($C_{p,s}$) and liquid ($C_{p,l}$) phases of each PCM. The measurements followed the procedures described in the standard test method, ASTM E1269-11 (2011), using a high-purity sapphire as a reference sample. The overall uncertainty in the heat capacity using this DSC technique was less than 10%, as determined from measurements of other reference materials with known C_p. The temperature-dependent heat capacities, $C_p(T)$, for both PCMs are shown in Fig. 4-3 and their corresponding values at 50 °Care presented in Table 4-1.

Table 4-1 Measured properties of *n*-eicosane and PT-37 (Ahmed *et al.*, 2016).

Properties	*n*-eicosane	PT-37
$\Delta_{fus}H$	239 ± 24 J/g	206 ± 21 J/g
T_{mpt}	35.6 ± 1.5 °C	36.4 ± 1.5 °C
$C_{p,s}$	1.8 ± 0.2 J/g K for T = 20 °C	1.8 ± 0.2 J/g K for T = 20 °C
$C_{p,l}$	2.3 ± 0.2 J/g K for T = 50 °C	2.1 ± 0.2 J/g K for T = 50 °C
k_s	0.46 ± 0.05 W/m K for T = -21 to 29 °C	0.28 ± 0.03 W/m K for T = -21 to 29 °C
ρ	0.79 gm/ml	0.84 gm/ml

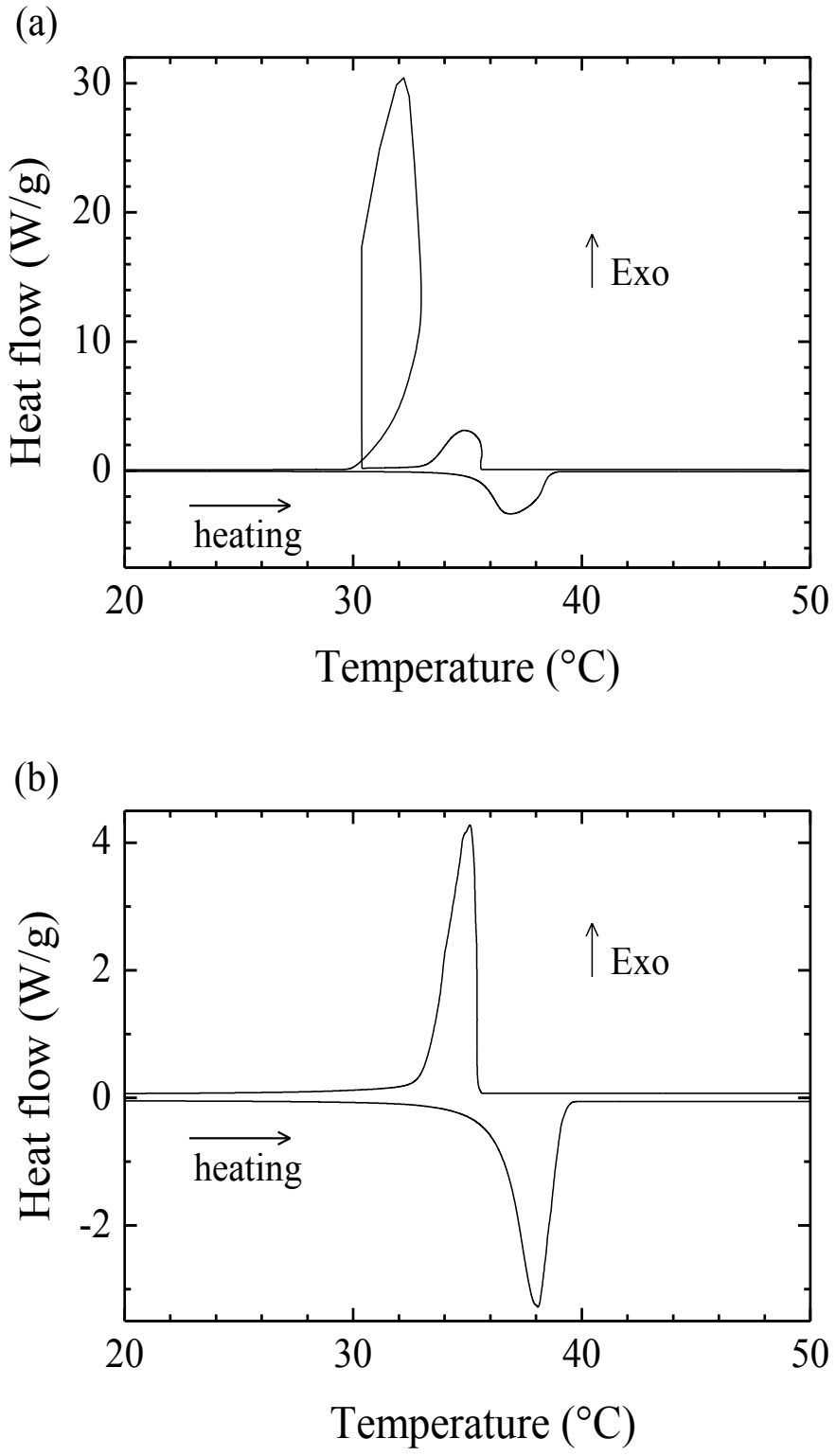

Figure 4-2 DSC thermograms of a) *n*-eicosane and b) PT-37. The loop on cooling for *n*-eicosane is characteristic of a supercooled PCM (Aubuchon, 2007; Ahmed *et al.*, 2016).

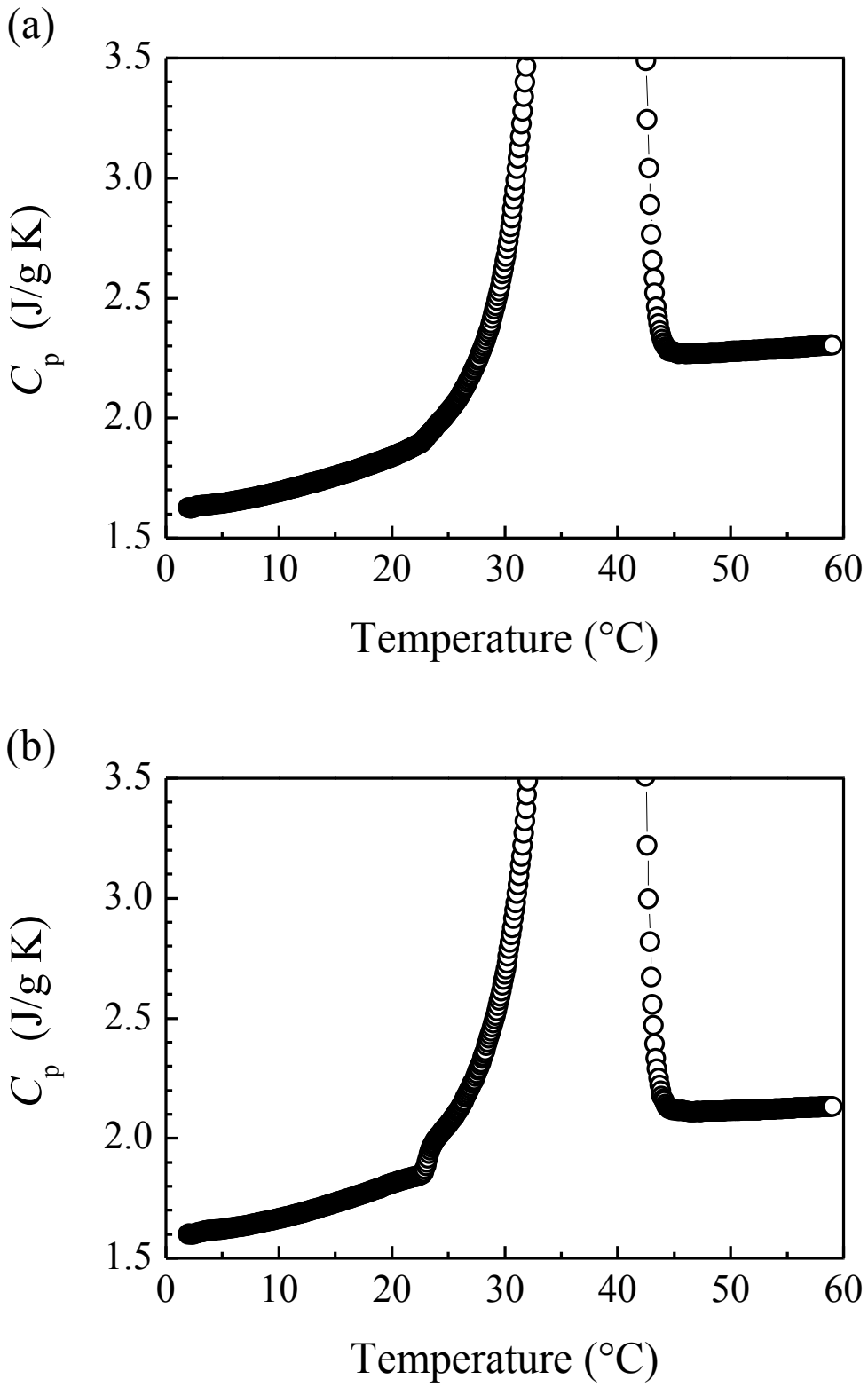

Figure 4-3 $C_p(T)$ measured by DSC: a) *n*-eicosane and b) PT-37. Both $C_p(T)$ curves show singularities in the solid-liquid transition regions (Ahmed *et al.*, 2016).

The thermal conductivities k_s, of solid samples of *n*-eicosane and PT-37 were measured in a high vacuum using a Quantum Design Physical Property Measurement System (PPMS), as shown in Fig. 4-4a. Each PCM sample was pressed into a pellet of approximately 5 mm diameter (Fig. 4-4b) and mounted on the thermal transport platform of the PPMS using gold-plated copper leads and a thin layer of high thermal conductivity epoxy. The thermal conductivity was measured via steady-state measurement (Johnson and White, 2014) as a function of temperature and the obtained results are shown in Fig. 4-5. Within the temperature range of -21 to 29 °C, the average values of k_s for *n*-eicosane and PT-37 are 0.46 ± 0.05 W/m·K, and 0.28 ± 0.03 W/m·K, respectively. A maximum uncertainty of 10% was estimated for the measurements of k_s, including uncertainty from the determination of the pellet dimensions.

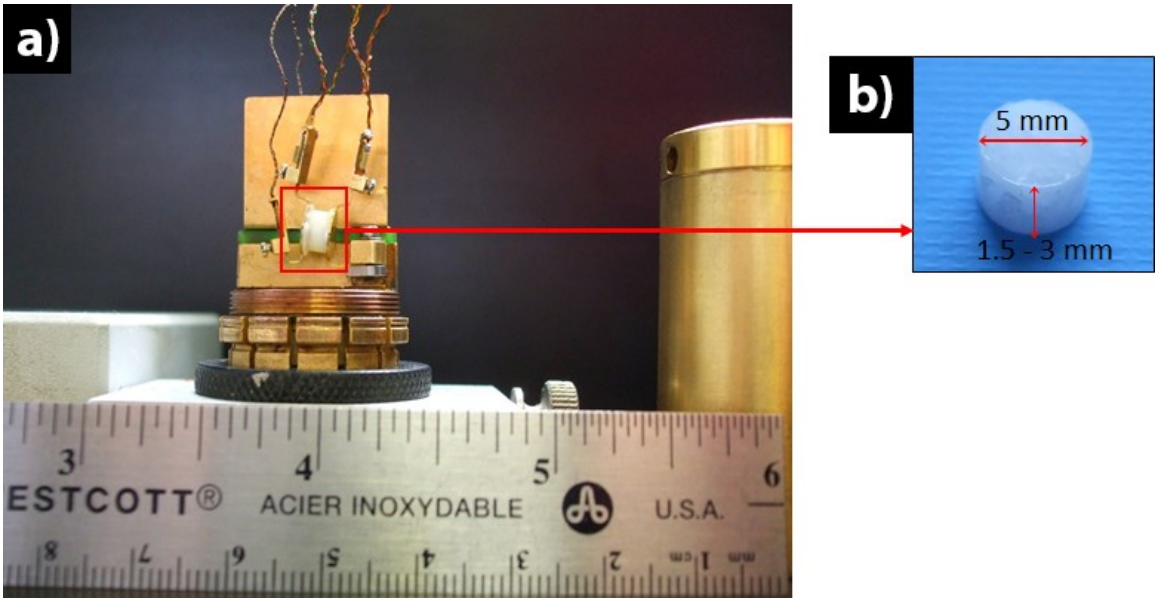

Figure 4-4 Photo of the apparatus used to measure the thermal conductivity (k_s) of PCMs: a) PPMS thermal transport platform b) Pellet sample (used with permission from Dr. White and Dr. Kahwaji).

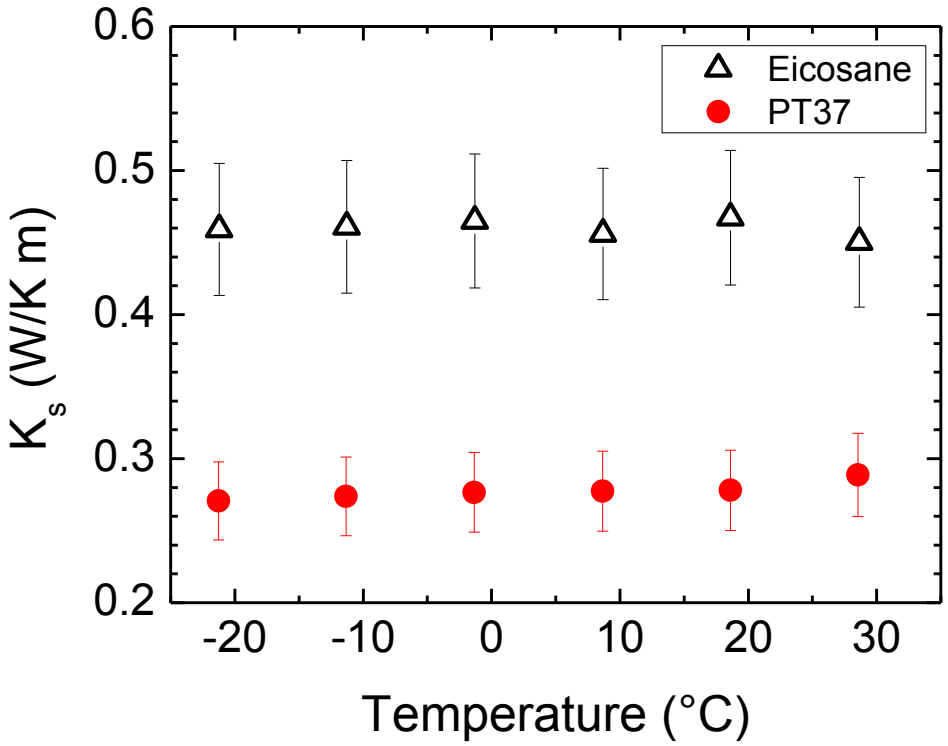

Figure 4-5 Thermal conductivities, $k_s(T)$ of solid samples of *n*-eicosane and PT-37 measured with the PPMS (used with permission from Dr. White and Dr. Kahwaji).

4.2 Description of the Experimental Setup

Details of the experimental setup and apparatus used for data collection are discussed in this section. The description of different parts of the setup are presented first, afterwards, equipment used in the data acquisition system are introduced with few notable points on data processing procedures.

4.2.1 Test Stand

The test stand, can be seen in Fig. 4-6, was built to isolate the experimental tablet PC from potential external thermal interference by minimizing physical contacts. The test stand holds the experimental tablet PC using four 3D printed clamps and provides the provision to rotate the experimental tablet PC at any angle, both in the clockwise and anti-clockwise directions. The 3D printed clamps provide low contact (provides line contact between the tablet PC surface and the clamp) with the experimental tablet PC and facilitate holding a

tablet PC with thickness up to 14 mm. The test stand also features a thermal camera holder which is housed in a rack and pinion system so that it can slide upward and downward to get an appropriate focus on the test tablet PC. Moreover, a spirit level is attached to one end of the frame to indicate the angle of inclination. The whole test stand was built from 2″ wide high density polyethylene (HDPE) bar. The HDPE material provides light weight, good machinability, and structural strength along with a certain level of flexibility. The overall height of the test stand is 26.5″ from the base to the top of the IR camera carriage. The distance from one leg to another is 20″. The test stand can hold a tablet PC having width up to 10″ and length up to 13″. Detailed technical drawings of the test stand and its constituent parts can be found in Appendix B.

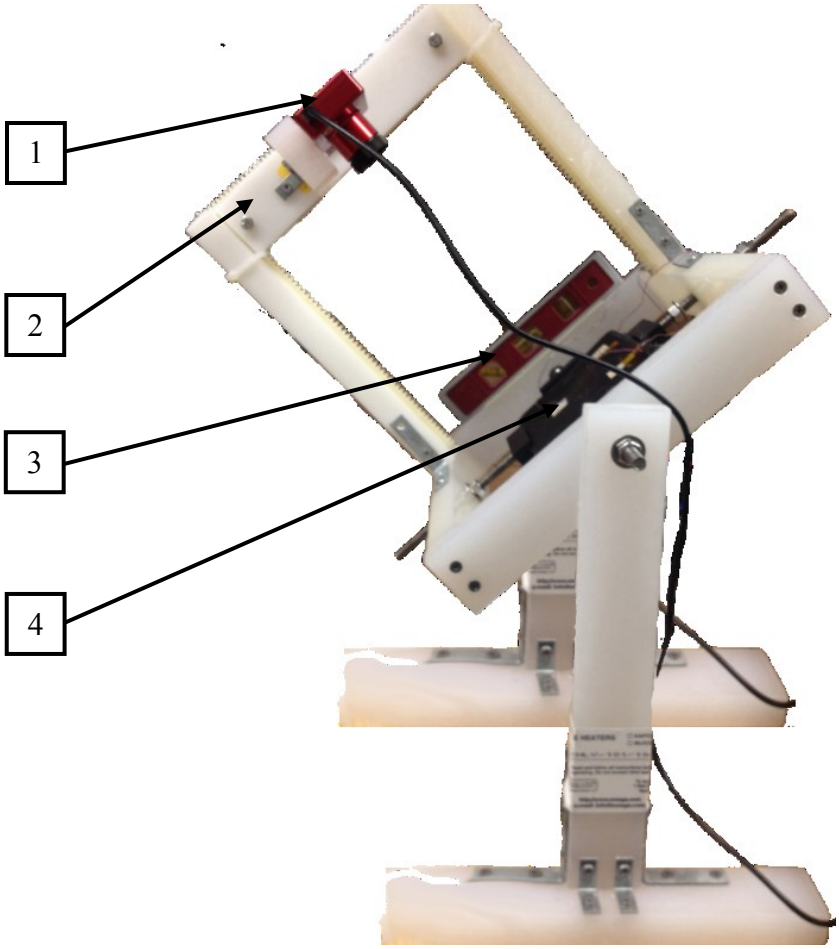

1 - IR camera
2 - Camera carriage
3 - Spirit level
4 - Experimental tablet PC

Figure 4-6 Photograph of the test stand holding the experimental tablet PC and the IR camera inclined at a certain angle.

4.2.2 Experimental Tablet PC

The experimental tablet PC (8.5″×5.1″×0.4″, 216 mm × 116 mm × 9 mm) (Fig. 4-7) was used to assess the effects of integrating PCM-based TES units into a system comparable to a real-life tablet PC. It consists of the original Windows tablet PC (Dell Venue 8 Pro) parts as a substrate. These parts were used to ensure the right physical properties and dimensions of a commercial tablet PC into the experiments. The Windows tablet PC was selected for this experiment based on the results obtained from the stress test showing that the Windows tablet PC performed poorly in terms of thermal performance as illustrated in Fig. 3-2b.

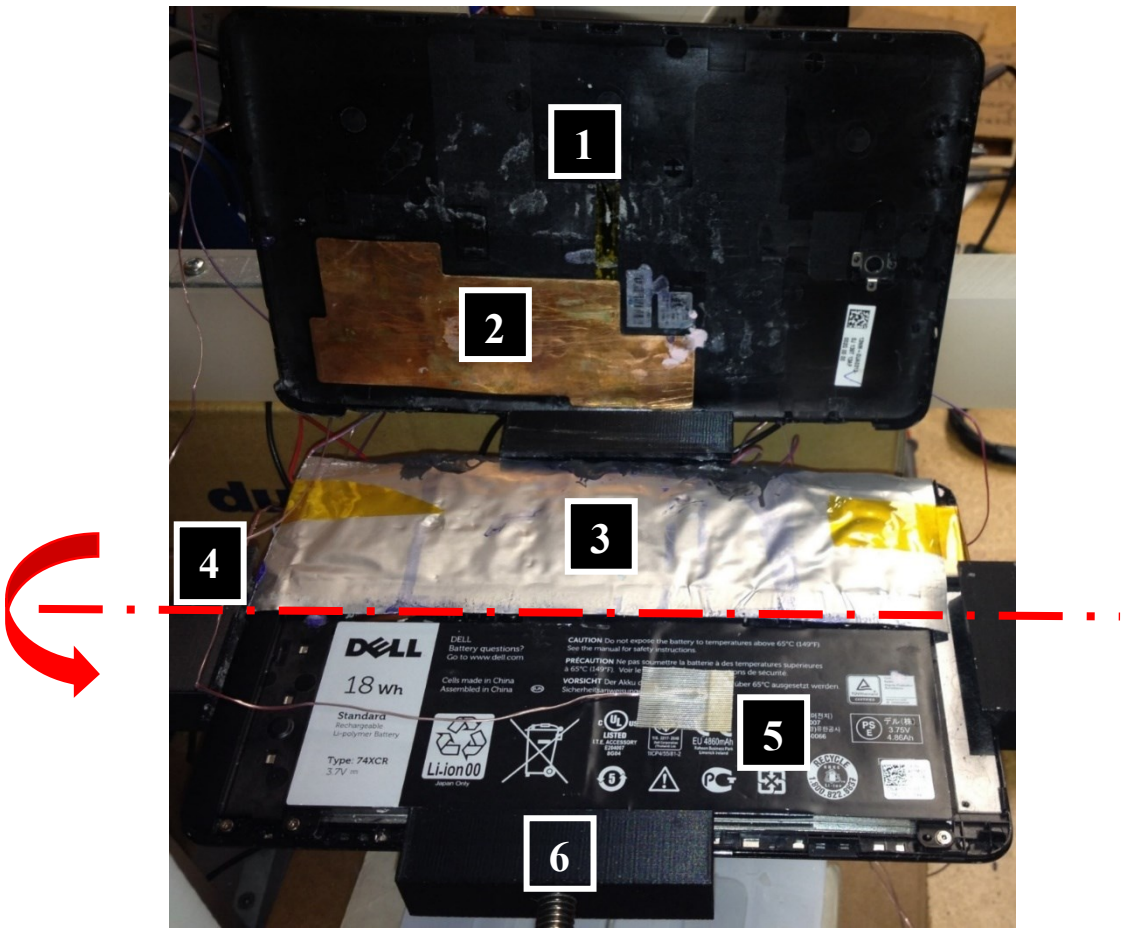

1 – Back Cover
2 – Copper heat spreader
3 – PCM TES Unit (Size 2)
4 – Axis of rotation
5 – Type – T thermocouple
6 – 3D printed clamp

Figure 4-7 Photograph of the experimental tablet PC with PCM encapsulation.

The most important part of the experimental tablet PC was the mock printed circuit board (PCB). It was made from FR4 copper clad board (Fig. 4-8b), which has similar thermal conductivity as regular circuit boards (through plane 0.343 W/m·K and in plane 1.059 W/m·K (Sarvar *et al.*, 1990). The heat dissipation from the tablet's electronics was applied using a 1″× 1″ (25.4 × 25.4 mm^2) Kapton heater (manufactured by Omega, KHLV-101/10) with a rated power density of 10 W/in^2 at 28 VAC. The placement of the heater can be seen from Fig. 4-8b which was based on the IR image of internal components showed in Fig. 4-8a. Input heat fluxes were calculated by the following formula:

$$q'' = \frac{PV^2}{V_R^2} \tag{4.1}$$

where, q'' is the heat flux, P is the rated power density of the heater, V is the voltage supplied to the heater, and V_R is the rated voltage of the heater.

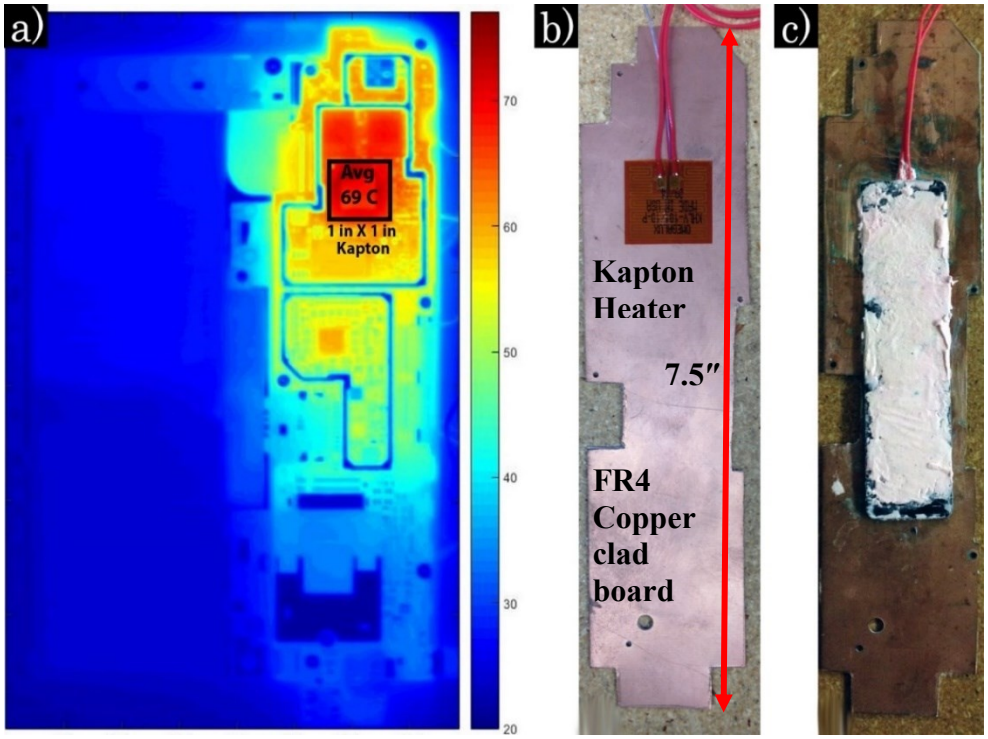

Figure 4-8 a) IR Temperature contour of the internal components of the working Dell tablet PC, b) Placement of the heater on the FR4 board, c) Heater and heat spreader assembled on the PCB.

As can be seen from Fig. 4-9, the experimental tablet PC with mock PCB provided a thermal response which is very close to the actual Windows tablet PC. The thermal behaviour of the tablet PC under different usage load was obtained by different power input from an analog variac (Fig. 4-10).

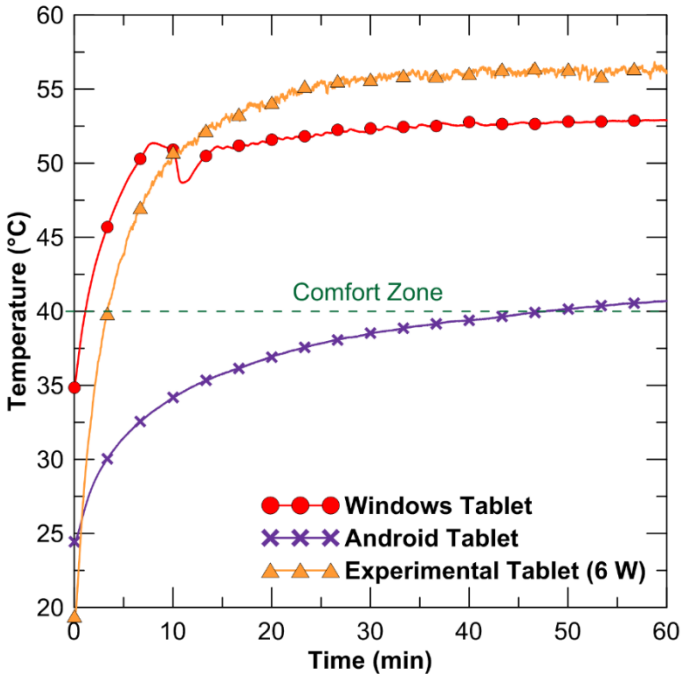

Figure 4-9 Comparison of the thermal response of the experimental tablet PC at 6 W power input with Windows (Dell) and Android (Samsung) tablets.

Figure 4-10 An analog variac to provide different voltages to the heater.

Table 4-2 Suggested voltage supply from the variac for required power input.

Power Input	Required Voltage Supply
2 W	12.5 V
4 W	17.7 V
6 W	21.7 V
8 W	25 V

A heat spreader was attached to the heater to reproduce the heat spreading behaviour obtained with the original device (see Fig. 4-8a) and to spread heat to the PCM-based TES unit efficiently. A thermal paste (Parker Chomerics, T670 Thermal grease) with a thermal conductivity of 3.0 W/m·K was also used on both sides of the heat spreader to eliminate air gaps and reduce contact resistances. The whole assembly made of different components constituting the mock PCB can be seen from Fig. 4-11. Nine Type T thermocouples were used in the mock tablet PC to observe heat spreading on the front surface, back cover, and internal components. The locations of these thermocouples in the mock tablet PC are shown in Fig. 4-12.

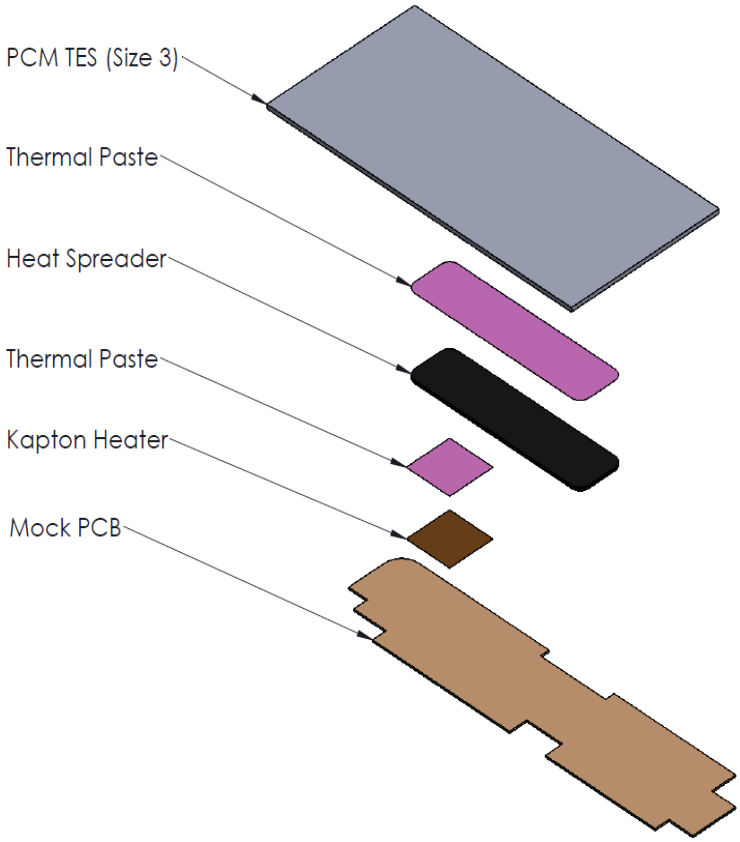

Figure 4-11 Components of the mock PCB in an exploded view.

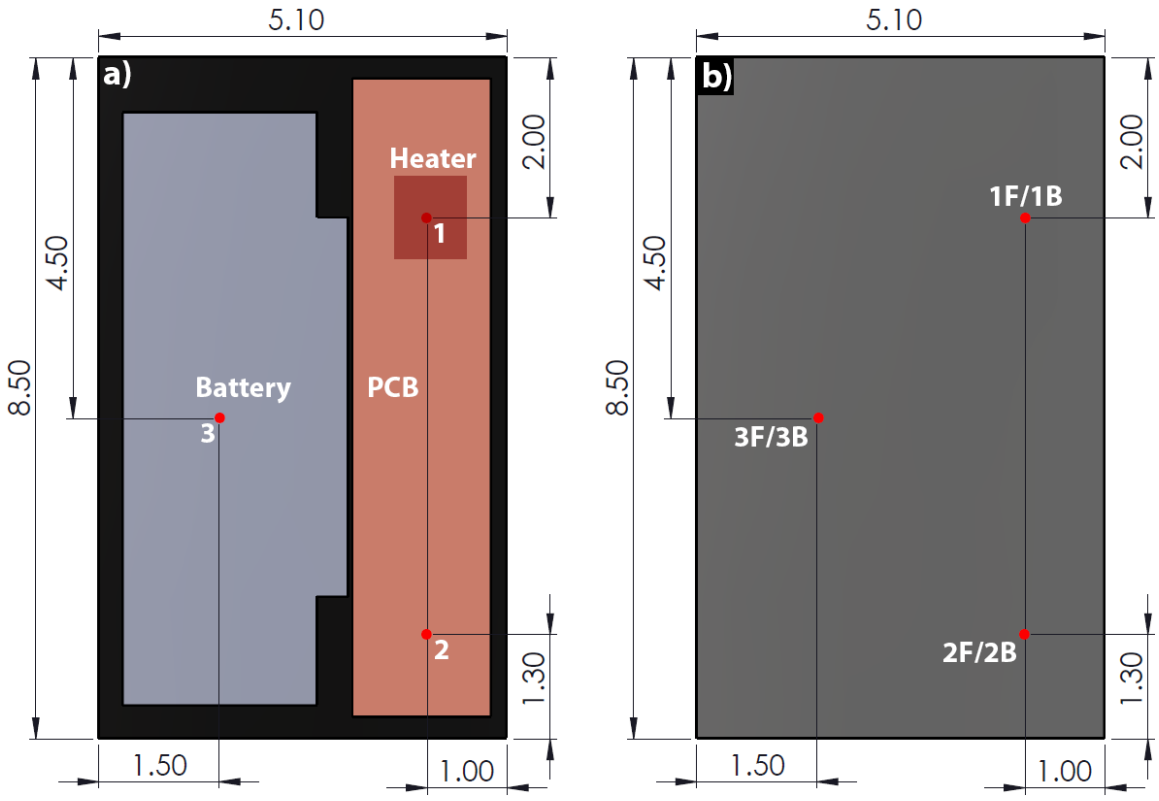

Figure 4-12 Position of the thermocouples (dimensions are in inches) a) attached to internal components and b) attached to the front and back surfaces (F – Front, B – Back).

4.2.3 Thermal Imaging Camera

Two-dimensional temperature contour plots are widely used to present overall thermal profiles of any surfaces under study. Creating a complete contour plot using discrete temperature sensors (*i.e.* thermocouples) is difficult (requires temperature reading at numerous points on the surface) and erroneous due to certain level of interpolation involved. Therefore, an ICI 7320 USB Infrared (IR) camera (Fig. 4-13) was used to capture bulk surface temperature contour of tablet PCs and PCM encapsulations. This types camera forms the image using infrared radiation from the device. The IR camera was factory calibrated and had an accuracy level of ± 2 °C. This accuracy can vary with the emissivity of surface materials. For reflective surfaces, the emissivity level was adjusted by calibrating with Type-T thermocouples, where thermocouple temperature was considered as the standard. In some experiments, a temperature difference between the

thermocouple and the IR camera readings of up to ± 3 °C were observed, can be seen from Fig. 4-14. This might occur due to slight reflection from external light sources (*i.e.* windows and neighboring rooms) interfering with the IR measurement. Image Touch-up feature was frequently used as suggested by the manufacturer, which is a non-uniformity correction (NUC) operation. NUC averages the color scheme over the whole image frame to remove stripes (can be seen in Figs. 4-15a and 4-15b) that happen due to lens reflection (Haghighi, 2012).

Figure 4-13 Thermal imaging camera (ICI 7320) used to capture infrared images (from: www.infraredcamerasinc.com).

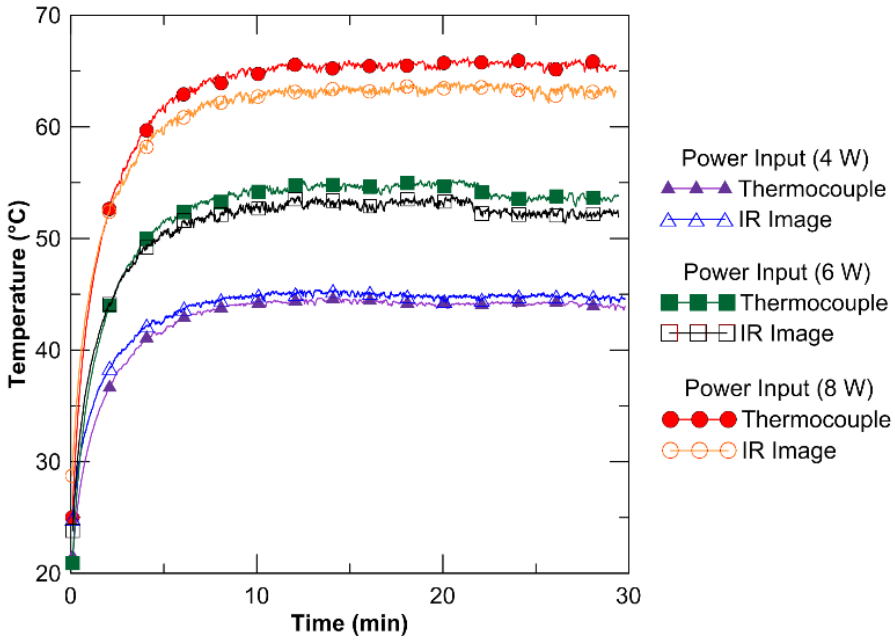

Figure 4-14 Comparison between temperatures of the back cover obtained from IR camera and thermocouple for different heat input levels.

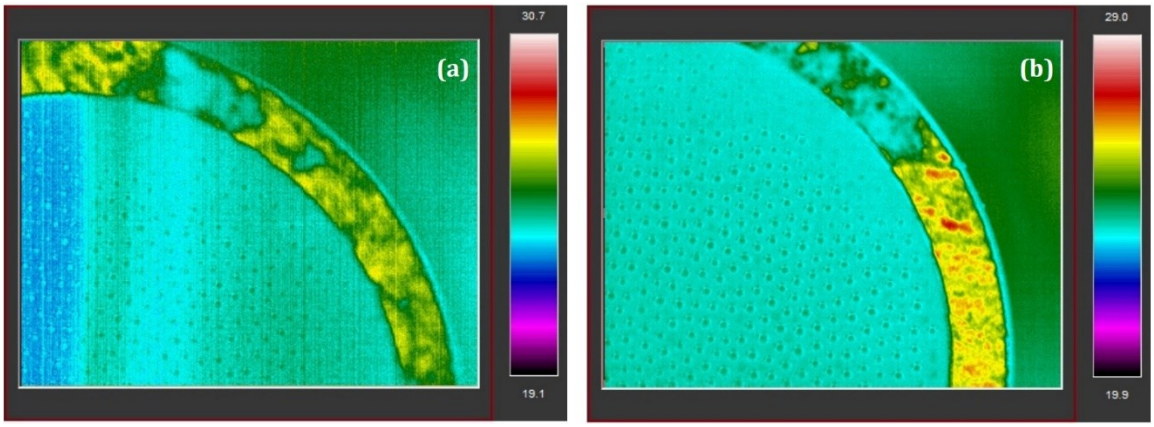

Figure 4-15 The effect of NUC (bottom) (Haghighi, 2012): a) before touch-up b) after touch-up.

4.2.4 Encapsulations

Three encapsulations with different base area for both *n*-eicosane and PT-37 were used: Size 1 had 6″ × 2.6″ (152.4 × 66 mm^2), Size 2 had 7″ × 1.5″ (177.8 × 38 mm^2), and Size 3 had 7″ × 3.4″ (177.8 × 86 mm^2) base areas. Figure 4-16 shows pictures of the encapsulations. The average thickness of all encapsulations was 1/16″ (2 mm). However, due to flexible encapsulation material, the thickness of the encapsulations was not uniform throughout. It varied from a minimum of 1.7 mm to a maximum of 2.2 mm throughout the surface of the encapsulation. Size 1, 2, and 3 encapsulations held 16 g, 11 g, and 25 g of PCM respectively. Encapsulations were shaped by pressing laminate film into HDPE molds, made by a CNC milling machine shown in Fig. 4-17. First a sheet of laminate film was pressed into the mold to get the proper shape. Then another sheet of laminate film was heat sealed with the shaped laminate film on three sides. After that melted PCM was poured into the encapsulation and the open side was heat sealed. Four T Type thermocouples were inserted into size 1 and size 2 encapsulations to observe the thermal behaviour of the PCMs during experiments. Thermocouple insert points were leak-proofed with PVC cement. Even sealing with PVC cement, slight leakage was observed after doing several experiments with same encapsulations. Hence, no thermocouples were inserted into the size 3 encapsulation because it was necessary to observe the leak prevention effectiveness of heat sealed edges. The approximate positions of each thermocouple along with

encapsulation dimensions are shown in Fig. 4-18. Thermocouples were secured into place by using small pieces of Kapton tapes (Fig. 4-19).

Figure 4-16 Actual photographs of PCM encapsulations: size 1 (Left), size 2 (middle), size 3 (right).

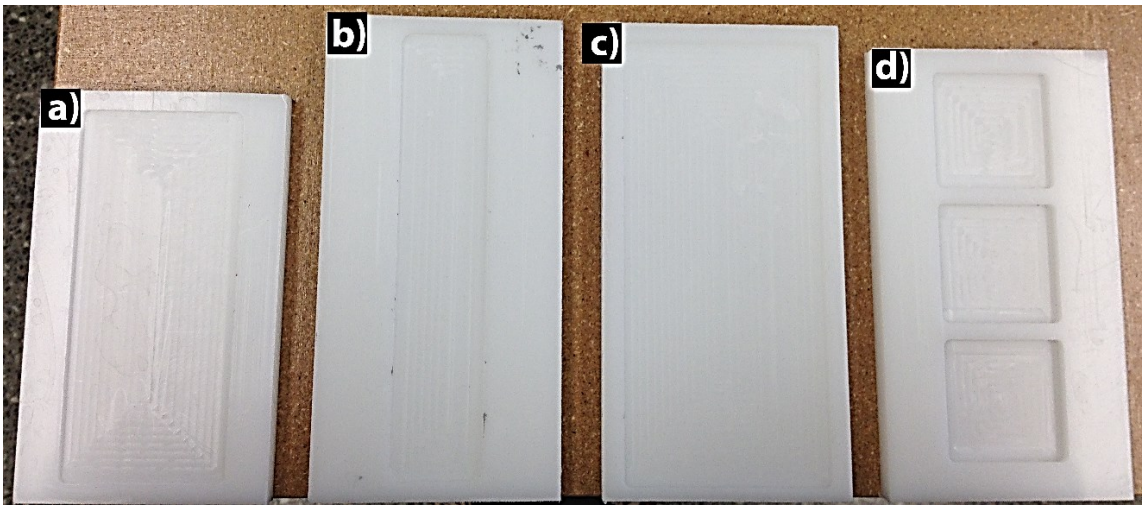

Figure 4-17 Molds used to prepare different encapsulations; a) Size 1 b) Size 2 c) Size 3 d) 2″ × 2″ base area with different thicknesses.

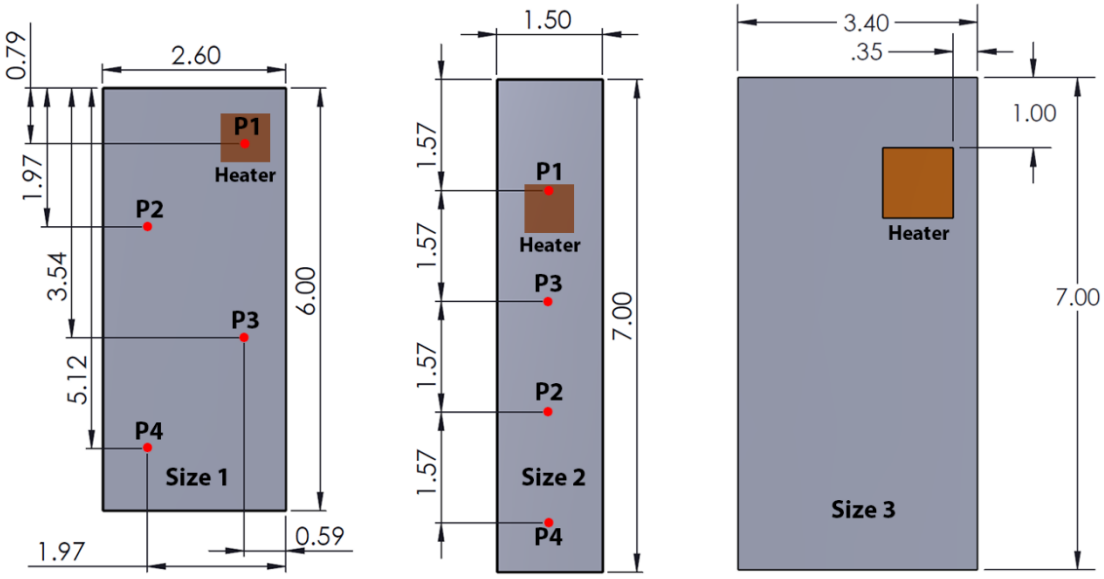

Figure 4-18 Schematics of three encapsulations showing their dimensions and approximate positions of thermocouples and the heater (dimensions are in inches).

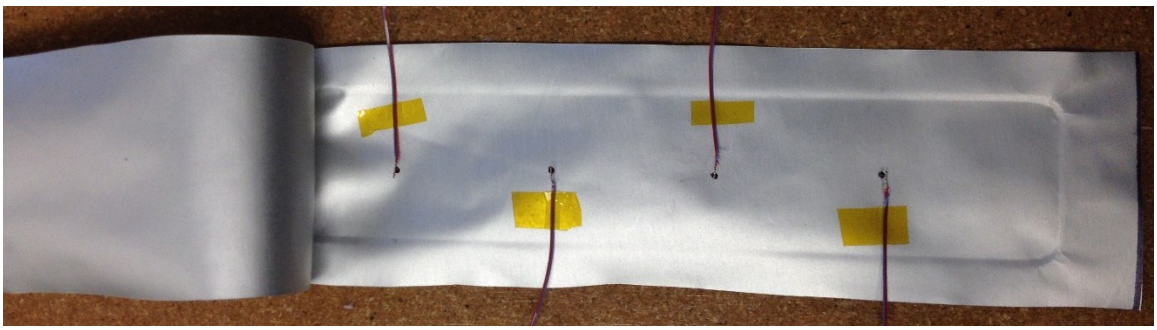

Figure 4-19 Placement of thermocouples using Kapton tapes inside PCM-based TES units (Size 2).

In our preliminary experiments PCM melting in the first three sizes of PCM TES units was partial. As a result, it was hard to determine the real amount of latent heat used in those. Therefore, to clearly observe the effect of varying latent heat, three additional smaller encapsulations for each PCM were used right on the top of the heat source where complete PCM melting is expected. These encapsulations have the same base area (2″ × 2″, 51 × 51 mm^2) but different thicknesses: 0.13″ (3 mm, 6 g PCM), 0.16″ (4 mm, 8 g PCM), 0.20″ (5 mm, 10 g PCM), as shown in Fig. 4-20. The summary of the dimensions of all encapsulations used in this study can be found in Table 4-3.

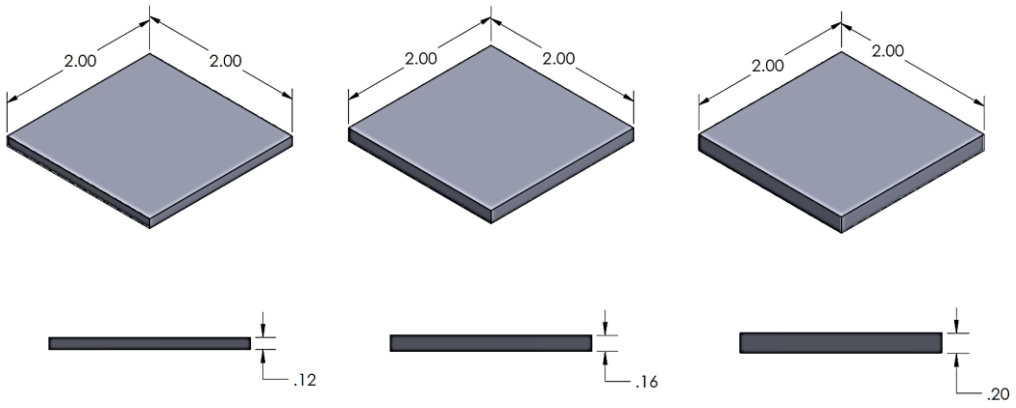

Figure 4-20 Encapsulations having the same base area but different thicknesses (dimensions are in inches).

Table 4-3 Summary of dimensional attributes of encapsulations, amount of PCMs, and latent heat used.

Encapsulation	Base area	Average thickness	Amount of PCM	Total latent heat (kJ)	
				n-eicosane	PT-37
Size 1	6″ × 2.6″ (152.4 × 66 mm^2)	1/16″ (2 mm)	16 g	3.82	3.25
Size 2	7″ × 1.5″ (177.8 × 38 mm^2)	1/16″ (2 mm)	11 g	2.63	2.27
Size 3	7″ × 3.4″ (177.8 × 86 mm^2)	1/16″ (2 mm)	25 g	6.00	5.15
6g	2″ × 2″ (51 × 51 mm^2)	0.13″ (3 mm)	6 g	1.43	1.24
8g	2″ × 2″ (51 × 51 mm^2)	0.16″ (4 mm)	8 g	1.91	1.65
10g	2″ × 2″ (51 × 51 mm^2)	0.20″ (5 mm)	10 g	2.39	2.06

4.2.5 Data Acquisition and Processing

Continuous data collection was accomplished at 1 Hz frequency through the use of a National Instruments' (NI) CompactDAQ-9174 (cDAQ), a 4-Slot USB chassis which can house four NI modules at a time, and a NI 9213, sixteen-port thermocouple module interfaced with LabVIEW 2013. NI 9481, A 60 VDC/250Vrms, 4 channel SPST relay module, was programmed in LabVIEW to turn the heater on and off as per requirement of the experiments. Figure 4-21 shows how all components of the data-acquisition system were connected with each other.

Type - T thermocouples with self-adhesive backing was used as temperature sensor in the current study (SA1-T Omega thermocouples). These thermocouples have ±0.5 °C accuracy and operating temperature range of -60 °C to 175 °C. The adhesive pad is made of polymide film with a silicone pressure sensitive adhesive (PSA).

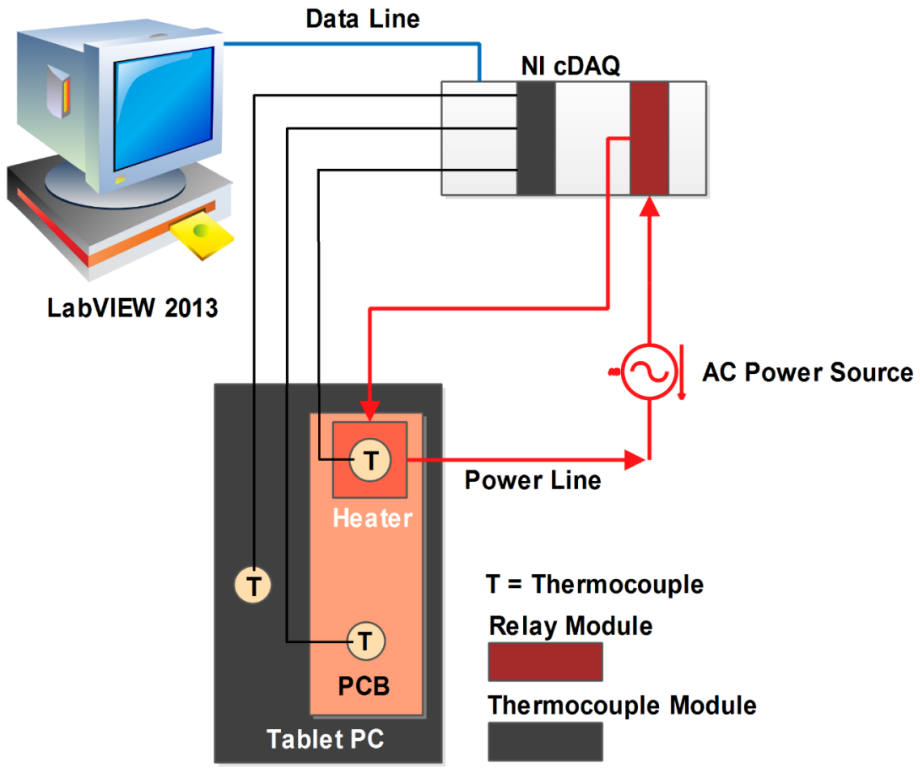

Figure 4-21 Schematic showing the network of electronic components for digital data acquisition.

Digital images from the IR camera were captured by IR Flash software, which was provided by ICI, the manufacturer of the IR camera. This software facilitates capturing fully radiometric images, thus storing temperature information of those images pixel by pixel in a 2D array. Temperature data were then exported as a CVS file and later opened in MATLAB to create a contour plot using the following code:

```
temp_complete_data = csvread('file_name.csv'); % reads the whole CSV
temperature data file

row = 1255;         % Specify tablet PC dimension in pixels
column = 787;

temp_tablet_data = zeros(row,column);

for i = 1:row
        for j = 1:column
            temp_tablet_data(i,j) = temp_complete_data(i, 32+j);
        end
end

[xq,yq] = meshgrid(0:1:column-1, row-1:-1:0);
contourf(xq, yq, temp_tablet_data, 500, 'LineColor', 'none')
colorbar
```

4.3 Experimental Procedure

In carrying out the experiments, the turning on-off of the heater was controlled by a NI really module which was connected in series between the variac and the heater. The variac was set to supply a certain AC voltage in order to generate the required heat which was calculated using Eq. (4.1). The LabVIEW program has a timer to turn on and off the relay module thus turning on and off the heater as per requirement of both continuous and intermittent operations. The LabVIEW program was also configured to save all thermocouple data at 1 Hz frequency. During each experiment the PCM TES unit was placed on the PCB and the back cover was attached, then the experimental tablet PC was placed on the test stand using 3D printed clamps. The software to record IR images was configured to save images at a frequency of 3 images/minute for 90 minutes in total. In the beginning of each experiment, NUC operation of the IR camera was done to avoid non-uniformity in the IR image data. After that, the frame of the test stand was inclined at a certain angle as per the experiment's requirements. Cardboard shades were used all around the setup to avoid any unwanted light coming towards the tablet PC to avoid reflections from the back cover. Summaries of all experiments can be found in Table 5-1 and Table 6-1 for continuous and intermittent operations respectively.

4.4 Sources of Uncertainties

As all physical measurements carry uncertainties to some degree, it is necessary to examine uncertainties to draw meaningful observations from experiments and to help explain any probable reason behind abnormal results. The source of uncertainty associated with the various measuring device used in the experiments are discussed below.

The scale (Cole Parmer Symmetry CS counting scale EW-10000-61) that was used to measure the weight of the PCMs had an accuracy of ± 0.1g. However, this uncertainty is negligible and did not result in any noticeable deviations in the thermal response of the tablet PC. The uncertainties imposed by Omega type-T thermocouples during temperature measurement was ± 0.5 °C. The uncertainties of power measurement were up to ±8% due to the inconsistent voltage supply which had an uncertainty up to ± 4%. Uncertainties in

the supplied power were calculated using Eq. (4-1). Maximum uncertainties in the supplied power and supplied voltage for different power input levels can be seen in Table 4-4. The inconsistency in voltage supply mainly occurred due to the voltage drop of the variac caused by other lab equipment, which were using the same power line. As high as 2 V drop caused by certain lab equipment. Though 2 V seems small, this slight fluctuation of the supplied voltage can result in a significant deviation of the transient temperature response, as the heater had an operating range of only 0 – 28 VAC. As high as 15 °C deviation was found after observing the thermal response curves and measuring the voltage of corresponding tests. However, that was an extreme case which was avoided by unplugging equipment having high wattage from the power line.

Table 4-4 Uncertainties in supplied voltage and supplied power.

Power Input	Maximum uncertainty in the supplied voltage	Maximum uncertainty in the supplied power
2 W	± 4%	± 8%
4 W	± 2.8%	± 5.75%
6 W	± 2.3%	± 5%
8 W	± 2%	± 3.75%

Figure 4-22 shows that there is a shift of the melted PCM and its accumulation away from the heater at lower section of the encapsulation at 90° inclination (marked with dashed rectangular box in Fig. 4-22). The high temperature zones marked with dashed lines shows the location of PCM after 60 minutes of charging. Compared to 0° inclination the location of the PCM is shifted slightly down in the 90° inclination. This phenomenon mainly occurred due to gravity at inclined position (90° and 45°) and a result of the use of flexible encapsulation material in the TES unit. However, in few cases, the same occurrence happened even at horizontal position (inclination 0°) due to the clamping pressure of the experimental tablet PC's back cover which pushed melted PCM away from the heater. Accordingly, the distribution of PCM all over the TES unit became uneven and the amount of PCM on the top of the heater was reduced after several consecutive experiments. This, in turns, resulted in a slight variation in transient response curves of the experimental tablet PC and melting curves of PCMs. To eliminate this problem, TES units were held under hot water to melt all PCMs after each experiment. After that, TES units were placed into

HDPE molds to redistribute PCMs throughout the TES units. However, PCM shifting did not have any impact on the peak temperature of PCM melting curves.

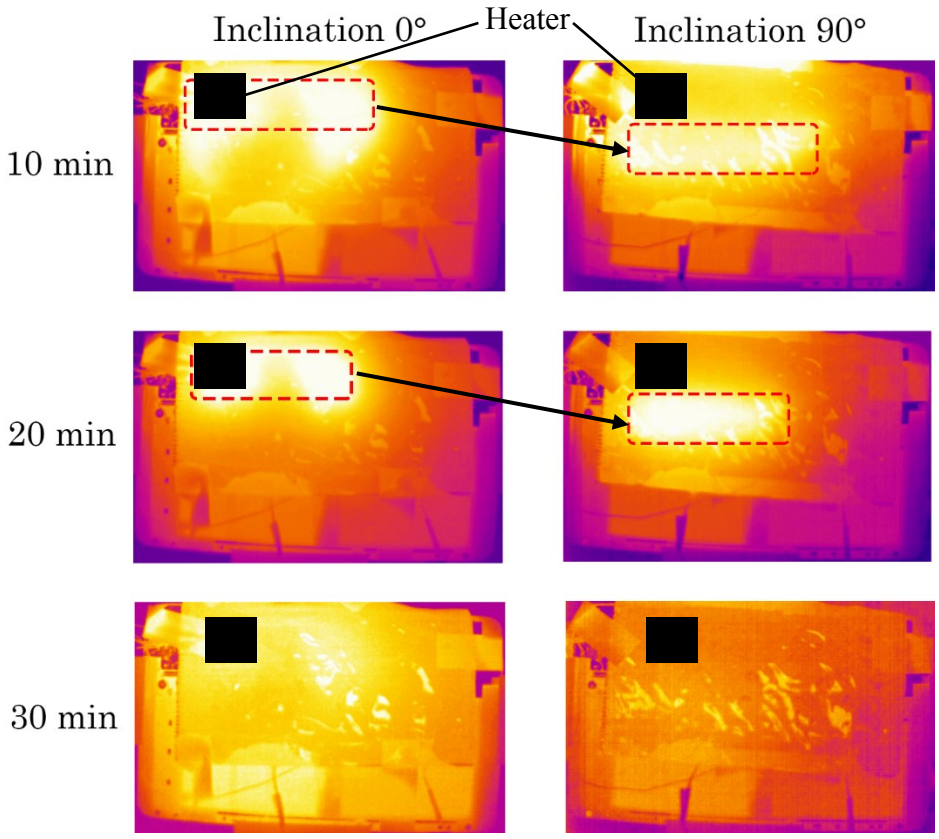

Figure 4-22 The thermograph during discharging phase is showing downward shifting of PCMs at inclined orientation (size 1 *n*-eicosane TES Unit with 6 W power input and 90° inclination, brighter area represents higher temperature).

Most tests were conducted more than once to ensure repeatability. One typical repeated test can be seen from Fig 4-23. Overall ± 5% deviations occurred in recorded temperatures measured between two consecutive experiments. The deviation in the temperature was measured by observing multiple trials of thermal response curves of similar experiments. Nevertheless, it is interesting to note that the deviation in the transient response of the experimental tablet PC and in the melting of PCMs mainly occurs in high-temperature zones where the heater is located. This implies that uncertainty in the supplied voltage can be considered as the main reason behind the deviations in the thermal response of experimental tablet PC and PCM melting.

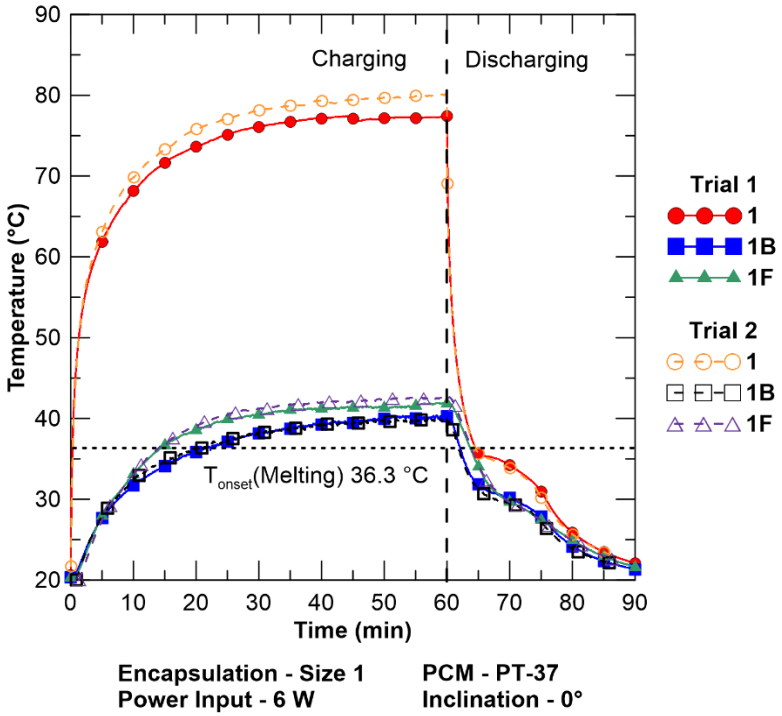

Figure 4-23 Comparison of experimental results using Size 1 PT-37 based TES unit at 0° inclination and 6 W power input.

Chapter 5

Results and Discussion: Continuous Operation

This chapter presents the results obtained during the tests performed under continuous operation, as well as observations from the experiments and discussions of the notable points of interest from those experiments. The present chapter is divided into two main sections: i) melting and solidification of PCMs and ii) performance of the tablet PC. In the first section, only melting and solidification phenomena of PCMs with size 1 and size 2 PCM-based TES units are discussed. In the second section, the performance of the tablet PC under the application of PCM-based TES units is presented. Results with all three PCM-based TES units along with three additional PCM-based TES units having same base area but different thicknesses are also covered. Table 5-1 shows the summary of all experiments done during the continuous operation of the tablet PC.

Table 5-1 Summary of experiments done in the continuous operation.

Observations	PCMs	Size of TES Unit (mass of PCMs)	Inclination	Power Input	Operation Mode
Melting-Solidification of PCMs	• *n*-Eicosane • PT-37	• Size 1 (16 g) • Size 2 (11 g)	• 0° (horizontal) • 45° • 90° (vertical)	• 2 W • 4 W • 6 W • 8 W	• Charging – 60 minutes. • Discharging – 30 minutes.
Performance of the Tablet PC	• *n*-Eicosane • PT-37	• Size 1 (16 g) • Size 2 (11 g) • Size 3 (25 g) • 2″ ×2″ ×0.12″ (6 g) • 2″ ×2″ ×0.16″ (8 g) • 2″ ×2″ ×0.20″ (10 g)	• 0° (horizontal) • 45° • 90° (vertical)	• 2 W • 4 W • 6 W • 8 W	• Charging – 60 minutes. • Discharging – 30 minutes.

5.1 Melting and Solidification of PCMs

During the charging (heating) process, the PCM undergoes three distinguishable stages. In the initial stage, the temperature of the PCM increases up to its melting temperature, quickly storing energy in the form of sensible heat. The PCM then changes phase, storing most of the energy as latent heat. In the final stage, the temperature of the melted PCM increases further by storing energy in the form of sensible heat, but at a slower rate eventually reaching a steady-state. The amount of heat storage into the PCM can be calculated using the following equation:

$$Q = \int \left(\int_{T_i}^{T_{onset}} \rho C_p dT + \rho a_m \Delta_{fus} H + \int_{T_{onset}}^{T_f} \rho C_p dT \right) dV \quad (5.1)$$

Where for the PCM, T_i is the initial temperature, T_{onset} is the onset melting temperature, ρ is the density, C_p is the specific heat, a_m is the melt fraction, $\Delta_{fus}H$ is the latent heat, T_f is the final temperature.

This equation shows that amount of heat storage in PCMs is dependent on the melt fraction of PCMs (a_m). The more PCM melts, the more heat storage occurs by latent heat storage in PCMs.

A typical melting curve for size 2 *n*-eicosane TES unit at 45° inclination and 8 W input can be seen in Fig. 5-1. Interestingly, even with 8 W of power input, not all *n*-eicosane melted inside the encapsulation. This can be seen from the P4 thermocouple readout which is the farthest away from the heater; the peak temperature encountered is less than the melting point of *n*-eicosane, 35.6 °C. Similar temperature profiles were obtained for all encapsulations, inclination and power input, and can be found in Appendix C.

Similar to the charging phase, during the discharging process, the PCM also undergoes three different stages. First, immediately after the heater was turned off at 60 minute (Fig. 5-1) a very sharp decrease in the temperature of the PCM was observed until it reached its solidification temperature, sensible heat was released during that process. In the second step, latent heat rejection occurred for 8 to 10 minutes at the constant solidification temperature of the PCM. Finally, the temperature of the PCM decreased further, until it

reached the room temperature. This entire process took approximately 30 minutes, which can be considered short duration and bodes well for the use of PCMs in the thermal management of electronic devices. In following sections, results with size 1 PCM TES unit is presented. The effect of size 2 TES unit on the melting and solidification of PCMs can be found in Appendix C.

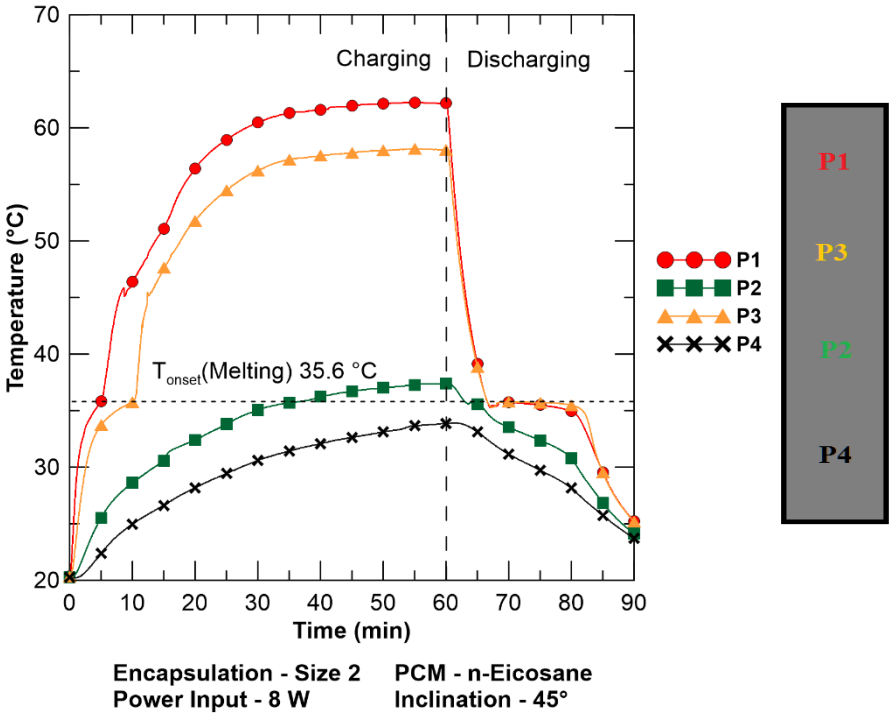

Figure 5-1 Melting curves of *n*-eicosane for size 2 TES unit at 45° inclination and 8 W power input.

5.1.1 Effect of Inclination

All experiments were conducted with three different orientations: 0° (horizontal), 45° (slanted), and 90° (vertical). Figure 5-2 shows the temperature responses of four thermocouples inserted into a size 1 PCM TES unit (see Fig. 4-17) for different inclination angles when the power level was kept at 6 W. During the sensible heating phase, the curves corresponding to the various inclination angles look almost identical. Such a result was expected since conduction was the governing mode of heat transfer during the sensible heat storage phase which is not influenced by inclination. However, very slight deviations, as

can be seen in Fig 5-2, can be attributed to the differences in PCM distribution throughout the PCM TES unit from one experiment to another.

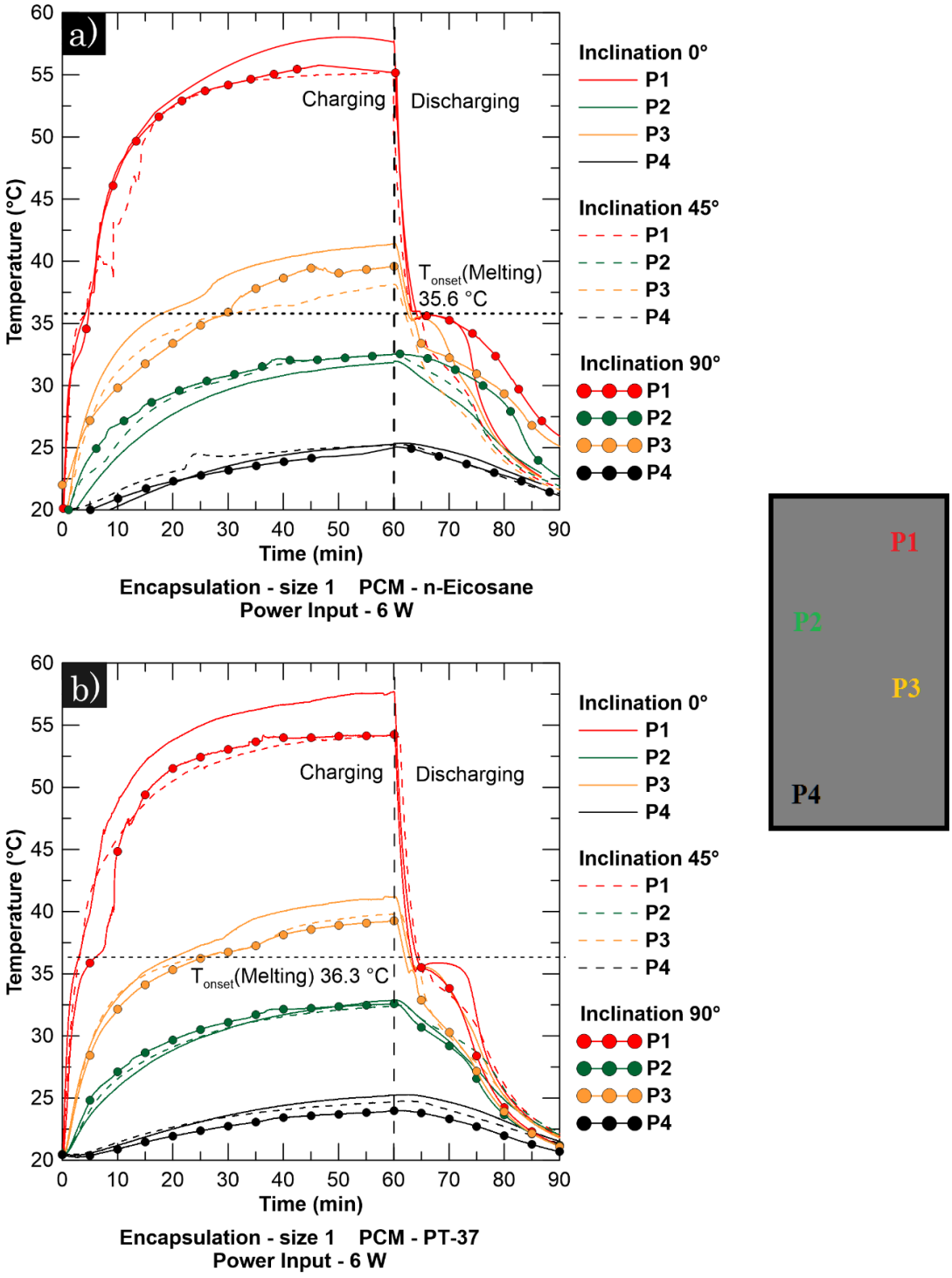

Figure 5-2 Effect of inclination on PCM melting for continuous operation at 6 W power input with size 1 PCM TES Unit: a) *n*-eicosane b) PT-37.

At 0º inclination, the entire heat transfer process was controlled by conduction. The temperature responses at 45° inclination show almost identical trends to those of the 90° inclination, except for some minor fluctuations in temperature during transient heating which may be attributed to the three-dimensional and unstable flow structures in the liquid PCM (Kamkari *et al.*, 2014). At 45º and 90º, the characteristic length for natural convection of the encapsulation changes from 1/16″ (the thickness of the encapsulation) to a maximum of 2.6″ (width of the encapsulation). The increment of characteristic length may facilitate the three dimensional flow structure which results in an increasing Grashof number (Gr_L) and thus intensifying the convection effect. Grashof number (Gr_L) can be defined as follows:

$$Gr_L = \frac{g\cos\theta\ \beta\ (T_S - T_\infty)L^3}{\nu^2} \qquad \text{for } 0 \leq \theta \leq 60° \qquad (5.2)$$

Where, g is the gravitational acceleration, θ is the inclination angle, β is the coefficient of thermal expansion, T_s is the average temperature of the back cover, T_∞ is the surrounding temperature, L is the characteristic length of the tablet PC, and υ is the kinematic viscosity of air.

Observations of the solid–liquid interface morphology by Webb and Viskanta (1986) also confirms the presence of three-dimensional flow structures in inclined rectangular enclosures (25.4 cm × 6.35 cm × 4.06 cm). Similar flow structures were confirmed by Sharifi *et al.* (2013) during the observation of melting of PCMs in a cylindrical enclosure (45.8 mm diameter and 18.9 mm height) with small tilt angles. However, as a very thin layer of PCM with non-uniform heat input from a finite heat source is a unique case, different phenomena with PCM melting in this study are less prevailing than studies by previous researchers. Additionally, aluminized laminate film acts as an IR shield which prevents the observation of flow behaviour of PCMs inside TES units. As a result, it was difficult to confirm if the three-dimensional flow behaviour of our experiments is identical to the ones observed in the previous studies (Webb and Viskanta, 1986; Sharifi *et al.*, 2013). Numerical investigations would be required to confirm the presence of such flow structures.

Lu *et al.* (2014) observed two stages of melting phase: initial and developed based on the change of slope in temperature profiles while investigating the effect of inclination on the thermal performance of PCM-based heat sinks. For the horizontal case (0° inclination), they observed much lower slope in the transient temperature curves. They attributed the inflection point to the two sub-stages during melting: conduction-dominated and convection-dominated. This inflection point can be observed at point P3 in Fig 5-2. At point P3, conduction dominated stage occurred during the first 25-30 minutes of charging phase. After that, when PCM at point P3 started melting, convection starts playing a role. This phenomenon can hardly be identified in point P1 on the melting curves due to the rapid melting of a small amount of PCM on the top of the heater compared to studies done by Lu *et al.* (2014) where 60 g of PCM was placed on top of the heater. No significant effects of inclination were observed at the low temperature (P2 and P4) regions because PCMs at those points did not melt and therefore convection had no effect. PCMs at these points did not contribute to any latent heat storage as well.

It is interesting to note that, although *n*-eicosane has a 16% greater latent heat of fusion than PT-37, in these experiments, this difference in latent heat did not cause significant variation on the melting curve of PCMs during transient heating (Fig. 5-2a and 5-2b). This might occur from having a small amount of PCMs in the system and from the resulting smaller melt fraction (< 1.0) after 60 minutes of operation. Similar trends were observed and can be considered as a norm for other experiments as well.

Melting of PCMs under 8 W of power input for *n*-eicosane and PT-37 can be seen in Fig. 5-3. Results obtained at 8 W are very similar to the results obtained at 6 W power input. Due to the higher rate of PCM melting at 8 W, the observed deviation between 45° and 90° inclination was more prevailing. Slight deviation between *n*-eicosane and PT-37 can be seen in Fig 5-3a and 5-3b. The main reason behind the deviation was the uncertainties in power input caused by the variability of voltage supply form the variac. Uncertainty in power input in turn may lead to slightly more heat storage in one PCM than other. During the discharging phase, time required to release the latent heat was higher at 8 W than 6 W power input; since at 8 W power input, more energy was absorbed in the PCM, the amount of heat rejection during discharging is also higher.

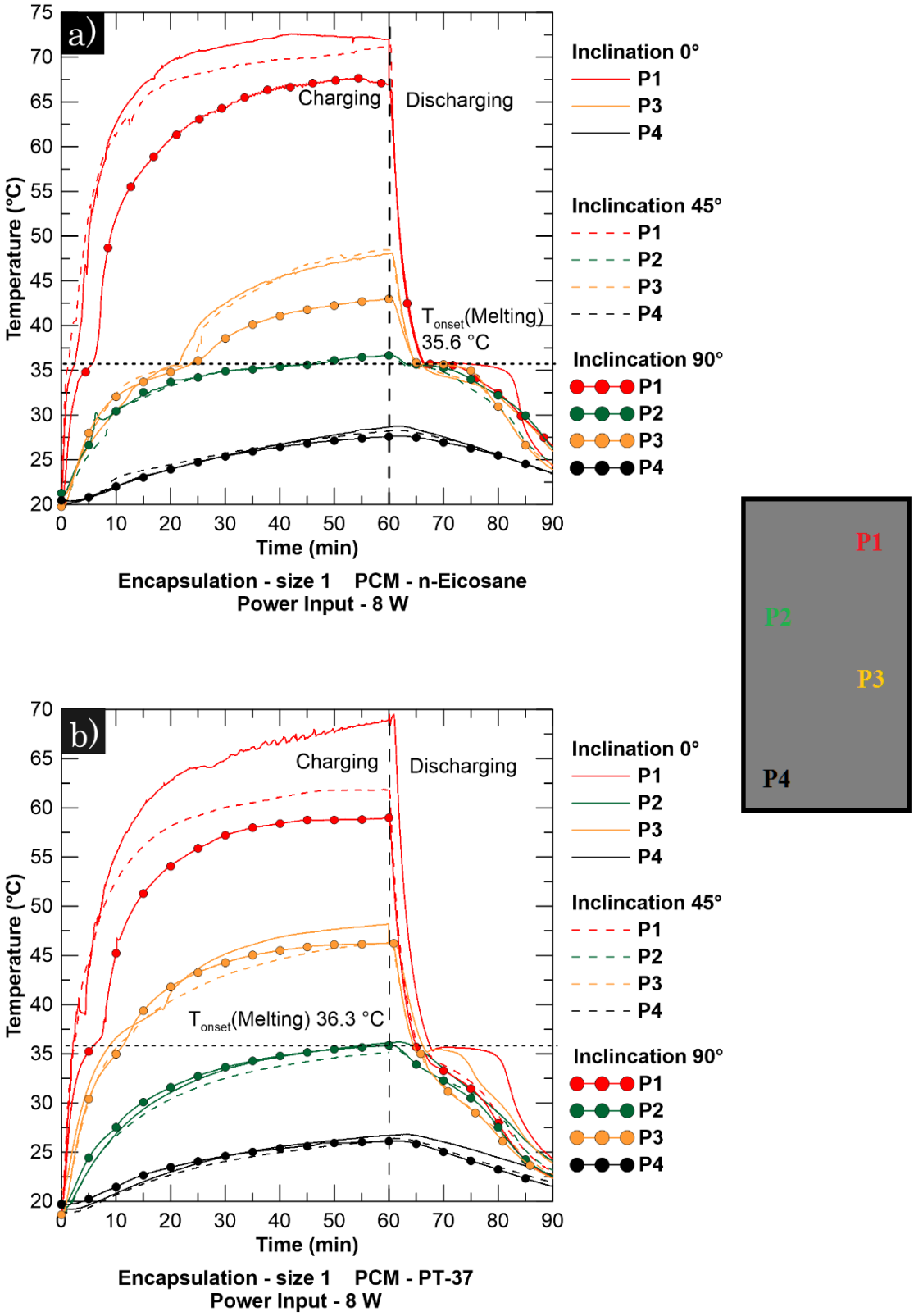

Figure 5-3 Effect of inclination on PCM melting for continuous operation at 8 W power input with size 1 PCM TES Unit: a) *n*-eicosane b) PT-37.

However, in case of PT-37, during the discharging phase, latent heat rejection of PCM was less prevailing at point P1 at higher inclination. As presented in Fig 4-21, at higher inclination, the melted PCM tends to accumulate on the bottom of the TES unit. This was expected to be extreme at 8 W power input with most PCM melted. As a result, during the discharging phase, the P1 thermocouple at 45° and 90° inclination was in contact with less liquid PCM. That resulted in a quicker decrease in temperature compared to the 0° inclination case during the discharging phase.

5.1.2 Effect of Power Input Levels

As the power generated through the electronics depends on the level and type of usage of the tablet PC, therefore, various power input levels had to be considered in the design. In this study, four different power levels (2, 4, 6, and 8 W) were used to observe the performance of PCM-based TES units under different usage load of the tablet PC.

Figure 5-4 shows the effect of different power input levels on the melting of both PCMs for size 1 PCM TES unit at 0° inclination. Only temperatures recorded by thermocouples P1 and P3 are shown because these regions experienced the most melting during experiments. It is evident that the rate of PCM melting is directly related to the supplied power. With increased heat input, faster PCM melting was observed as well as higher steady-state temperature. In addition, it is also apparent that no PCM melting effect was observed at 2 W of supplied power. As a result, during the discharging phase, no latent heat rejection was observed at 2 W power input. Similar phenomena were mentioned by Kandasamy *et al.* (2007). Isothermal heat rejection time was increased with increasing heat input during the discharging phase which implies that more latent heat was stored with increasing power input level. Also, as can be seen from Fig. 5-4, the time required for PCM solidification at point P1 and P3, during which the absorbed latent heat was dissipated, is much longer than that for the melting phase. Melting during the charging phase was initiated by the high heat flux applied by the heater, whereas during the discharging phase the heater was turned off and PCM was solidified by natural convection. Saha and Dutta (2012) have also showed that the thermal resistance for heat flow from the

PCM to the surrounding during the discharging phase is significantly higher in comparison to that of the charging phase due to natural convection cooling of the setup.

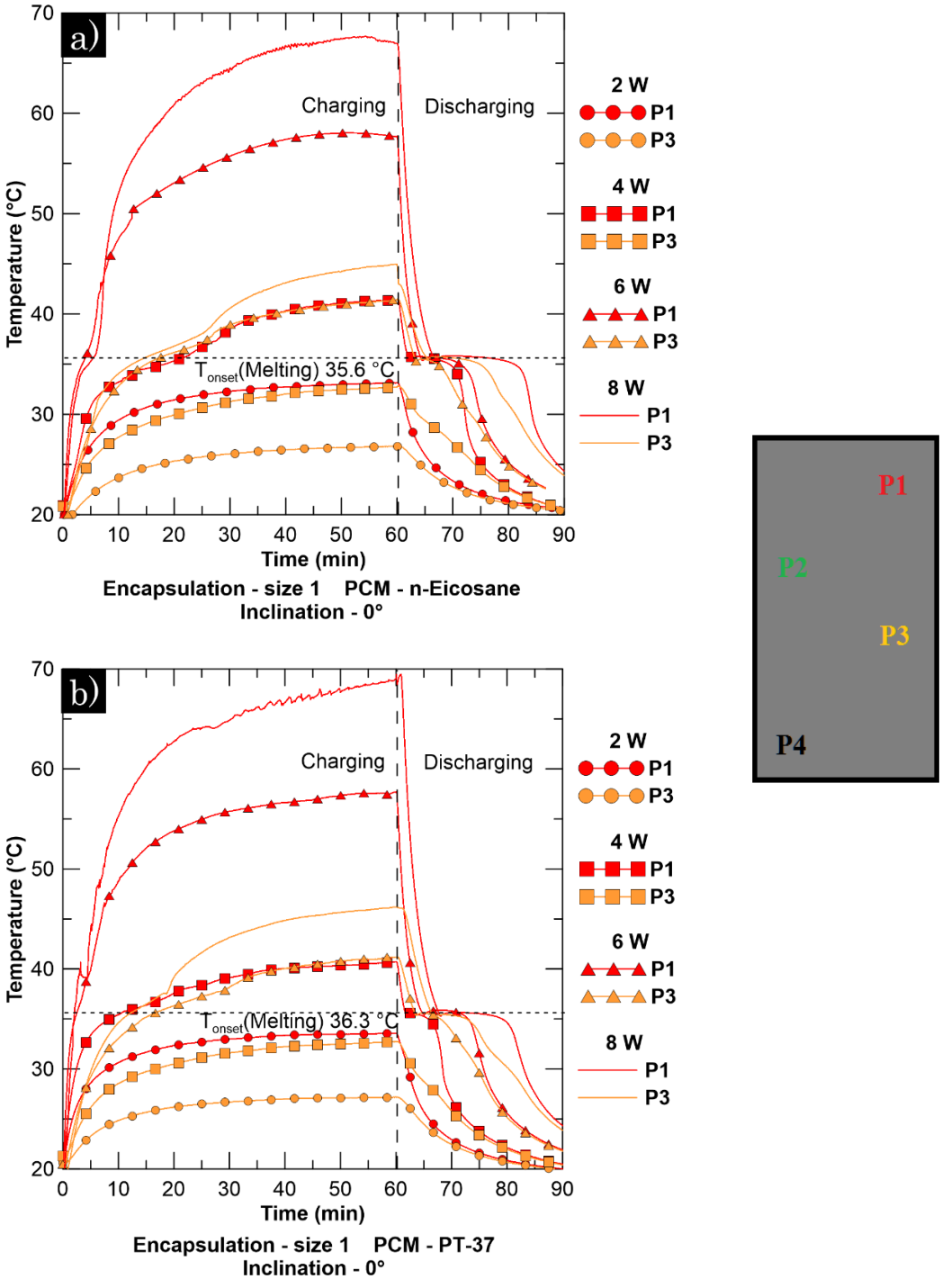

Figure 5-4 Effect of power input levels on PCM melting for continuous operation at 0° inclination with size 1 PCM TES Unit: a) *n*-eicosane b) PT-37.

5.1.3 Effect of TES Unit Size

Figure 5-5 shows the effect of PCM-based TES unit size on the melting curve of both PCMs at 6 W power input and 0° inclination. Noticeable deviations between size 1 and size 2 PCM TES units were observed for both *n*-eicosane and PT-37. This deviation was attributed to the differences in the position of thermocouples as well as the difference in total latent heat of PCM which varied depending on the size (therefore amount of PCM) of the TES units. From Fig. 4-17, it is clear that P2, P3, and P4 thermocouples in size 1 PCM TES unit were located farther away from the heater compared to size 2 PCM TES unit. Moreover, having a width similar to the PCB itself, the entire size 2 PCM TES unit was set on the top of the highly conductive PCB. Hence, PCM melting in size 2 PCM TES unit was more extensive compared to size 1 PCM TES unit because of better heat conduction to PCMs through the PCB surface, and therefore, a lower thermal resistance between the heater and PCMs was expected.

Results in this section also show that larger TES unit (size 1) did not contribute much compared to smaller TES unit (size 2) in terms of latent heat storage (similar amount of latent heat rejection during discharging phase). This in turns shows the necessity of having good heat spreading throughout the PCMs from the heater or using smaller PCM-based TES units placed component-wise (*i.e.* placed on the top of the heater only) to utilize all latent heat of PCMs. This reduction in size is critical for keeping the overall size and weight of the device small. Similar concept was recommended by Kandasamy *et al.* (2007).

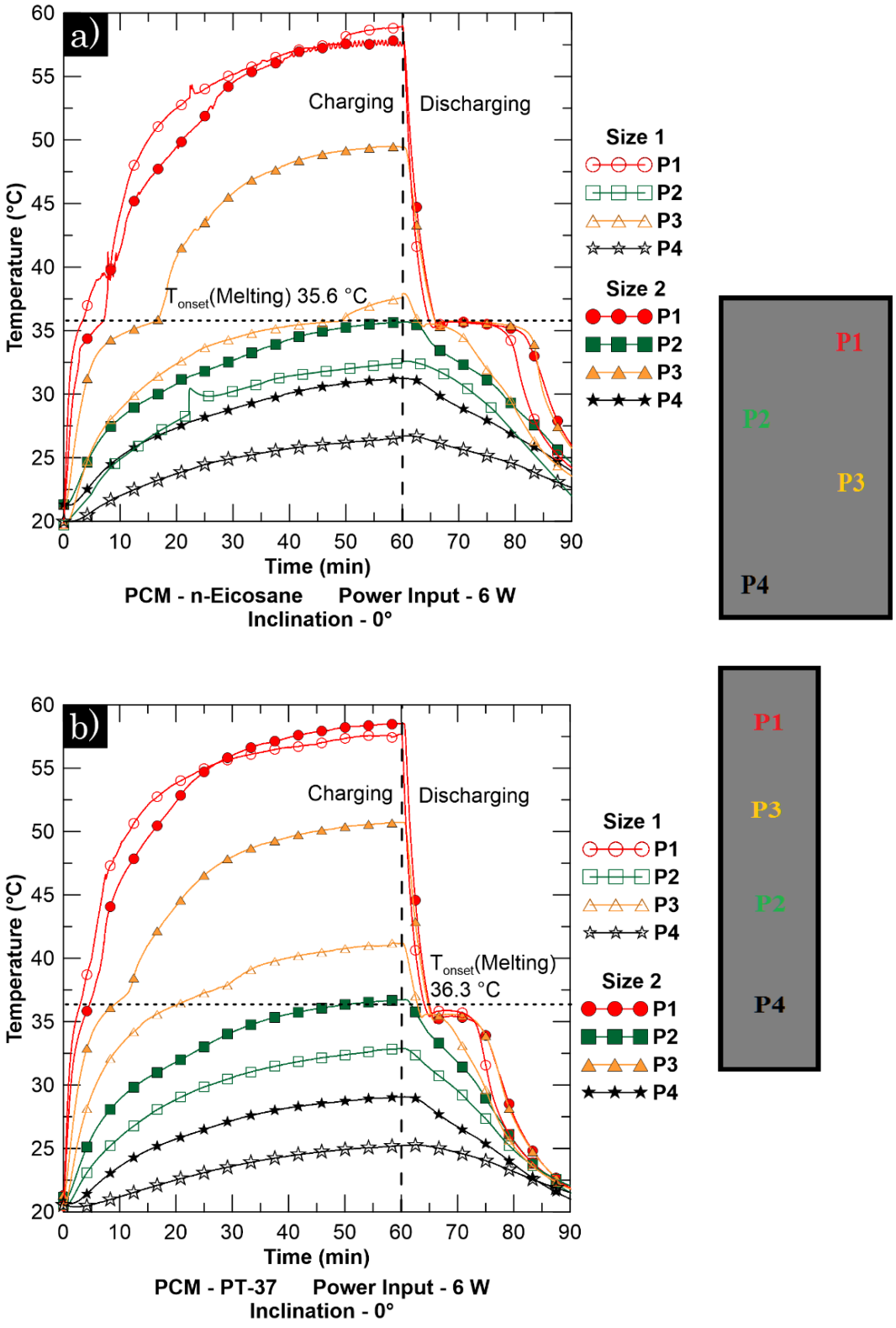

Figure 5-5 Effect of PCM TES size on PCM melting at 6 W power input and 0° inclination: a) *n*-eicosane b) PT-37.

5.2 Performance of the Tablet PC

All experiments using the experimental tablet PC were conducted for 60 minutes of continuous charging (heating) followed by 30 minutes of continuous discharging. Continuous operation of the experimental tablet PC without any PCM-based TES unit in a horizontal position (inclination 0°) was considered as the baseline condition for this study. The temperature response of the experimental tablet PC at various power inputs can be seen in Fig. 5-6. The operating comfort zone of users was considered here to be a device outer surface temperature less than or equal to 40°C which is slightly lower than indicated (42 °C–45 °C) in previous studies (Greenspan *et al.*, 2003; Patapoutian *et al.*, 2003) to maintain a safer margin of comfort. Interestingly, point 2F had a higher temperature than point 2B (see Fig. 4-12), even though the heater was placed on the back side of the PCB. This mainly happens due to a large metal stiffener residing between the PCB and the display which conducts and spreads heat on the front side better than the back side at that location. Moreover, thermal resistance on the back was higher compared to the front side due to the presence of air gaps in between the circuit board and the back cover.

A typical comparison of size 1 PT-37 TES unit performance on the tablet PC with baseline operation at 6 W heat input and 0° inclination can be seen in Fig. 5-7. The heater (point 1) temperature was reduced slightly during the transient heating due to latent heat storage in the PCMs. The back surface immediately above the heater (point 1B) experienced an almost 15 °C reduction in temperature compared to baseline operation. Similarly, the point on the front (display), in line with the heater (point 1F), had almost 5 °C reduction using the PCM TES unit. As the PCM TES unit was placed between the heater and the back cover, temperature reduction on the back cover was greater than on the front. It took almost 57 minutes more to reach the 40 °C limit compared to the baseline operation.

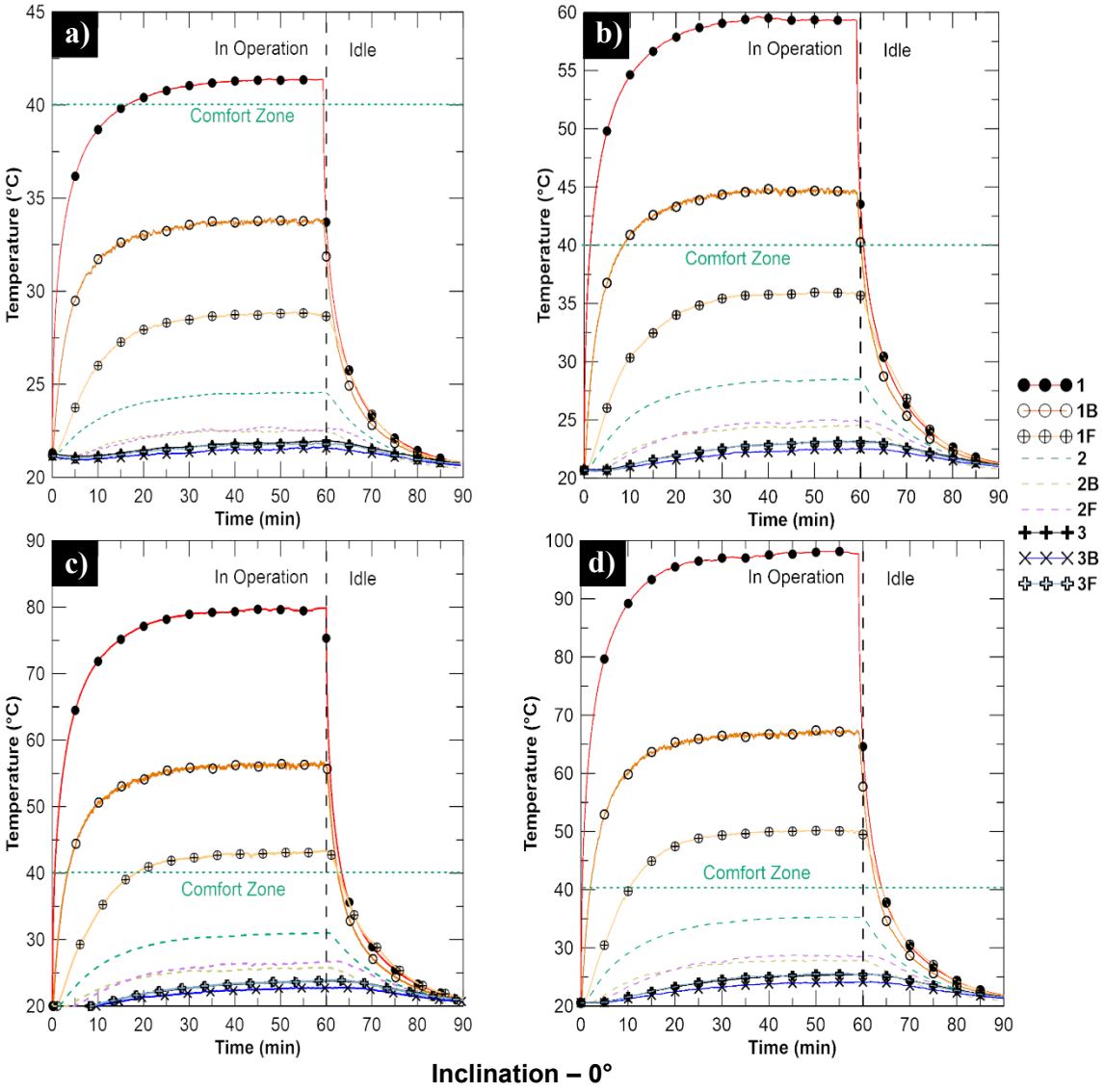

Figure 5-6 Baseline temperature profile for the experimental tablet PC at various power input without any PCM TES units: a) 2 W b) 4 W c) 6 W d) 8 W.

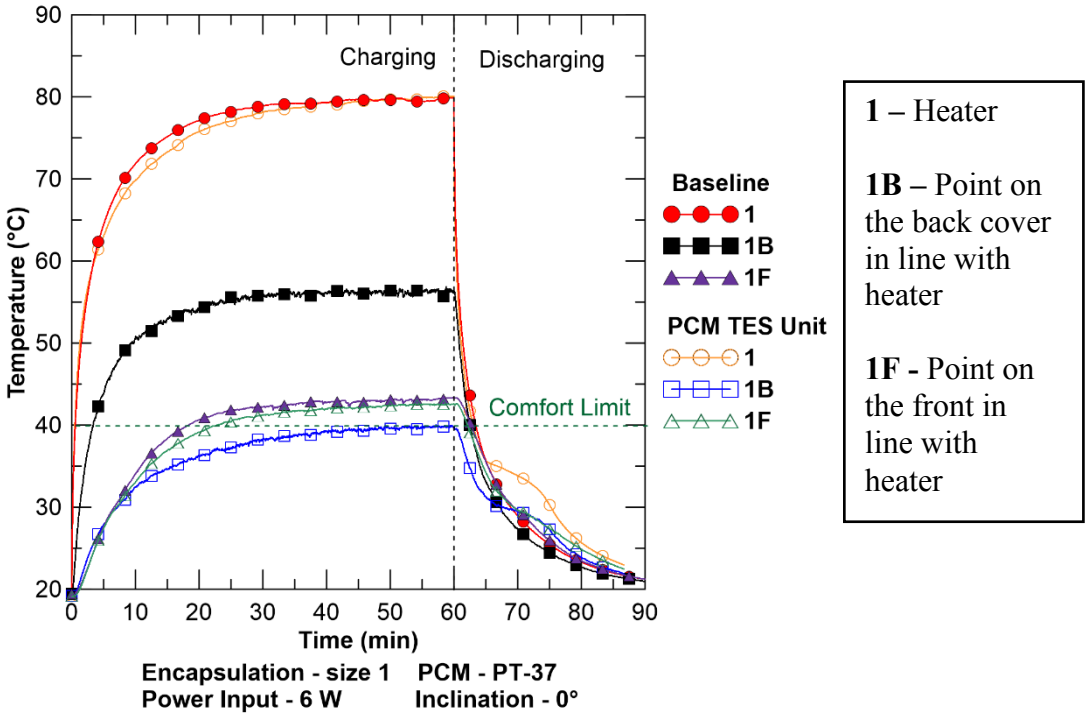

Figure 5-7 Effect of Size 1 PT-37 TES unit on the thermal response of the experimental tablet PC at 0° inclination and 6 W power input.

From Fig. 5-8, it can be seen that point 2 and 3 (see Fig. 4.12) had higher temperature with size 1 PCM TES unit compared to the baseline operation. This mainly happens because the PCM TES unit acts as a thermal barrier which offers a greater resistance to the heat flow from internal components (*i.e.* PCB, battery) to the outside. Due to relatively high thermal conductivity of the PCB material, heat spreading at point 2 (on the PCB) was higher compared to point 3 (battery) at baseline operation. Strong spatial and temporal variation of the thermal conditions inside a tablet PC were considered as the major thermal management challenge by Chiriac *et al.* (2015). The same authors suggested using heat spreaders to achieve good internal thermal management of tablet PCs which provides a consistent lower exterior temperature of the device. In the present study, at 2W power input, no PCM melting was observed (see Fig. 5-4). However, the heat spreading resulted in lower back cover temperature even without any PCM melting, can be seen from Fig. 5-9.

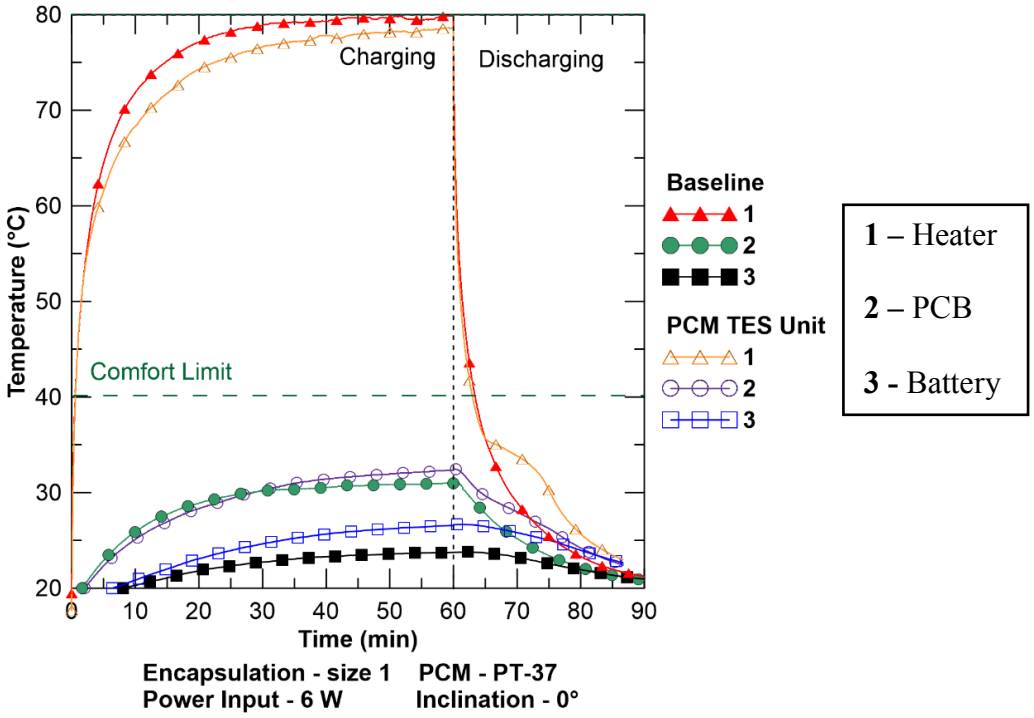

Figure 5-8 Effect of heat spreading on the thermal response of the tablet PC with size 1 PT-37 TES unit at 0° inclination and 6 W power input.

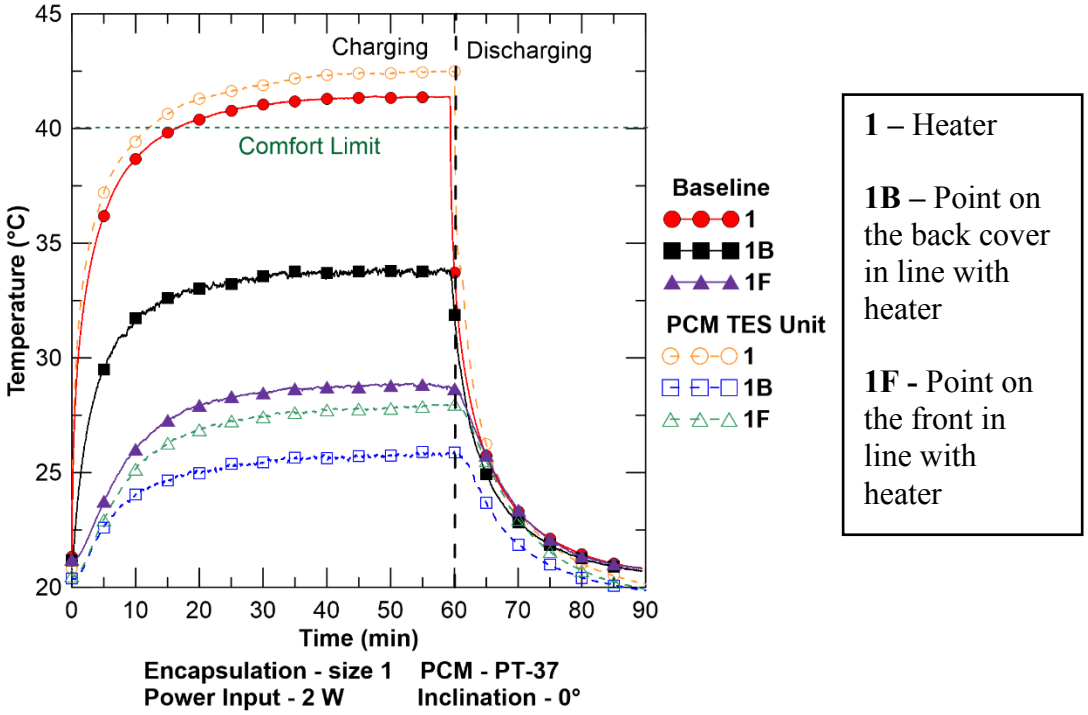

Figure 5-9 Thermal response of the experimental tablet PC at 2W power input with size 1 PT-37 TES unit and at 0° inclination under the continuous operation.

Based on baseline operations, only temperature variations of the heater (point 1), point 1B on the back cover and point 1F on the front (display) are considered as performance parameters, as only these specific areas suffered from temperatures higher than the comfort zone. In this section results with size 1 PCM TES units is presented. The effect of size 2 and size 3 TES units on the thermal performance of the tablet PC can be found in Appendix D.

5.2.1 Effect of Inclination

During the use of a tablet PC, the position and orientation of the device can be subjected to arbitrary change. Hence, it is necessary to observe the effectiveness of the PCM TES units at different angular orientations. Figure 5-10 shows the thermal response of the experimental tablet PC for various orientations at 6 W power input with size 1 PCM TES unit: horizontal (0°), vertical (90°), and inclined at 45°. Experimental results show that the orientation of the tablet PC affected its steady-state temperature slightly. From Fig. 5-10a slight deviation between 45° and 90° inclination (point 1) can be seen which is absent in Fig. 5-10b with PT-37. This can be attributed to the inconsistency of the supplied power.

In the case of point 1B and 1F, the maximum temperature decreases from horizontal (0°) to slanted (45°), to the vertical (90°) position. It is caused by the thermal response of point 1 (heat source), as point 1B and 1F reside immediately on the top and below point 1 respectively. However, in the case of point 1F, the role of natural convection comes into play. This can be explained by looking at the expected convection coefficients on the display (which is oriented downward in the experiment), determined by calculating Nusselt numbers (Nu) using accepted correlations form Bergman *et al.* (2011).

For a vertical plate, the Nusselt number is calculated from:

$$\mathrm{Nu_L} = 0.68 + \frac{0.670\mathrm{Ra}_L^{1/4}}{[1+(0.492/\mathrm{Pr})^{9/16}]^{4/9}} \tag{5.3}$$

For the lower surface of an inclined hot plate:

$$\mathrm{Nu_L} = 0.52\ \mathrm{Ra}_L^{1/5} \tag{5.4}$$

Where, P_r is the Pandtl number of air and Ra_L is the Rayleigh number defined as follows:

$$\mathrm{Ra_L} = \mathrm{Gr_L Pr} \tag{5.5}$$

Where, Gr_L is the Grashof Number calculated from the Eq. 5-2. And finally, the convection coefficient (h) was calculated from:

$$\mathrm{Nu_L} = \frac{hL}{k} \tag{5.6}$$

Where, h is the convection coefficient, L is the characteristic length of the tablet PC, and k is the thermal conductivity of air. Calculated values of aforementioned dimensionless numbers can be found in Table 5-2. For the 45º and 90º experiments, the convection coefficients are found to be 3.7 and 4.1 W/m^2·K respectively. However, for the 0º inclination test, the resulting convection coefficient is 3.1 W/m^2·K; this 24% difference in the strength of convection explains the 5 ºC temperature difference on the display. Similar to the front side, it can be assumed that the back cover temperature was also affected by natural convection with the surroundings. However, there are no empirical relations to calculate Nusselt number (Nu_L) for the back cover. As a result, numerical values of convection coefficient for the back cover are not available.

By considering the slight effect of orientation on the performance of the tablet PC with PCM-based TES units, thermal management of tablet PCs using PCMs is expected to work safely in a real environment.

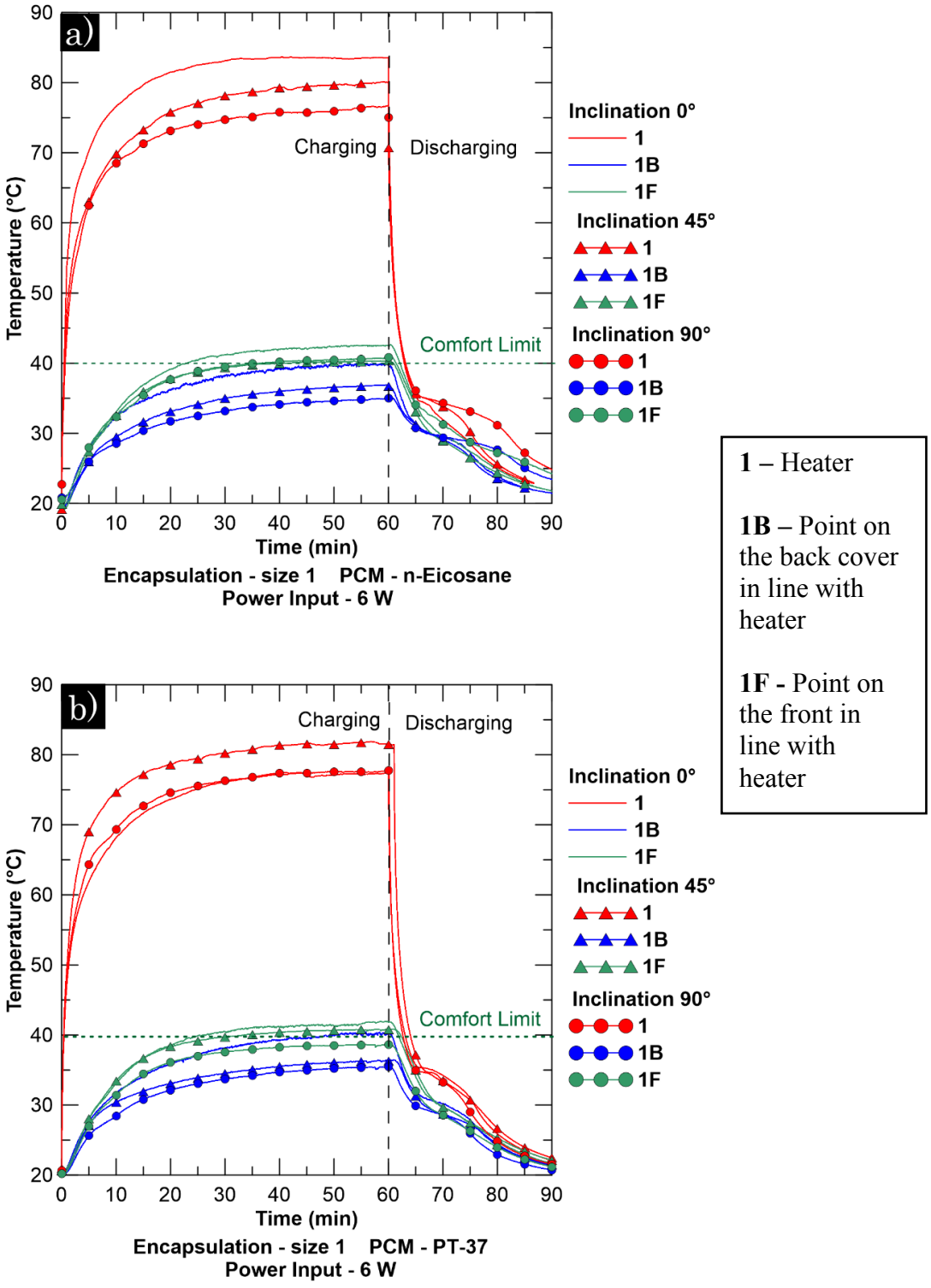

Figure 5-10 Effect of inclination on the thermal response of the experimental tablet PC at 6 W power input with size 1 PCM TES Unit: a) n-eicosane b) PT-37.

Table 5-2 Values of dimensionless numbers and convection coefficient with different angular orientations.

Angular Orientation	Grashof Number (Gr_L)	Rayleigh Number (Ra_L)	Nusselt Number (Nu_L)	Convection Coefficient, h (W/m^2K)
0°	9.21×10^4	6.5×10^4	4.78	3.1
45°	2.44×10^5	1.73×10^5	5.8	3.7
90°	2.83×10^6	2.0×10^6	20.0	4.1

5.2.2 Effect of Power Input Levels

Similar to the effect on PCM melting curves, Fig 5-11 shows that increased power input level increases the temperature of the heater as well as the display and the back cover. At all power input levels and with both PCMs, the front (display) temperature was higher than the back cover temperature. This occurs due to the fact that the PCM TES unit was placed in between the PCB and the back cover and some of the energy is absorbed by the PCM. On the other hand, some of the energy that was lost through the back during baseline operation now goes out through the front.

At 8 W power input, the heater (point 1) temperature reaches almost 100 °C (can be seen in Fig. 5-6) for both *n*-eicosane and PT-37 based PCM TES units. Most of the Intel CPU thermal control circuits (TCC) activate at 85 °C (Tian, 2010) which indicates that chip temperature above 85 °C can be harmful for the proper functioning of tablet PCs. Every electronic device has a certain design limit beyond which thermal management using passive cooling does not remain useful. In this tablet PC, 8 W power input goes beyond that limit. This can also be confirmed from the thermal analysis of the original tablet PC which even at severe stress test only produced a maximum of 5 W of power leading to a heater temperature of 69 °C. It is still very interesting to note that, even at 8 W power input, the back cover temperature remained close to the user comfort zone. This mainly occurred due to significantly higher latent heat storage at 8 W power input compared to other power input levels. From the discharging phase, it can be seen that rejection of latent heat took a longer period of time for 8 W power input, 16 minutes compared to 8 minutes for 6 W power input. As a result, temperature control using PCM TES units at various power input levels deemed effective for all mode of usage loads (regular to heavy).

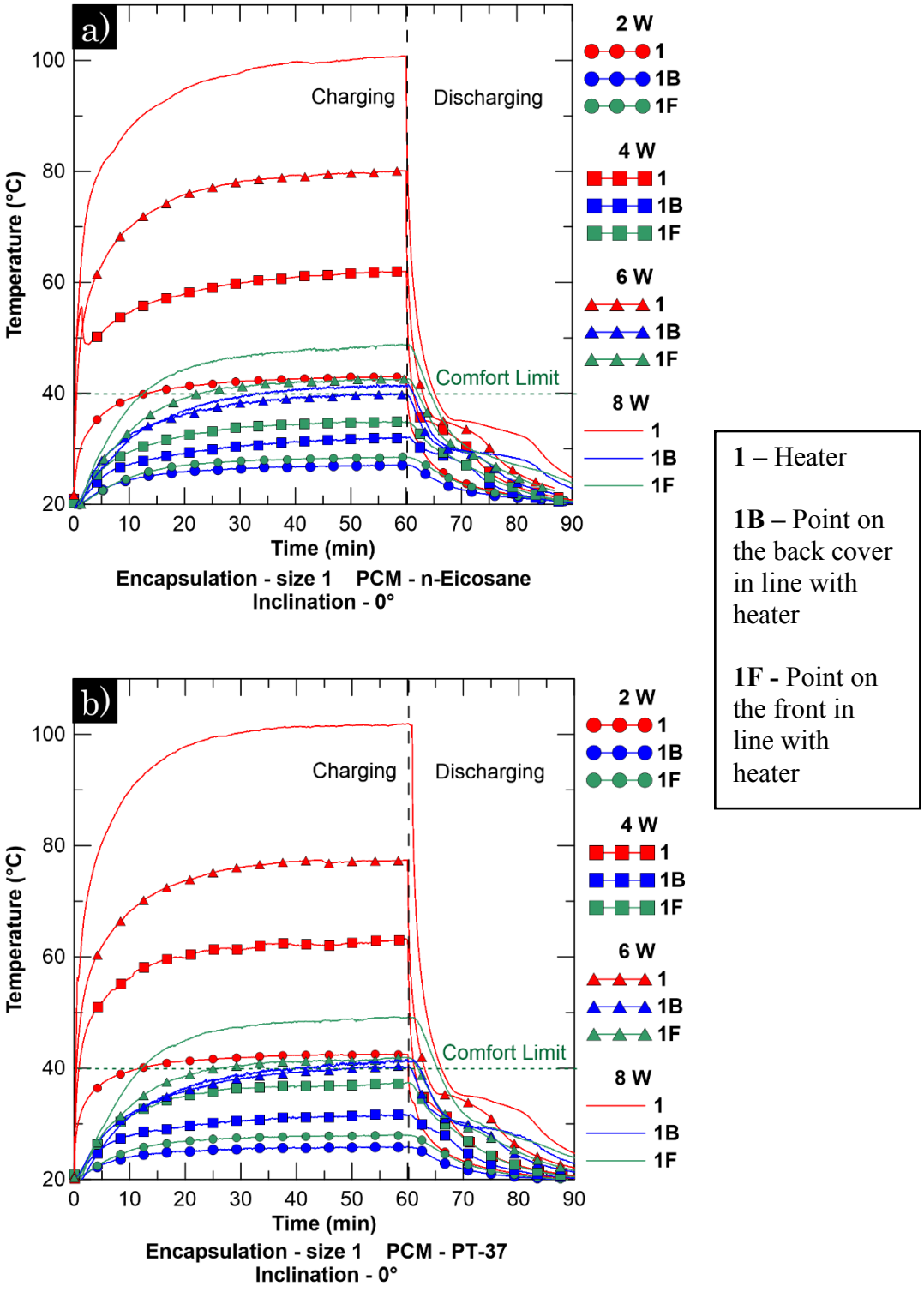

Figure 5-11 Effect of power input levels on the thermal response of the experimental tablet PC at 0° inclination with size 1 PCM TES unit: a) n-eicosane b) PT-37.

5.2.3 Effect of TES Unit Size

Effect of encapsulation size on the thermal response of the experimental tablet PC at 6 W power input and 0° inclination can be seen from Fig. 5-12. Similar to previous analyses no significant variation between *n*-eicosane and PT-37 was observed. Both for *n*-eicosane and PT-37, size 3 TES unit provided the lowest temperature of the back cover (point 1B) after 60 minutes of charging phase. This can be attributed to the higher heat storage and greater surface area of the size 3 TES unit compared to the two other TES units (size 1 and size 2). Due to the greater surface area, removal of air gaps inside the tablet PC was higher. As a result, uniform distribution of heat was possible with size 3 TES unit during the charging phase. Size 2 TES unit resulted in highest back cover temperature due to the least latent heat storage and thus transferring most heat to the back by conduction through the PCM. In all cases, size 1 TES unit provided a thermal response in between size 2 and size 3 TES unit. This was expected, since the base area and quantity of PCMs inside size 1 TES unit lies in between size 2 and size 3 TES unit.

In Fig. 5-13, IR images show the back cover temperature contours of the experimental tablet PC after 60 minutes of charging and 30 minutes of discharging with different PCM-based TES units at 6 W power input and 0° inclination. IR images with PT-37 and *n*-eicosane have showed similar trends, therefore results presented in this section are limited to the case of PT-37 based TES units. After 60 minutes of charging the baseline condition resulted in an average temperature of 57.5 °C on area X (a certain area marked on the back cover) (Fig. 5-13a). This hotspot temperature was reduced to 40 °C with size 1 PCM TES unit. By adding size 1 TES unit, the heat was slightly more distributed away from the upper-right region, therefore, removing the hotspot. Similarly, size 2 and size 3 TES units had 42 °C and 38 °C respectively on area X after 60 minutes of charging (Fig. 5-13c and 5–13d). Equipping the tablet PC with size 2 TES unit resulted in slightly higher area X's average temperature compared to size 1 and size 3 TES units as discussed earlier. As size 2 TES unit had the least width, it allowed the largest air gap inside the tablet PC. This air gap in turns increased the internal thermal resistance which caused heat to conduct more easily to the back cover through the PCM encapsulation. Latent heat storage, however, slows down the heat rejection slightly compared to the baseline condition. This can be

seen from the IR images of discharging phase in Fig. 5-13. After 30 minutes of discharging the baseline condition had 23 °C on area X which was almost 24.7 °C with size 1 TES unit. On the contrary, size 2 had the best thermal performance after 30 minutes of discharging due to less energy storage during the charging phase in a fewer amount of PCMs compared to the two other TES units. Size 2 and 3 had 24 °C and 26.5 °C of area X temperature respectively.

Further software analysis of these IR images was done to analyze the temperature distribution of the back cover with different PCM TES units. The summary of software analysis data can be found in Table 5-3. For the baseline operation, the average back cover temperature was found to be 33 °C with a standard deviation of 11 °C. For the size 3 TES unit, standard deviation was only 5 which is 15% lower than size 1 (5.8 °C) and 45% lower than size 2 (7.0 °C) TES unit. As a result, it can be concluded that size 3 PCM TES unit provided the best heat spreading resulting in the most uniform back cover temperature.

Table 5-3 Summary of statistical analysis of IR images.

Operation	Average Temperature (°C)	Standard Deviation (°C)
Baseline (6 W)	33	11
PT-37 Size 1 TES Unit (6 W)	29.6	5.8
PT-37 Size 2 TES Unit (6 W)	30.3	7
PT-37 Size 3 TES Unit (6 W)	29.3	5

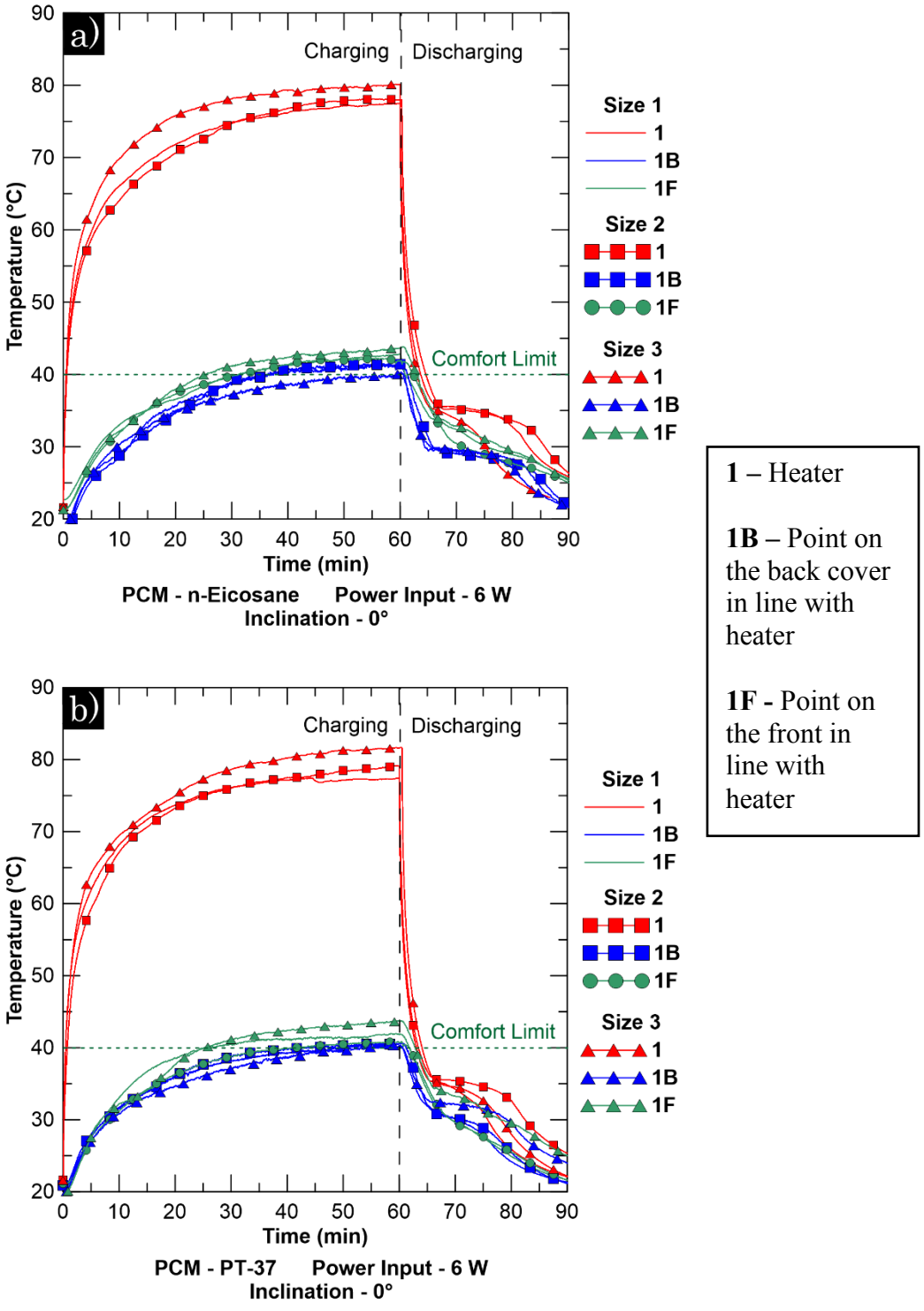

Figure 5-12 Effect of PCM TES size on the thermal response of the experimental tablet PC at 6 W power input and 0° inclination: a) *n*-eicosane b) PT-37.

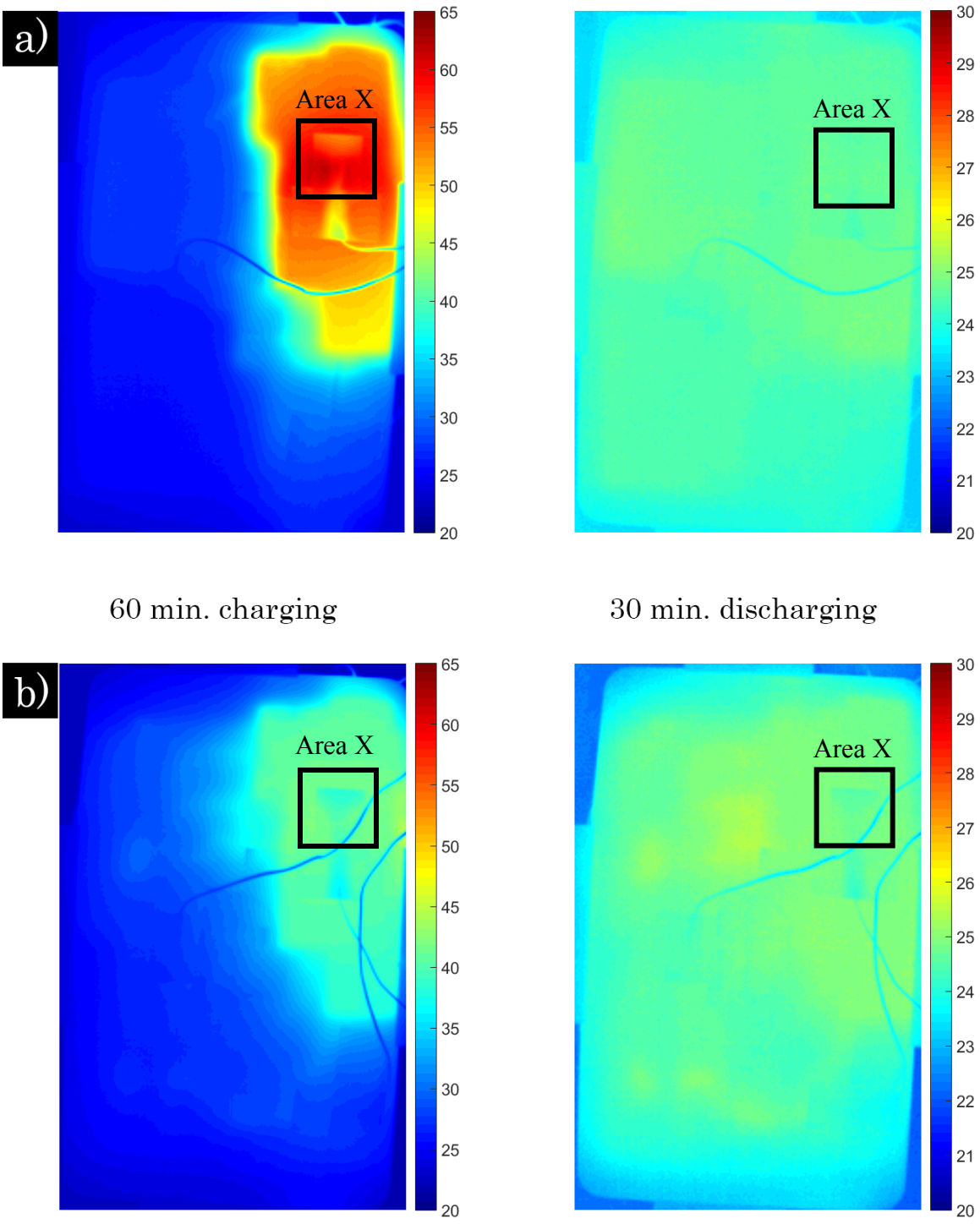

Figure 5-13 Thermal images showing the effect of PCM TES size on the thermal response of the experimental tablet PC at 6 W power input and 0° inclination: a) Baseline b) Size 1 PT-37 TES Unit.

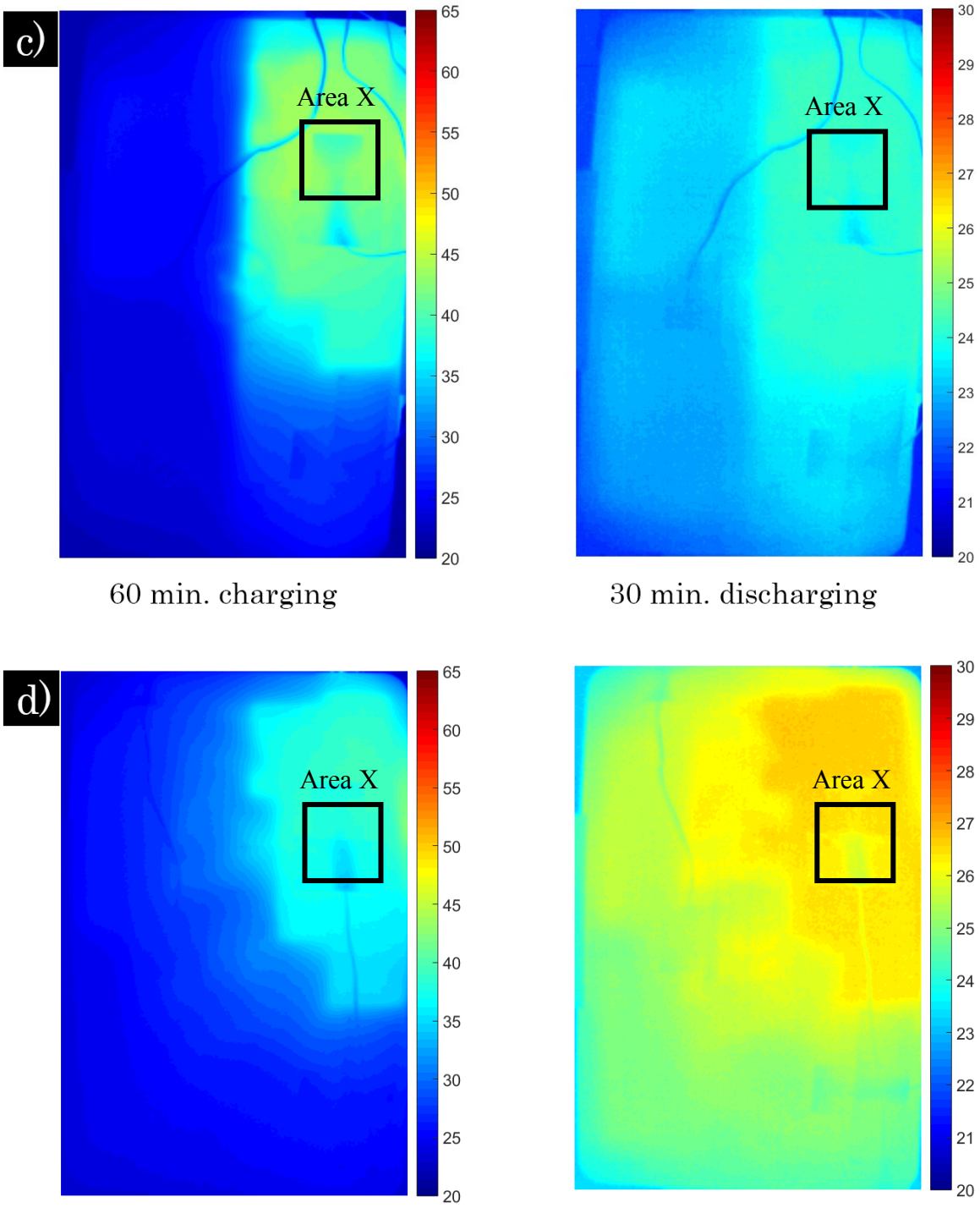

Figure 5-13 (cont'd) Thermal images showing the effect of PCM TES size on the thermal response of the experimental tablet PC at 6 W power input and 0° inclination c) Size 2 PT-37 TES Unit: c) Size 2 PT-37 TES unit d) Size 3 PT-37 TES Unit.

5.2.4 Effect of Varying Latent Heat

Based on the results obtained from studying the effect of varying PCM TES unit size on the PCM melting (section 5.1.3), it was deduced that, smaller PCM TES units, placed on the components only, could be more useful by utilizing all of the latent heat of PCMs through complete PCM melting. This in turn could provide better transient operation of the tablet PCs. This can be confirmed from Fig. 5-14 which shows a comparison between typical size 1 PCM TES unit and smaller encapsulations with different latent heat placed on the top of the heater for PT-37. Clearly, all smaller PCM TES units provided a better transient response as well as lower peak temperature of the heater (point 1). For the size 1 PT-37 TES unit, the latent heat was only 970 J on an area of 2″ × 2″ on the top of the heater which is 53% lower than the 10g case. However, it is interesting to note that with smaller TES units the heater temperature was lowered. Moreover, the temperature on the back was increased almost 12 °C which is 7 °C beyond the user comfort limit.

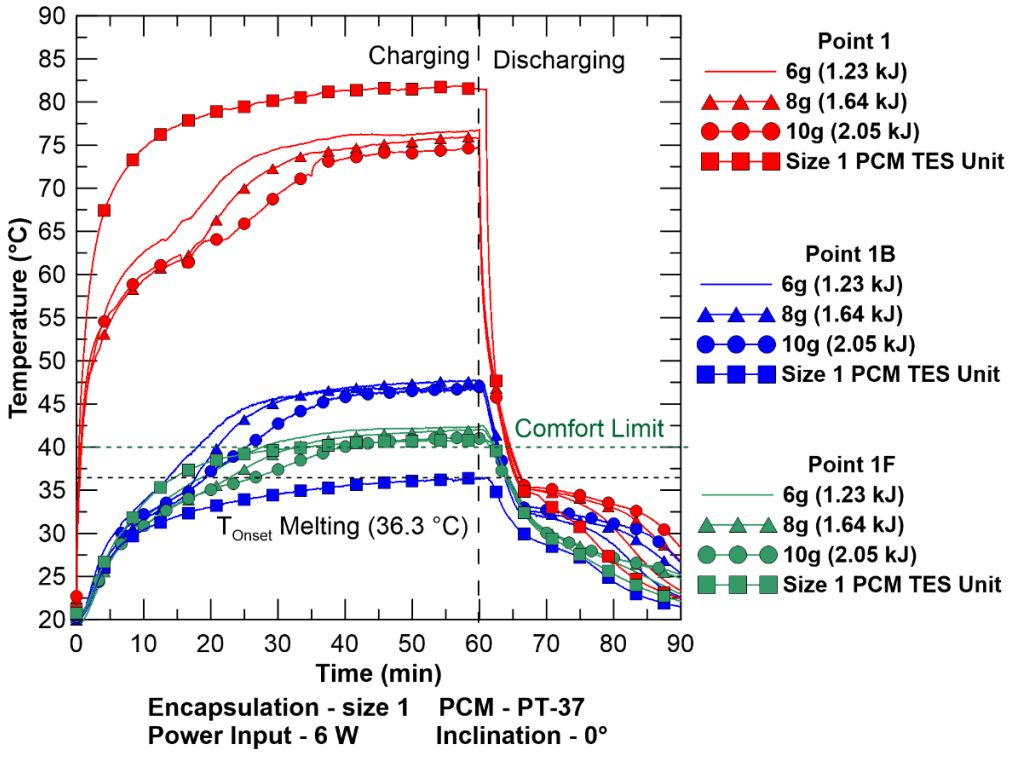

Figure 5-14 Comparison between size 1 PT-37 TES unit with smaller PT-37 TES units having different latent heat at 6 W power input and 45° inclination.

Due to the smaller sizes, these TES units had a significantly lower surface area compared to the previous types of TES units (size 1-3). As a result, more heat was conducted through the PCM to the back causing higher back cover temperature due to the presence of a large air gap inside the tablet PC. IR mages of the back cover with small TES units (Fig. 5-15) clearly show that after 60 minutes of charging the back cover temperature is not as well distributed as shown in Fig. 5-13 for bigger TES units. As all of these small TES units had similar base area (2″ × 2″), the air gap and thus thermal resistance inside the tablet PC is expected to be the same for all three cases. After 30 minutes of discharging, however, increasing back cover temperature was observed with increasing latent heat. This mainly happened as more energy was absorbed with increasing latent heat which took longer to release.

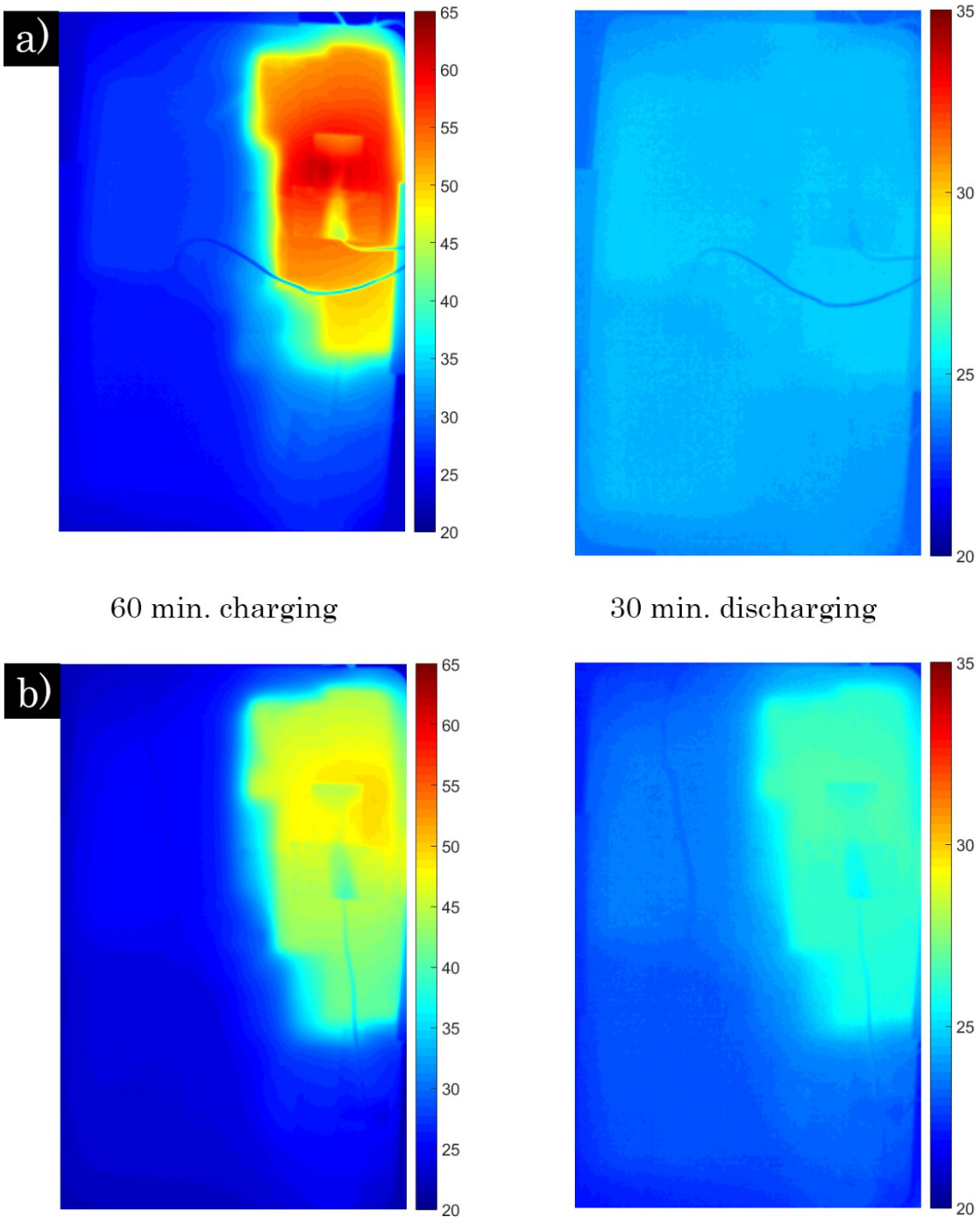

Figure 5-15 Thermal images showing the effect of latent heat on the thermal performance of the experimental tablet PC at 6 W power input and 45° inclination during continuous operation: a) Baseline b) 6g PT-37 (ΔH - 1.23 kJ).

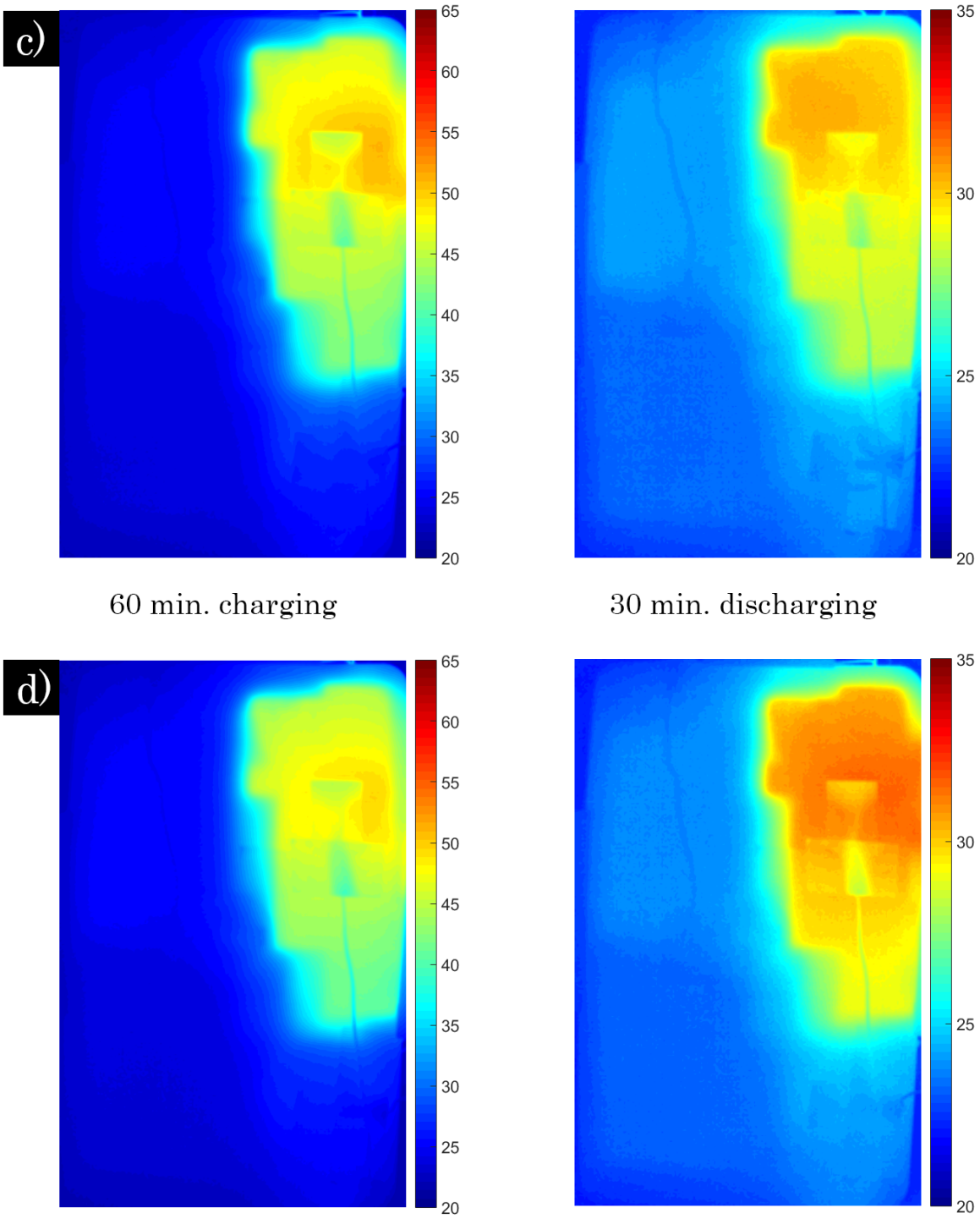

Figure 5-15 Thermal images showing the effect of latent heat on the thermal performance of the experimental tablet PC at 6 W power input and 45° inclination during continuous operation: c) 8g PT-37 (ΔH - 1.64 kJ) d) 10g PT-37 (ΔH - 2.05 kJ).

From Fig. 5-16, it is evident that increasing latent heat provided a better transient response of the tablet PC. Slight decrease of the peak temperature of the heater was observed with increasing latent heat. With increasing latent heat more energy from the heater was absorbed into the PCM which resulted in a decrease in the heater temperature. Increasing latent heat also delayed reaching a threshold temperature selected as 70 °C for illustration purposes; a 33% increase in latent heat (8 g case) delayed by 5 minutes and a 66% increase in latent heat (10 g case) delayed by almost 10 minutes the time need to reach 70 °C compared to 6 g case (see Fig 5-16a). The comparison between Fig. 5-16a and 5-16b shows that variation on latent heat between *n*-eicosane and PT-37 resulted in slight deviation during the transient heating phase. With 16% higher latent heat, *n*-eicosane provided lower transient temperature of the back cover and increased operation time of the tablet PC before crossing the user comfort limit.

During the discharging phase, supercooling might cause a sudden jump in the temperature with *n*-eicosane (Fig. 5-16a) which was less prevalent in the case of PT-37 (Fig. 5-16b). During the measurement of thermo-physical properties of PCMs (section 4.1), the DSC curve of *n*-eicosane indicated the presence of supercooling in *n*-eicosane. Due to the high level of purity (99%) of the used PCM (Alfa-Aesar, 2015) and the absence of nucleation agent during solidification, slight supercooling in *n*-eicosane can be expected. However, with thin 1/16″ (2 mm) typical TES units (size 1-3) supercooling was rare for both PCMs.

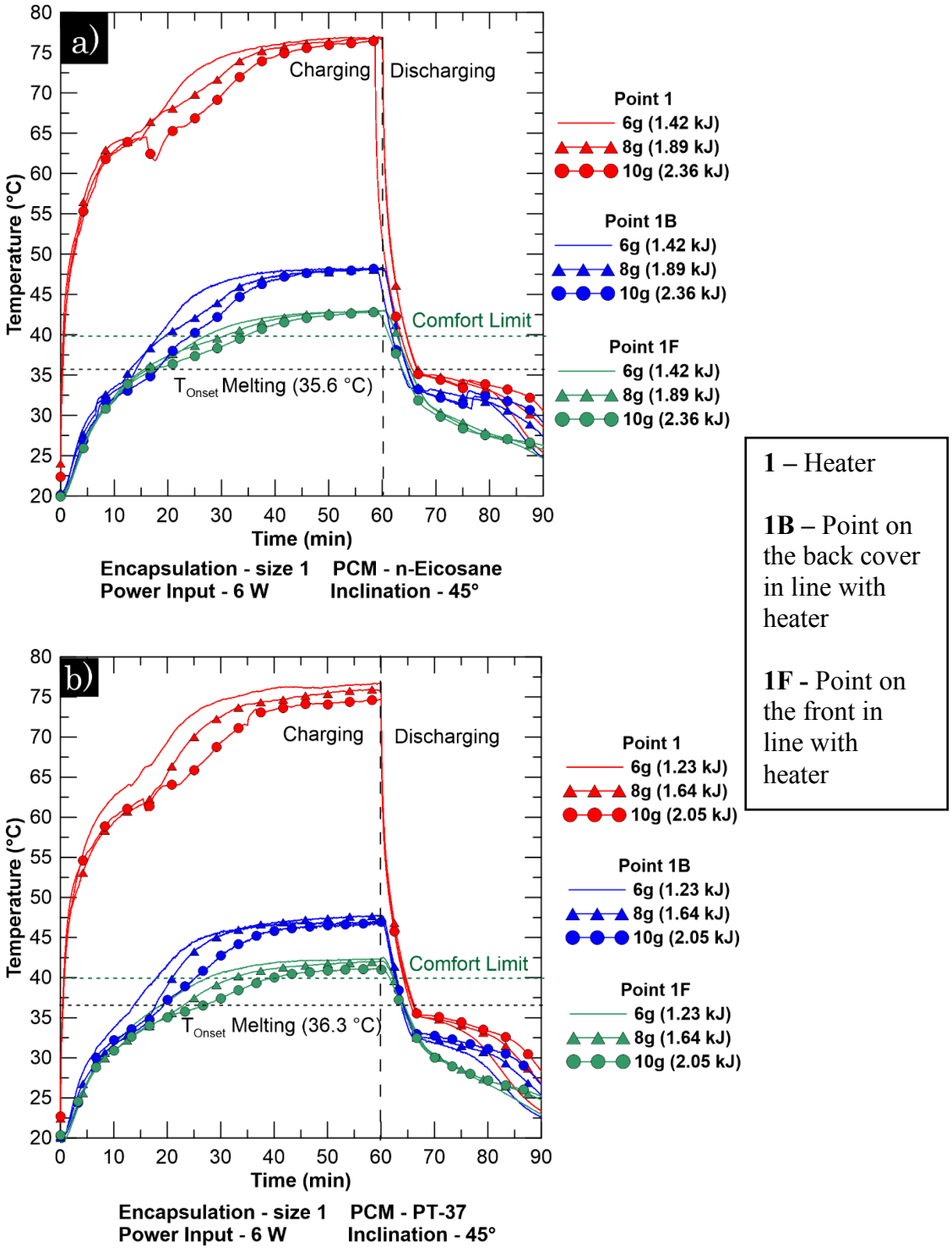

Figure 5-16 Effect of varying latent heat on thermal response of the experimental tablet PC at 6 W power input and 45° inclination: a) *n*-eicosane b) PT-37.

5.3 Summary

Thermal management of a tablet PC using PCMs was investigated under continuous operation. Performance of the tablet PC was observed at various operating conditions such as different power input levels and angular orientations. Moreover, effect of varying size of PCM TES unit and variation of latent heats were also investigated.

Increasing the angle of orientation resulted in slight decrease in the peak PCM temperature. This can be attributed to the complex three dimensional flow structures inside the PCM TES units. The back cover temperature was also reduced with increased inclination. The front temperature of the tablet PC, however, was mainly dependent on the natural convection coefficient. Increased inclination resulted in increased convection coefficient and thus resulting in a lower front temperature.

Increased power input level resulted in higher rate of PCM melting. With increasing power input level melting of PCMs was also increased. As a result, more latent heat was absorbed with increasing power input levels which provided a comfortable back cover temperature at all power input levels tested.

The PCM TES unit provided lower back cover temperature even without any PCM melting. PCM TES units reduced the amount of air gaps inside the tablet PC which resulted in better distribution of heat from the reduction of thermal resistance of air gaps. Better thermal performance of the tablet PC during the transient operation was observed with increasing latent heat of PCMs. Increasing latent heat of PCMs also provided lower heater temperature due to more energy storage in PCMs.

In this section, results show that during continuous operation PCM TES units can be used effectively under different usage conditions of a tablet PC. Tablet PC manufacturers can be benefitted from this study by incorporating PCMs into the system as an inexpensive thermal management technology.

Chapter 6

Results and Discussion: Intermittent Operation

The results obtained during the intermittent operation tests along with observations from the experiments and discussions of the noteworthy points from those experiments are presented in this chapter. The present chapter is arranged in a fashion similar to Chapter 5 with two main sections: i) melting and solidification of PCMs and ii) performance of the tablet PC. In the first section, only melting and solidification phenomena of PCMs with size 1 and size 2 PCM-based TES units are discussed. In the second section, the performance of the tablet PC under the application of PCM-based TES units is presented. Results with all three PCM-based TES units along with three additional PCM-based TES units having same base area but different thicknesses are also covered. Table 6-1 shows the summary of all experiments done during the continuous operation of the tablet PC.

During normal usage of tablet PCs, the load on the chip varies randomly from time to time. There are situations where tablet PC users make an online video call or play games for a certain short duration of time and immediately after that the tablet PC goes into an idle state releasing the chip from the heavy computational load. Hence, it is necessary to observe the effectiveness of PCM-based TES units under regular usage patterns unlike the experiments conducted in the previous section. To accomplish this task, all experiments for the experimental tablet PC with and without PCM-based TES units were conducted for three cycles of 15 minutes of charging followed by 15 minutes of discharging.

Table 6-1 Summary of experiments done in the intermittent operation.

Observations	PCMs	Size of TES Unit (mass of PCMs)	Inclination	Power Input	Operation Mode
Melting-Solidification of PCMs	• *n*-Eicosane • PT-37	• Size 1 (16g) • Size 2 (11g)	• 0° (horizontal) • 45° • 90° (vertical)	• 2 W • 4 W • 6 W • 8 W	3 cycles of: • Charging – 15 minutes. • Discharging – 15 minutes.
Performance of the Tablet PC	• *n*-Eicosane • PT-37	• Size 1 (16g) • Size 2 (11g) • Size 3 (25g) • 2″ ×2″ ×0.12″ (6g) • 2″ ×2″ ×0.16″ (8g) • 2″ ×2″ ×0.20″ (10g)	• 0° (horizontal) • 45° • 90° (vertical)	• 2 W • 4 W • 6 W • 8 W	3 cycles of: • Charging – 15 minutes. • Discharging – 15 minutes.

6.1 Melting and Solidification of PCMs

A typical melting curve for size 2 *n*-eicosane TES unit at 45° inclination and 8 W power input can be seen in Fig. 6-1. Similar to continuous operation, even with 8 W of power input, melting of *n*-eicosane inside the TES unit was partial. During the discharging phase, the time required to reject the latent heat (almost 5 minutes) during the intermittent operation is significantly lower compared to the continuous operation (almost 15 minutes as can be seen in Fig. 5-1). This mainly occurs due to the higher latent heat storage during the continuous operation even at the same heat input level (8 W) due to longer operation time. After 15 minutes of discharging the temperature registered at P1 and P3 thermocouples are almost 30 °C which is significantly higher than room temperature (~20 °C). This means that after 15 minutes of discharging, the PCM still stores some sensible heat which in turns results in a gradual increase of the peak temperature after 15 minutes of charging in subsequent cycles as can be seen from Fig. 6-1. Additional melting curves can be found in Appendix C.

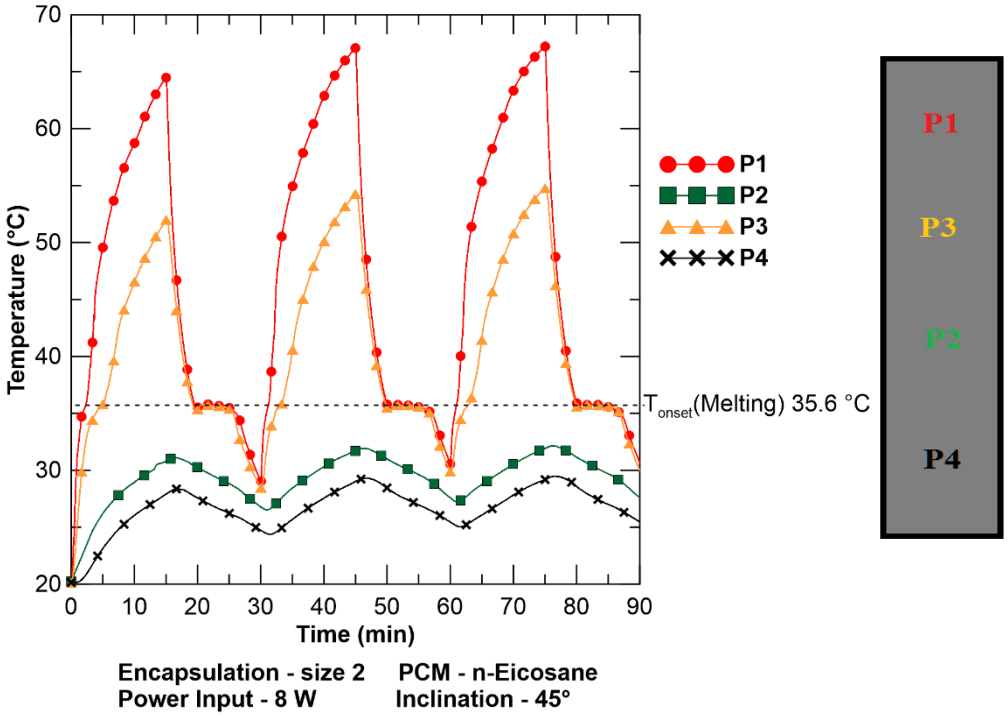

Figure 6-1 Melting curves of *n*-eicosane for intermittent operation with size 2 TES unit at 45° inclination and 8 W power input.

6.1.1 Effect of Inclination

Figure 6-2 shows the intermittent temperature responses of four thermocouples inserted into size 1 PCM-based TES units with both PCMs for different inclination angles when the power level was kept at 6 W. Observations similar to the continuous operation case can be seen during the sensible heating phase. Identical curves during sensible heat storage imply that conduction is the main form of heat transfer. Unlike the continuous operation, the effect of inclination is not very noticeable after 15 minutes of charging as can be seen from Figs. 6-2a and 6-2b. The fluctuations among 0°, 45°, and 90° inclination were attributed to the three-dimensional and unstable flow structures in the liquid PCM in case of the continuous operation (section 5.1.1). However, only 15 minutes of charging (heat addition) does not melt enough PCM to produce the unstable flow structures and thus no noticeable fluctuations among 0°, 45°, and 90° inclinations occur. Also unlike the continuous operation, no PCM melting was observed at point P3 after 15 minutes of charging. This can be explained by the fact that there is not enough time to reach the melting temperature

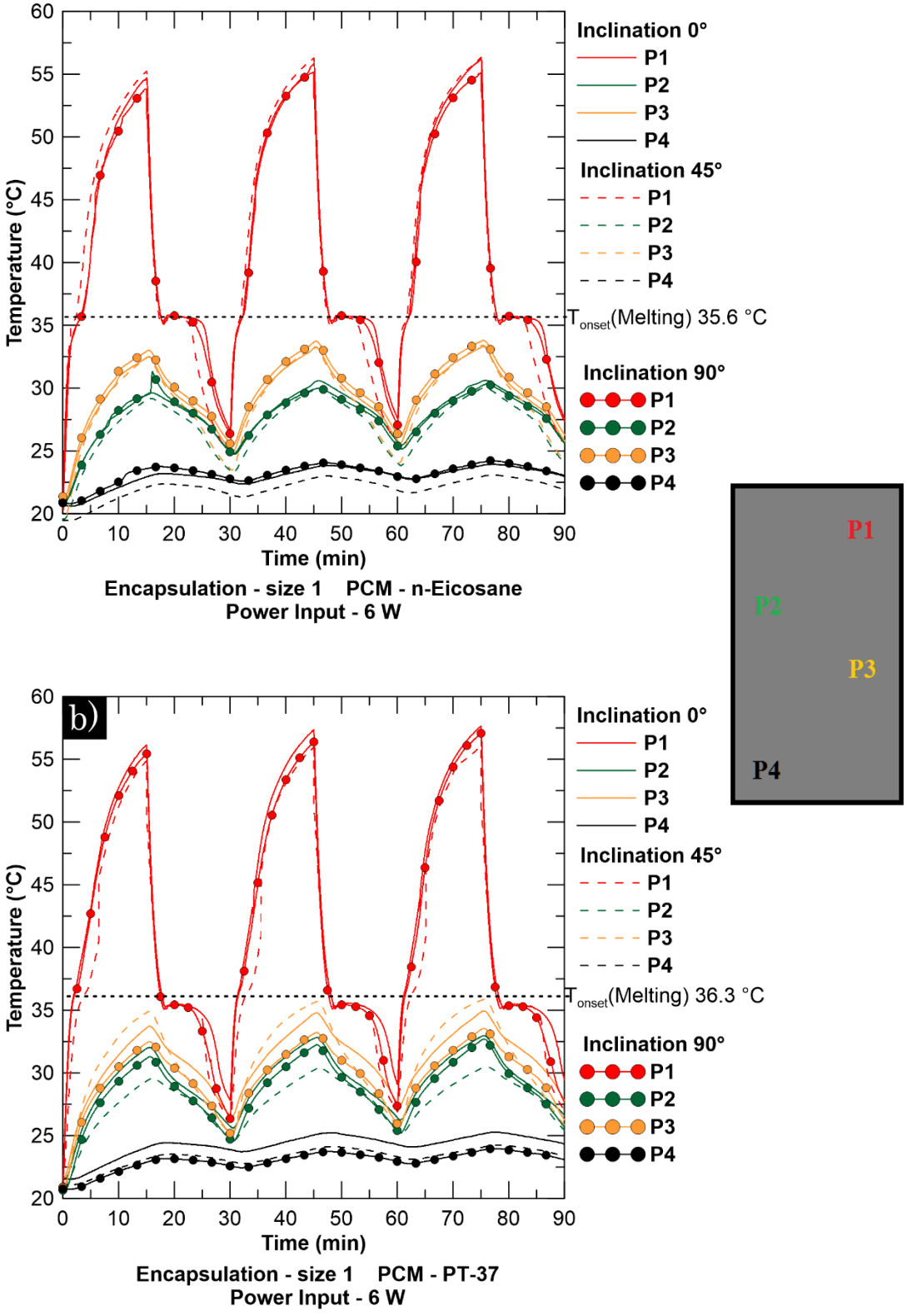

Figure 6-2 Effect of inclination on PCM melting during intermittent operation at 6 W power input with size 1 PCM-based TES Unit a) *n*-eicosane b) PT-37.

of PCMs. From Fig. 5-2, it can be seen that a time interval of almost 20 minutes of charging (heat addition) is required to melt the PCM at point P3 during the continuous operation. Previous sections have shown that variation of latent heat between n-eicosane and PT-37 did not contribute much in the thermal response of the tablet PC. As a result, the slightly higher temperature in PT-37 can be attributed to the uncertainty in power input. Conclusions similar to continuous operation can be drawn for the low temperature region (P2 and P4) due to the lack of PCM melting. PCM at these points did not contribute to any latent heat storage as well.

6.1.2 Effect of Power Input Levels

Figure 6-3 shows the effect of different power input levels on the melting of the two PCMs, during the intermittent operation for size 1 PCM-based TES unit at 0° inclination. The increase of the peak temperature is proportional to the heat input. Moreover, an increasing trend of temperature in the following cycles was also observed which mainly occurs due to the partial heat rejection during the discharging phase. For instance, at 8 W power input, the sensible heat release was almost negligible in the second and the third cycle of discharging phase for PT-37 (Fig. 6-3b). Similar to the continuous operation higher heat input resulted in more latent heat storagewhich resulted in a longer duration of latent heat release during the discharging phase. At lower heat input, the melting rate was also lower. Hence, the slope of the melting curve becomes less steep. Due to smaller duration of the charging (heating) phase, the PCM at point P3 did not reach the melting temperature and no PCM melting was observed.

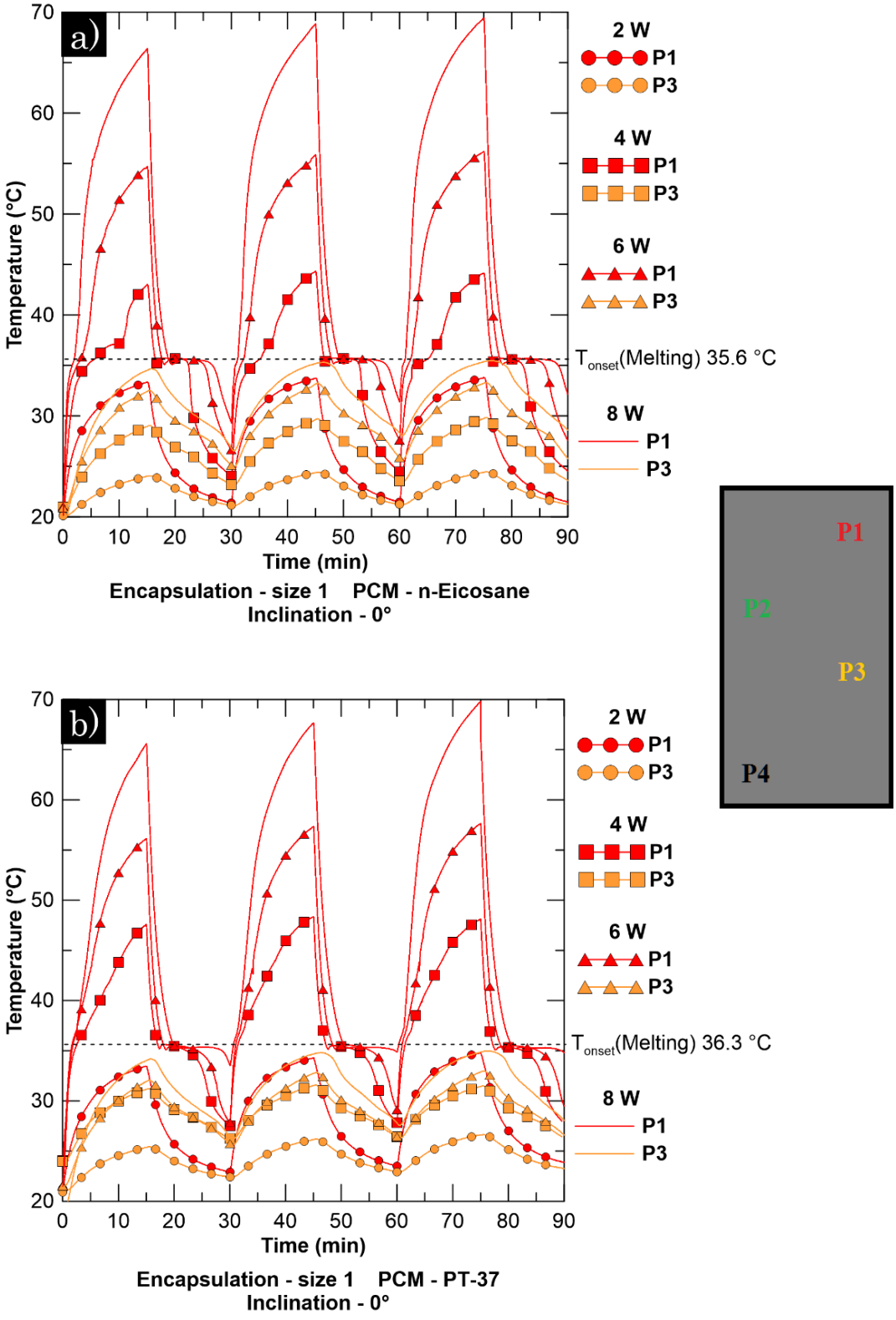

Figure 6-3 Effect of power input on PCM melting at 0° inclination with size 1 PCM-based TES Unit during intermittent operation: a) *n*-eicosane and b) PT-37.

6.1.3 Effect of TES Unit Size

Figure 6-4 shows the effect of PCM-based TES unit size on the melting curve of both PCMs, *n*-eicosane and PT-37, at 6 W power input and 0° inclination during the intermittent operation. After 15 minutes of charging, size 1 *n*-eicosane TES unit resulted in almost 5 °C increase of the peak temperature of point P1 compared to the size 2 *n*-eicosane TES unit (Fig. 6-4a). Similar occurrences were observed in the case of the continuous operation (Fig. 5-5) after 15 minutes of charging. In the case of PT-37, the deviation in the peak temperature of point P1 was almost 10 °C in the first cycle (Fig. 6-4b). This further deviation occurs due to a higher amount of PT-37 melting in size 2 TES unit compared to size 2 *n*-eicosane TES unit. This can be verified from the subsequent cycles of PCM melting where the melting effect is slightly less which leads to a higher peak temperature of point P1. Loading of more PCMs on the top of the heater in the case of size 2 PT-37 TES unit might be one of the reasons behind this phenomenon.

Due to the closer position of the P3 thermocouple to the heater, significant melting of the PCM was observed with size 2 PCM TES unit for both PCMs. However, with the size 1 PCM TES unit, the PCM at point P3 only stored sensible heat without experiencing any melting. Though for the continuous operation (Fig. 5-5) with size 1 PCM TES unit melting of PCMs at the P3 point was observed after a sufficient amount of time, at 15 minutes, point P3 temperature does not reach the melting point of PCMs. Hence, results for intermittent operation conform to the results found with continuous operation. In the case of point P2 and P4, no noticeable differences between continuous and intermittent operation were found.

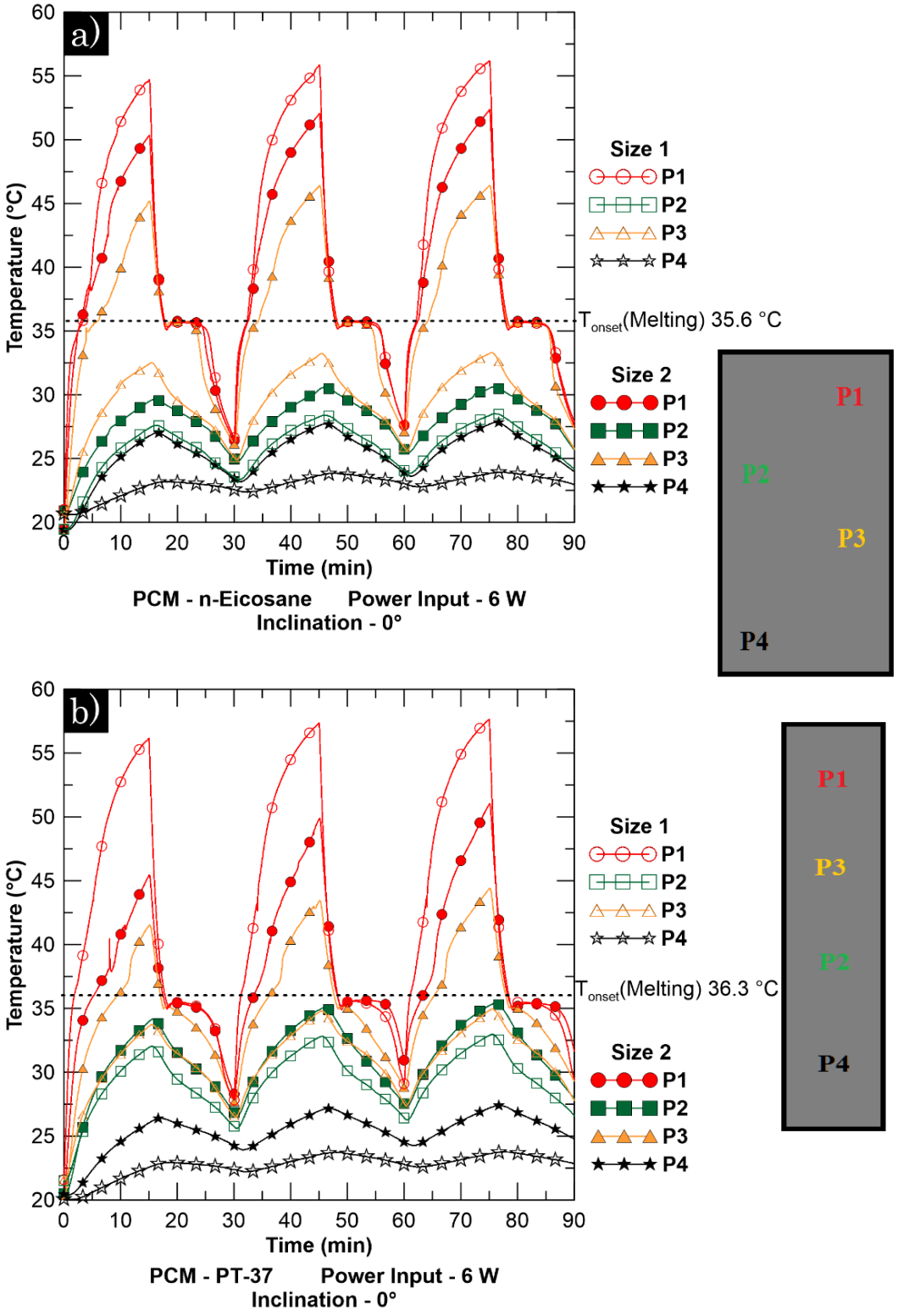

Figure 6-4 Effect of PCM TES size on PCM melting during intermittent operation at 6 W power input and 0° inclination: a) *n*-eicosane and b) PT-37.

6.2 Performance of the Tablet PC

All experiments using the experimental tablet PC were conducted for three cycles of 15 minutes of charging (heating) followed by 15 minutes of discharging. Similar to the continuous operation case, the operations of the experimental tablet PC without any PCM-based TES unit in a horizontal position (inclination 0°) are considered as baseline conditions for intermittent operation study. The temperature response of the experimental tablet PC at different power input levels can be seen in Fig. 6-5. Due to similar reasons as the continuous study, the point 2F has a higher temperature than point 2B (see Fig. 4-12), even though the heater is placed on the back side of the PCB. Based on all baseline operations, only temperature variations of the heater (point 1), point 1B on the back cover and point 1F on the front display are considered as performance parameters.

A typical comparison of size 1 PT-37 TES unit performance on the tablet PC with baseline operation at 6 W heat input and 0° inclination can be seen in Fig. 6-6. The back surface just above the heater (point 1B) experienced an almost 22 °C reduction in the temperature compared to the baseline operation case. Similarly, the point on the front (display), in line with the heater (point 1F), had almost 5 °C reduction using the PCM-based TES unit similarly to the case of the continuous operation. Moreover, throughout the whole intermittent operation, the back cover temperature never exceeded the user comfort limit of 40 °C at 6 W power input. The effect of size 2 and size 3 TES units on the thermal performance of the tablet PC during the intermittent operation can be found in Appendix D.

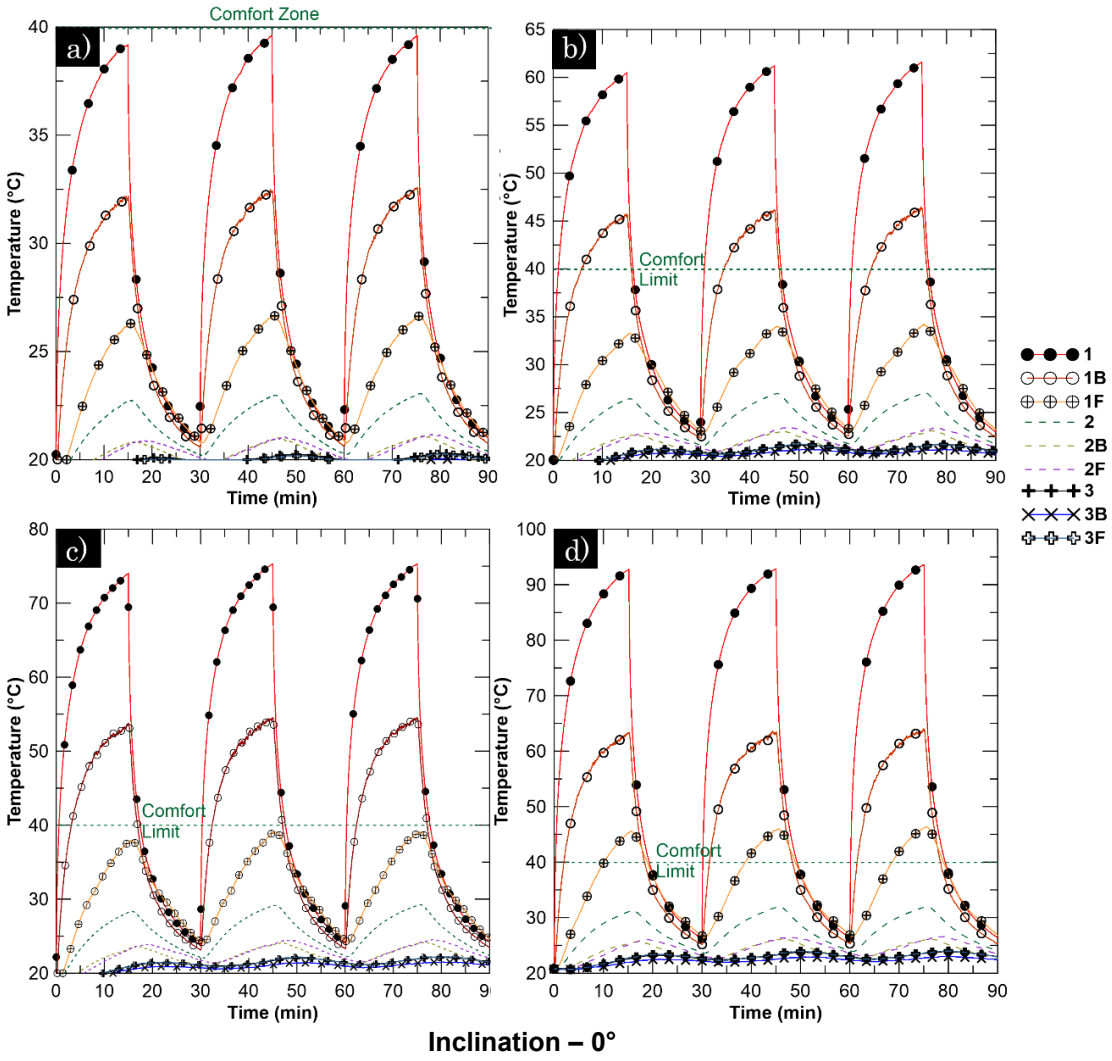

Figure 6-5 Baseline temperature curves of the experimental tablet PC at different power inputs for intermittent operation: a) 2 W b) 4 W c) 6 W d) 8 W.

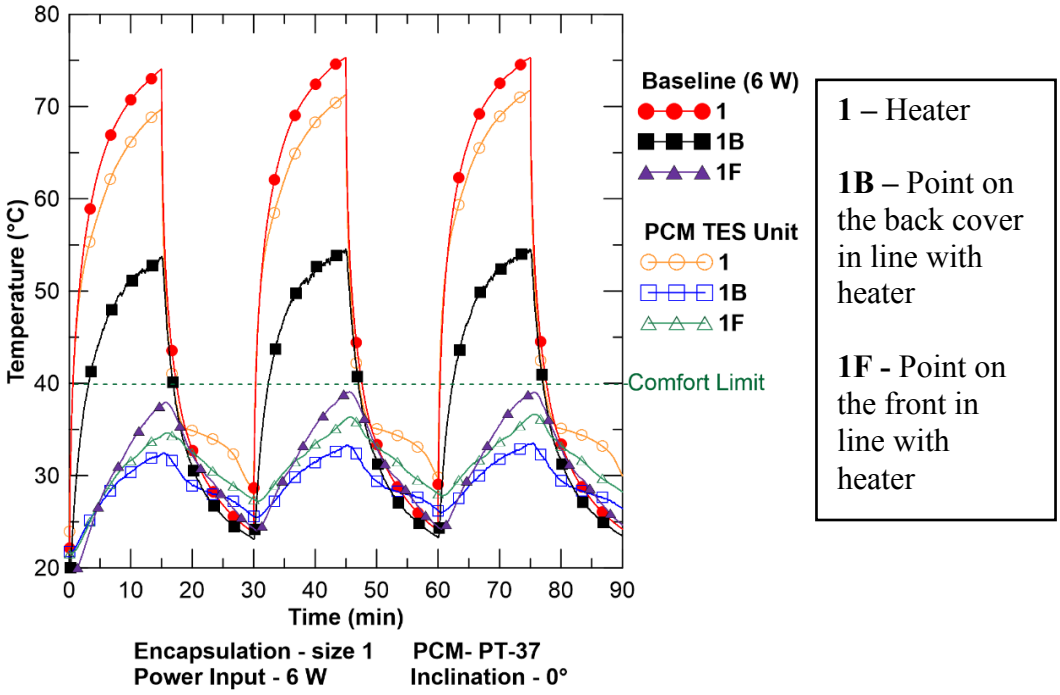

Figure 6-6 Effect of Size 1 PT-37 TES unit on the thermal response of the experimental tablet PC at 0° inclination and 6 W power input for intermittent operation.

6.2.1 Effect of Inclination

Figure 6-7 shows the thermal response of the experimental tablet PC for various angular orientations at 6 W power input with size 1 PCM TES unit. No specific variations in the peak temperature of the heater were found with inclination. As latent heat storage in PCM was almost similar at different inclination

The natural convection resulted in a slight deviation in the thermal responses between 0°, 45° and 90° inclination as expected. Unlike the continuous operation, deviations in the temperatures of points 1B and 1F were not significant after 15 minutes of charging during the intermittent operation. This deviation would be the same as the continuous operation case if sufficient time during the charging phase was allowed under intermittent operation. Looking at Fig. 5-10, it is clear that deviation at point 1B and 1F after 15 minutes of charging is smaller than the deviation after 60 minutes of charging.

The back and front (display) side temperatures recorded in case of the intermittent operation, were almost 7 °C lower compared to the continuous operation. Considering the slight effect of orientation on the thermal performance of the tablet PC and the favorable

back cover temperatures, the PCM-based TES units can be expected to work reliably in a practical situation with intermittent usage.

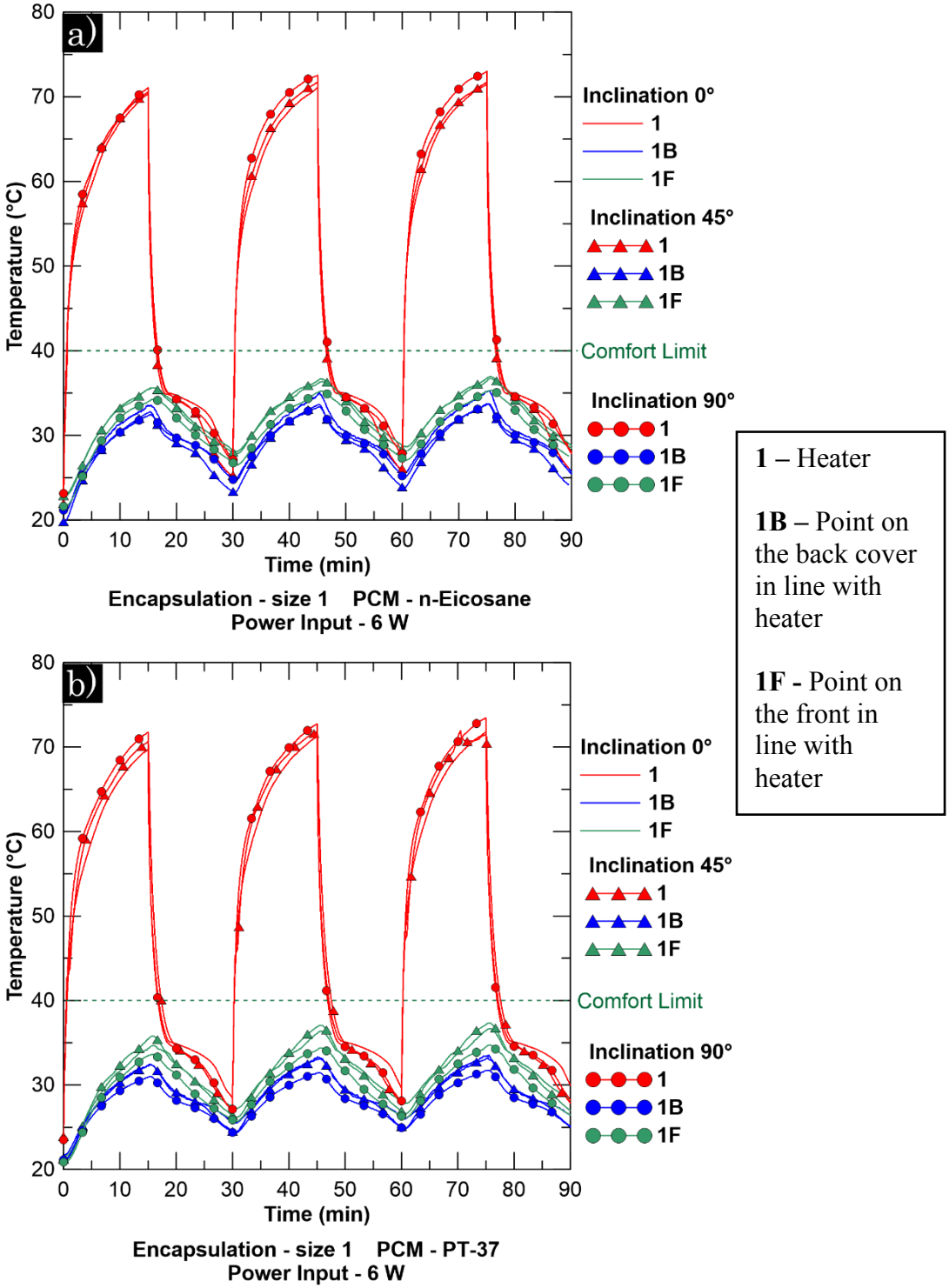

Figure 6-7 Effect of inclination on the thermal response of the experimental tablet PC during intermittent operation at 6 W power input with size 1 PCM TES Unit a) *n*-eicosane b) PT-37.

6.2.2 Effect of Power Input Levels

The effect of power input levels on the thermal performance of the experimental tablet PC with size 1 PCM TES units with both PCMs and at 0° inclination can be seen from Fig. 6-8. The peak heater temperature was found to be proportional to the power input levels and no effect of PCM melting can be observed. The comparison of the point 1F (display) temperatures in cases of continuous (Fig. 5-11) and intermittent operations shows no noticeable difference between their temporal evolutions, as no PCM-based TES units were placed on the front side of the PCB. At 8 W power input, the heater (point 1) temperature reaches almost 90 °C for *n*-eicosane and PT-37 based TES units (slightly more than 90 °C in PT-37 due to power input uncertainty). This means that even at intermittent operation the heater temperature crossed the threshold of 85 °C, the maximum chip temperature allowed by Intel Corporation in their electronic devices for safe operations. Hence, it is suggested that 8 W power input should be avoided in this particular tablet PC to maintain allowable maximum chip temperature using thin PCM-based TES units similar to the continuous operation. From the discharging phase, it can be seen that rejection of latent heat at 8 W power input also took a similar period of time as 6 W power input. However, back cover temperatures for all power input levels were within the user comfort limit.

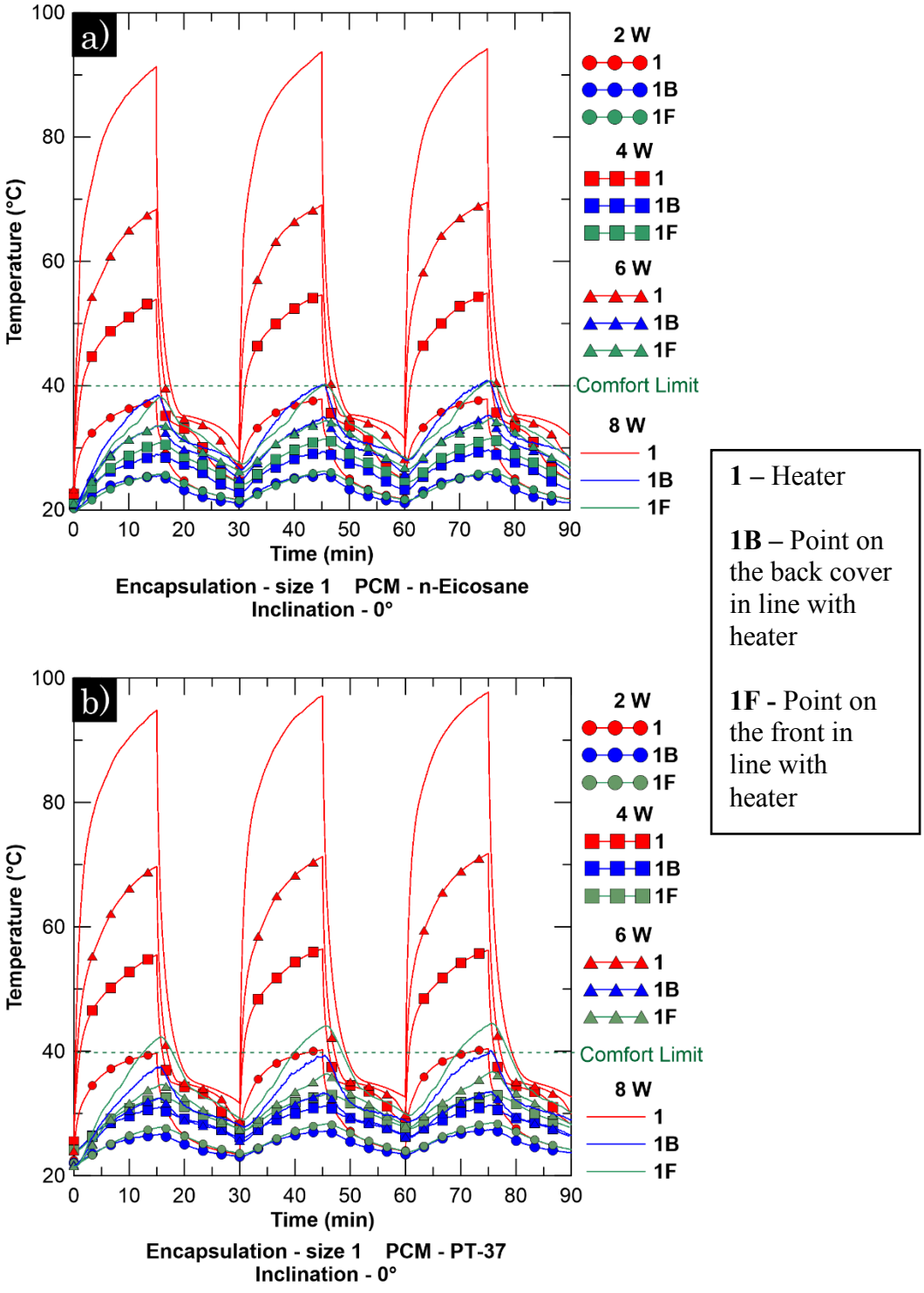

Figure 6-8 Effect of power input levels on the thermal response of the experimental tablet PC during intermittent operation at 0° inclination with size 1 PCM TES unit a) *n*-eicosane b) PT-37.

6.2.3 Effect of TES Unit Size

The effect of PCM TES unit size on the thermal response of the experimental tablet PC during intermittent operation at 6 W power input and 0° inclination can be seen from Fig. 6-9. The variation of the temperature response in cases between *n*-eicosane and PT-37 TES units due to the differences in their latent heat was not very noticeable. Similar to the case of continuous operation, both for *n*-eicosane and PT-37, size 3 TES unit provided the lowest temperature on the back cover (point 1B) after 15 minutes of charging. Having higher heat storage and allowing the least air gaps inside the tablet PC the size 3 TES unit resulted in a better thermal performance of the tablet PC compared to the two other TES units. Due to the similar reasons size 2 PCM TES unit resulted in the highest back cover temperature due to a smaller size and less heat stored into PCMs.

As seen from the continuous studies (Fig. 5-12), the front (display) side had a higher temperature compared to the back cover temperature. A very slight increase in the peak temperature of the heater, display, and back cover in subsequent cycles can be noticed. However, it largely depended on the amount of latent heat rejected at the discharging phase. This fact was more pronounced in systems with more latent heat and can be seen in the following section. IR images of the back cover showing the effect of PCM-based TES unit size during intermittent operation can be seen in Appendix E.

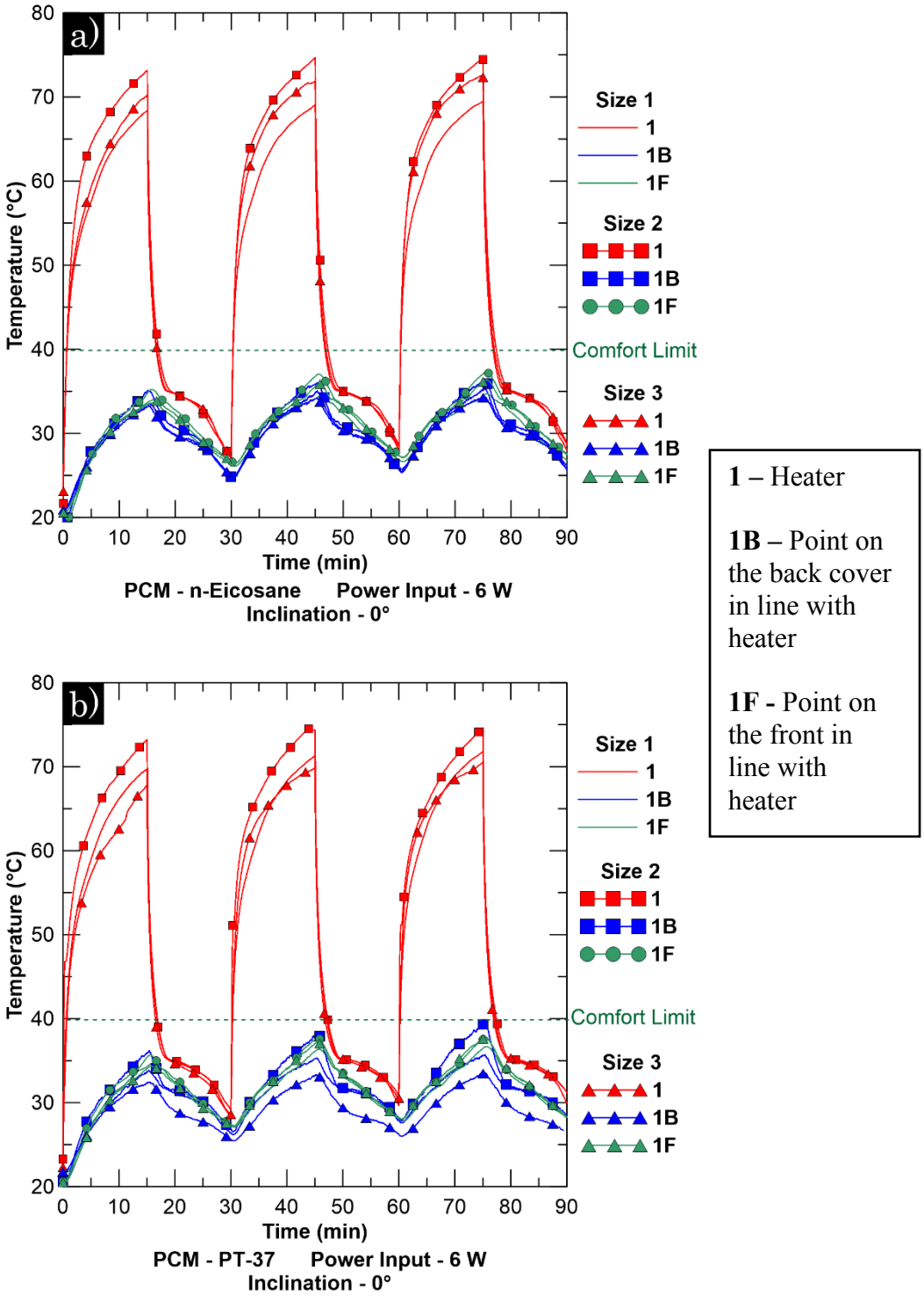

Figure 6-9 Effect of PCM TES size on the thermal response of the experimental tablet PC during intermittent operation at 6 W power input and 0° inclination: a) *n*-eicosane and b) PT-37.

6.2.4 Effect of Varying Latent Heat

Figure 6-10 shows the comparison between typical size 1 PCM TES unit and smaller encapsulations with different latent heat for PT-37 PCM during intermittent operation. Similar to the continuous operation (Fig. 5-14) heater temperature was reduced significantly due to more latent heat storage. Moreover, the back cover temperature was also significantly higher. Due to higher internal thermal resistance from the presence of air gaps in the tablet PC, heat tends to escape through the PCM TES units to the back cover thus leading to a higher temperature hot spot on the back cover. However, it is interesting to note that size 1 PCM TES unit had relatively quicker heat rejection. As a result, in subsequent cycles, peak temperatures of the heater and back cover remained almost constant. On the other hand, due to partial latent heat rejection during the discharging phase, peak temperatures of the heater and back cover increased in subsequent cycles with smaller encapsulations.

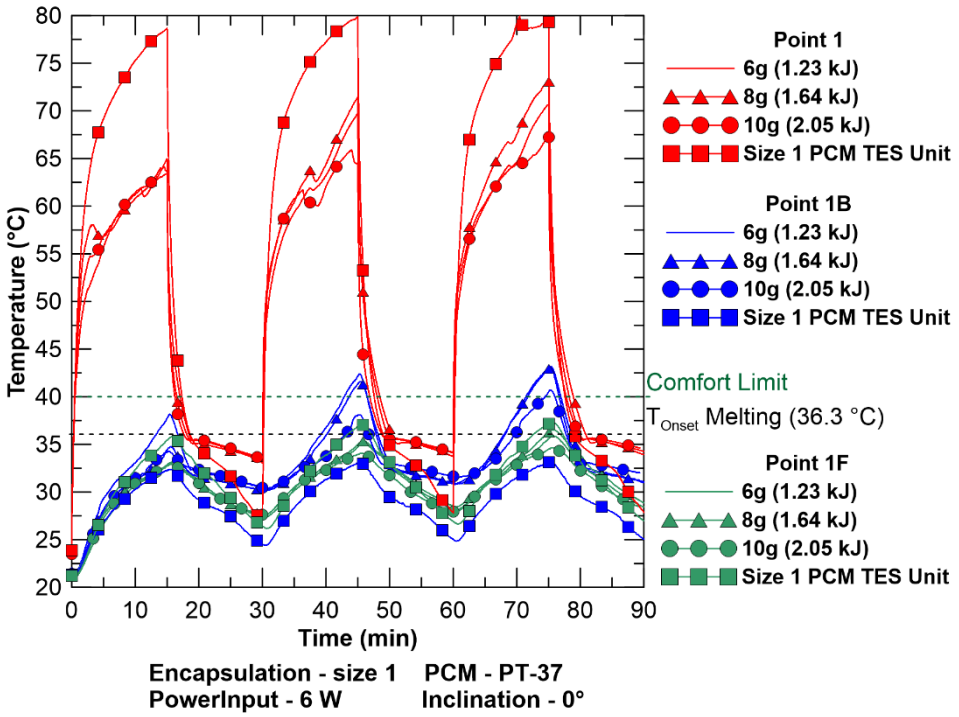

Figure 6-10 Comparison between size 1 PT-37 TES unit with smaller PT-37 TES units having different latent heat at 6 W power input and 45° inclination during the intermittent operation.

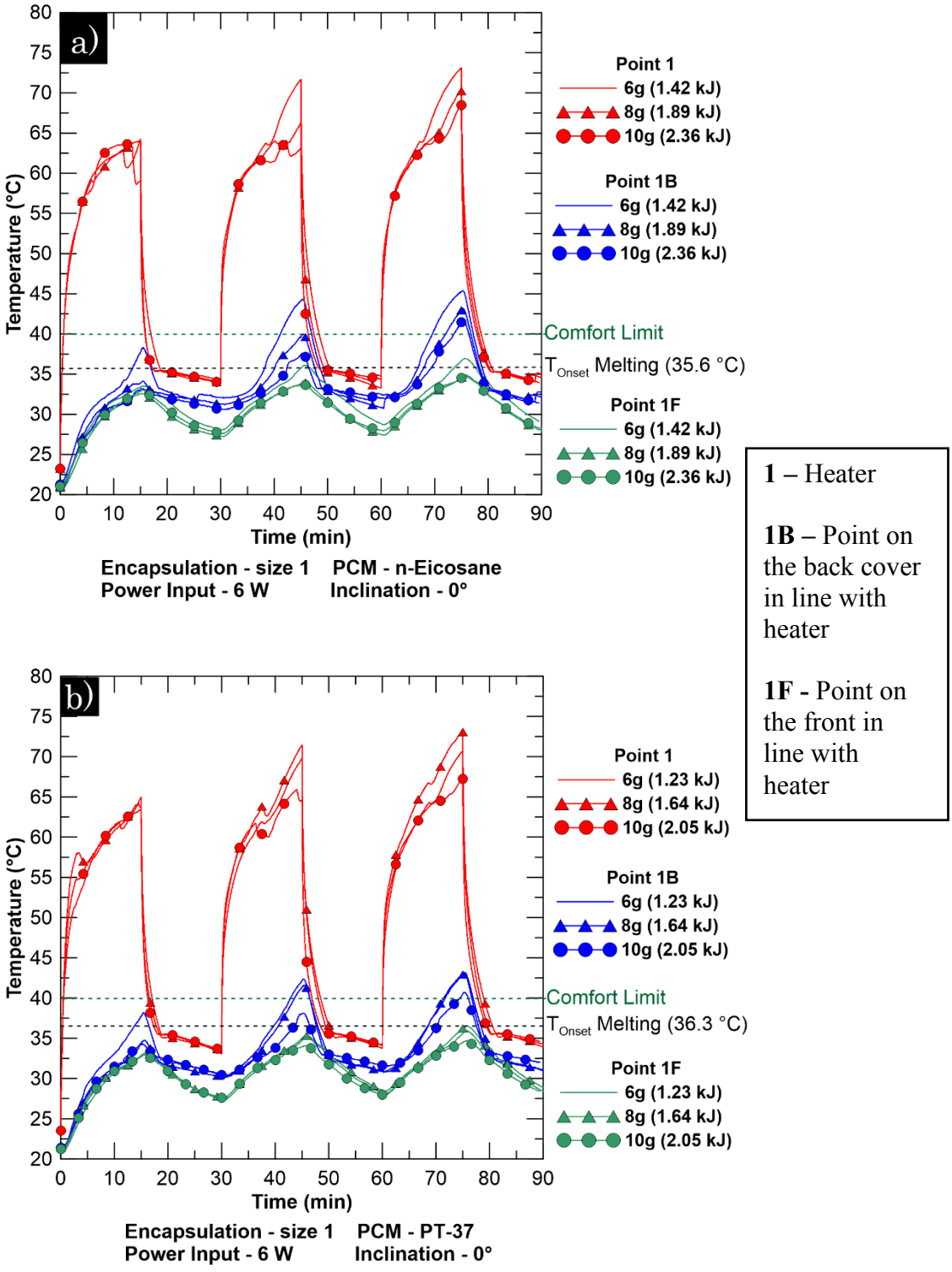

Figure 6-11 Effect of varying latent heat on the thermal response of the experimental tablet PC for the intermittent operation at 6 W power input and 45° inclination a) *n*-eicosane b) PT-37.

Figure 6-11 shows a very little deviation of peak heater temperature with varying latent heat after 15 minutes. From Fig. 5-14, it can be seen that, for continuous operation, the effect of varying latent heat on the heater temperature was more distinct in 20–40 minutes of heating range. Since during the intermittent operation, heating was stopped after 15 minutes, the effect of varying latent heat was negligible.

No noticeable difference between *n*-eicosane and PT-37 was observed as usual. Due to less heat storage in the TES unit with 6g of PCM, the back cover temperature was slightly higher compared to the two other (8, 10g) PCM-based TES units. The back cover temperature was increased from 37 to 45 °C in the final cycle of operation for both PCMs due to stored heat built up at the end of each previous cycles. Hence, component–wise PCM-based TES units should be used along with heat spreaders to distribute heat uniformly and avoid a concentrated hotspot on the back cover. IR images of the back cover showing the effect of varying latent heat during intermittent operation can be seen from Appendix E.

6.3 Summary

An approach similar to the one presented in Chapter 5 was undertaken for the study of thermal management of the tablet PC using PCM under intermittent operation. The performance of the tablet PC was observed at various operating conditions such as different power input levels and angular orientations. Moreover, the effect of the varying size of PCM TES unit and variation of latent heats were also investigated.

No effect of inclination was observed on the melting of PCMs. This was attributed to the absence of any significant amount of complex three dimensional flow structures inside the PCM TES units due to insufficient melting achieved with only 15 minutes of heating. The back cover temperature was also unaffected with increased inclination. The front temperature of the tablet PC, however, was dependent on the natural convection coefficient, similar to the continuous operation study. Increased inclination resulted in increased convection coefficient and thus resulting in a lower front temperature.

Increased power input level resulted in higher rate of PCM melting. With increasing power input level melting of PCMs was also increased. As a result, more energy was absorbed with increasing power input levels which provided a comfortable back cover temperature at all power input levels.

The reduction in the air gaps inside the tablet PC through the addition of PCM TES units resulted in better distribution of heat from the reduction of thermal resistance associated with air. Better thermal performance of the tablet PC during the transient operation was observed with increasing latent heat of PCMs. Increasing latent heat of PCMs also provided lower heater temperature due to more energy storage in the PCM. Results show that during intermittent operation, PCM TES units can be used effectively under different usage conditions of a tablet PC.

Chapter 7

Conclusions and Recommendations

7.1 Conclusions

In this study, the role of PCM-based TES systems in the thermal management of tablet PCs at different power input levels and different angular orientations for continuous operation as well as intermittent operation was investigated. Experiments were carried out for two PCMs, *n*-eicosane and PT-37, and for three different sizes of PCM-based TES units, loaded with different amounts of PCMs. The selection of the PCMs was based on their melting temperatures to fulfill the operating comfort limit required by the tablet PC users. Moreover, smaller PCM-based TES units, placed only on the component (*i.e.* heater), were also introduced and investigated under specific operating conditions. The 6 W power input tests were mainly used to compare the resulting thermal responses with the ones measured in case of the original tablet PC. The following conclusions can be made from the current work:

1. While the melting of PCM provided better thermal performance at transient operations, elimination of air gaps by placing PCM TES units inside the tablet PC provided overall lower steady-state temperature of the tablet PC due to better internal heat distribution. Even without any PCM melting at 2 W power input, size 1 PT-37 TES unit resulted in 8 and 7 °C temperature reductions of the back cover for continuous and intermittent operations respectively. It was found that larger PCM-based TES units provided lower back cover temperature due to a bigger base area which filled more air gaps and reduced internal thermal resistance. However,

more PCMs inside larger TES units had a very little effect on the transient thermal response of the tablet PC due to the incomplete melting of PCMs.

2. The thermal response of the experimental tablet PC with PCM-based TES units was observed at different angular orientations. PCM-based TES units were found to be useful to maintain a favorable thermal performance of the tablet PC at various angular orientations. Results showed that while the back cover temperature of the tablet PC was dictated by the PCM melting curves, natural convection played a major role in the thermal response on the front (display) side. Due to a higher convection heat transfer, the display temperatures at 45° and 90° (vertical) inclinations were lower than the one at horizontal orientation (0°).

3. PCM-based TES units effectively maintained the comfortable back cover temperature of the tablet PC at all power input levels. Hence, it can be concluded that the present PCM-based TES units can be used for regular usage loads as well as for the heavy usage loads without compromising tablet PC users' comfort. However, at 8 W power input the chip temperature was reached almost 90 to 100 °C for both continuous and intermittent operations which was higher than the allowable chip temperature (85 °C) prescribed by most computer chip manufacturers. But, this was an extreme test case which had a significantly higher power input level than the original tablet PC.

4. Smaller PCM-based TES units placed on heat generating components (*i.e.* heater) provided better transient response compared to the regular 1/16″ (2 mm) thick PCM-based TES units. As PCM was concentrated on the top of the heater, most PCM melted during the charging phase and more heat was stored as latent heat. However, the back cover temperature was above the user comfort limit due to additional thermal resistance from more air gaps inside the tablet PC causing higher internal thermal resistance and a warmer hot spot above the heater.

5. PCM-based TES units also resulted in a good thermal performance of the tablet PC during intermittent operation. Similar to continuous operation, PCM-based TES units remained effective at different power inputs and angular orientations.

However, due to incomplete release of stored heat after 15 minutes of discharging phase, the peak temperature gradually increased in subsequent cycles of operation.

7.2 Recommendations

Based on the findings of the present work, the following points can be recommended in particular for further studies:

1. To avoid an unstable shape and inconsistent performance which happened due to the melted PCM shifting over time, shape stabilized PCM-based TES units could be used. Shape stabilized PCM also provides a leak-free encapsulation of PCMs. Additionally, shape stabilized PCM allows easy inclusion of additives to enhance the thermal conductivity of the overall PCM-based TES units (Zhang *et al.*, 2006; Cheng *et al.*, 2010). Typically, shape stabilized PCMs are made by mixing the melted PCM with the melted carrier material at a certain high temperature, then adding thermal conductivity enhance additives to the melted composite samples. This process was mentioned in a study conducted by Cheng *et al.* (2010) where they were able to achieve 1.36 W/m·K thermal conductivity of PCMs (340% improvement ratio) with only 4.6% mass percentage of additives. Increasing the thermal conductivity of the PCM will facilitate the quick removal of heat during the discharging phase and thus will become more effective in intermittent operation. However, this in turn may lead to higher back cover temperature because of better heat conduction to the back. As a result, rigorous studies are necessary to obtain an optimized PCM TES unit with thermal conductivity enhancer.

2. During the 15 minutes of discharging phase in the intermittent operation, the heater was completely turned off to imitate the idle state of the tablet PC. However, even in the idle state, a certain amount of power is consumed to power the wireless adapter, memory, GPS, etc. Hence to replicate the idle state properly, instead of turning off the heater completely in the discharging phase, a certain power input should be imposed on the system during the intermittent operation study.

3. The thermal performance of the tablet PC with PCM-based TES units largely depends on the ambient temperature. Higher ambient temperature can result in a higher operating temperature in tablet PCs. The average summer ambient temperature in Nova Scotia, Canada where the study was conducted, varies from 20 to 25 °C. Many other countries have quite different weather patterns due to their geographic location. For instance, the temperature in the UAE can exceed 40 °C during the summer. Under such conditions, *n*-eicosane and PT-37 may not be the appropriate PCMs for cooling tablet PCs. As tablet PCs are used in countries where ambient temperatures can change substantially, more extensive studies are required to determine the effectiveness of the present approach with respect to different types of PCMs.

References

ASTM Standard E1269-11 (2011). Test Method for Determining Specific Heat Capacity by Differential Scanning Calorimetry. ASTM International, West Conshohocken, PA, USA,

Abhat, A., (1983) Low Temperature Latent Heat Thermal Energy Storage: Heat Storage Materials, Solar Energy, 30, pp. 313-332.

Abhat, A., Heine, D., Heinisch, M., Malatidis, N. and Neuer, G., (1981) Development of a modular heat exchanger with integrated latent heat energy store, Final Report, Dec. 1979 Institut fuer Kemtechnik und Energiewandlung eV, Stuttgart (Germany, FR). 1.

Adriaanse, N., Dekker, H. and Coops, J., (1964) Some physical constants of normal saturated fatty acids and their methyl esters, Recueil des Travaux Chimiques des Pays-Bas, 83, pp. 557-572.

Agyenim, F., Hewitt, N., Eames, P. and Smyth, M., (2010) A review of materials, heat transfer and phase change problem formulation for latent heat thermal energy storage systems (LHTESS), Renewable and Sustainable Energy Reviews, 14, pp. 615-628.

Ahmed, T., Bhouri, M., Kahwaji, S., Groulx, D. and White, M. A., (2016) Experimental Investigation of Thermal Management of Tablet Computers using Phase Change Materials (PCMs), ASME 2016 Summer Heat Transfer Conference, 10 p.

Alawadhi, E. M. and Amon, C. H., (2003) PCM thermal control unit for portable electronic devices: experimental and numerical studies, IEEE Transactions on Components and Packaging Technologies, 26, pp. 116-125.

Alfa-Aesar. (2015). "Information on A13853 n-Eicosane." 2015, from https://www.alfa.com/en/catalog/A13853/.

Amin, N. A. M., Bruno, F. and Belusko, M., (2014) Effective thermal conductivity for melting in PCM encapsulated in a sphere, Applied Energy, 122, pp. 280-287.

Amon, C. H., Nigen, J. S., Siewiorek, D. P., Smailagic, A. and Stivoric, J. (1994). Concurrent design and analysis of the Navigator wearable computer system: the thermal perspective. Thermal Phenomena in Electronic Systems, 1994. I-THERM IV. Concurrent Engineering and Thermal Phenomena., InterSociety Conference on.

JESD51-2A (2008). Integrated Circuits Thermal Test Method Environmental Conditions - Natural Convection (Still Air) JEDEC Solid State Technology Association, Arlington, VA 22201-3834

Aubuchon, S. R., (2007) Interpretation of the crystallization peak of supercooled liquids using Tzero® DSC, TA344, TA Instruments.

Baby, R. and Balaji, C., (2012) Experimental investigations on phase change material based finned heat sinks for electronic equipment cooling, International Journal of Heat and Mass Transfer, 55, pp. 1642-1649.

Bergman, T. L., Incropera, F. P. and Lavine, A. S. (2011). Fundamentals of heat and mass transfer, John Wiley & Sons.

Bremerkamp, F., Seehase, D. and Nowottnick, M. (2012). Selective cooling of sensitive PCB components by means of silica gel based cover coatings. Electronic System-Integration Technology Conference (ESTC), 2012 4th.

Cabeza, L. F. (2008). Heat And Cold Storage With PCM: An Up To Date Introduction Into Basics And Applications, Springer.

Cabeza, L. F., Castell, A., Barreneche, C., de Gracia, A. and Fernández, A. I., (2011) Materials used as PCM in thermal energy storage in buildings: A review, Renewable and Sustainable Energy Reviews, 15, pp. 1675-1695.

Cabeza, L. F., Illa, J., Roca, J., Badia, F., Mehling, H., Hiebler, S. and Ziegler, F., (2001a) Immersion corrosion tests on metal-salt hydrate pairs used for latent heat storage in the 32 to 36°C temperature range, Materials and Corrosion, 52, pp. 140-146.

Cabeza, L. F., Illa, J., Roca, J., Badia, F., Mehling, H., Hiebler, S. and Ziegler, F., (2001b) Middle term immersion corrosion tests on metal-salt hydrate pairs used for latent heat storage in the 32 to 36°C temperature range, Materials and Corrosion, 52, pp. 748-754.

Cabeza, L. F., Roca, J., Nogués, M., Mehling, H. and Hiebler, S., (2002) Immersion corrosion tests on metal-salt hydrate pairs used for latent heat storage in the 48 to 58°C temperature range, Materials and Corrosion, 53, pp. 902-907.

Carroll, A. and Heiser, G. (2010). An Analysis of Power Consumption in a Smartphone. USENIX annual technical conference.

Chalco-Sandoval, W., Fabra, M. J., López-Rubio, A. and Lagaron, J. M., Use of phase change materials to develop electrospun coatings of interest in food packaging applications, Journal of Food Engineering.

Cheng, W.-l., Liu, N. and Wu, W.-f., (2012) Studies on thermal properties and thermal control effectiveness of a new shape-stabilized phase change material with high thermal conductivity, Applied Thermal Engineering, 36, pp. 345-352.

Cheng, W.-l., Zhang, R.-m., Xie, K., Liu, N. and Wang, J., (2010) Heat conduction enhanced shape-stabilized paraffin/HDPE composite PCMs by graphite addition: Preparation and thermal properties, Solar Energy Materials and Solar Cells, 94, pp. 1636-1642.

Chiriac, V., Molloy, S., Anderson, J. and Goodson, K., (2015) A Figure of Merit for Smart Phone Thermal Management, Electronics COOLING.

Courtney, T. (2015). "How Much Power Do Common Devices Consume?" Retrieved April 4, 2016, from https://www.gozolt.com/blog/power-devices-consume/.

Desgrosseilliers, L., Groulx, D. and White, M. A. (2012). Reclaimed Laminate Waster as Novel, Heat Transfer Enhancing, Encapsulation for Long-term PCM Heat Storage. CleanTech 2012, San Jose, CA, USA.

Desgrosseilliers, L., Groulx, D. and White, M. A., (2013a) Heat conduction in laminate multilayer bodies with applied finite heat source, International Journal of Thermal Sciences, 72, pp. 47-59.

Desgrosseilliers, L., Groulx, D. and White, M. A., (2014) Thermographic validation of a novel, laminate body, analytical heat conduction model, Heat and Mass Transfer, 50, pp. 895-905.

Desgrosseilliers, L., Murray, R. E., Sefati, A., Marin, G., Stewart, J., Osbourne, N., White, M. A. and Groulx, D., (2011) Phase Change Material Selection in the Design of a Latent Heat Energy Storage System Coupled with a Domestic Hot Water Solar Thermal System, ASHRAE Annual Conference 2011, 8 p.

Desgrosseilliers, L., Whitman, C. A., Groulx, D. and White, M. A., (2013b) Dodecanoic acid as a promising phase-change material for thermal energy storage, Applied Thermal Engineering, 53, pp. 37-41.

Desgrosseilliers, L. R. J. (2012). Heat Transfer Enhancements Using Laminate Film Encapsulation for Phase Change Heat Storage Materials. (master's thesis). Dalhousie University, Halifax, NS, Canada. pp.101.

Dirand, M., Bouroukba, M., Briard, A.-J., Chevallier, V., Petitjean, D. and Corriou, J.-P., (2002) Temperatures and enthalpies of (solid + solid) and (solid + liquid) transitions of n-alkanes, The Journal of Chemical Thermodynamics, 34, pp. 1255-1277.

Elopak (2009) "Elopak environmental report," Buskerud, Norway.

Entropy Solutions, L. (2014). "PureTemp 37 technical data sheet." Retrieved March 2, 2016, from http://www.puretemp.com/stories/puretemp-37-tds.

Entropy Solutions, L. (2015). "Thermal cycling 101." from http://www.puretemp.com/stories/thermal-cycling-101.

Espeau, P., Mondieig, D., Haget, Y. and Cuevas-Diarte, M., (1997) 'Active'Package for Thermal Protection of Food Products, Packaging Technology and Science, 10, pp. 253-260.

Farrell, A. J., Norton, B. and Kennedy, D. M., (2006) Corrosive effects of salt hydrate phase change materials used with aluminium and copper, Journal of materials processing technology, 175, pp. 198-205.

Feldman, D., Shapiro, M. M. and Banu, D., (1986) Organic phase change materials for thermal energy storage, Solar Energy Materials, 13, pp. 1-10.

Ferrer, G., Solé, A., Barreneche, C., Martorell, I. and Cabeza, L. F., (2015) Corrosion of metal containers for use in PCM energy storage, Renewable Energy, 76, pp. 465-469.

Fok, S. C., Shen, W. and Tan, F. L., (2010) Cooling of portable hand-held electronic devices using phase change materials in finned heat sinks, International Journal of Thermal Sciences, 49, pp. 109-117.

Furbo, S. and Schultz, J. M., (2007) State of development of the work with seasonal PCM heat storage at the Department of Civil Engineering, Technical University of Denmark (DTU)," in "A Report of IEA Solar Heating and Cooling programme - Task 32: Advanced storage concepts for solar and low energy buildings, STREICHER W. (Ed.), International Energy Agency.

Ge, H., Li, H., Mei, S. and Liu, J., (2013) Low melting point liquid metal as a new class of phase change material: An emerging frontier in energy area, Renewable and Sustainable Energy Reviews, 21, pp. 331-346.

Ghali, E., Sastri, V. S. and Elboujdaini, M. (2007). Corrosion prevention and protection: practical solutions, John Wiley & Sons.

Greenspan, J. D., Roy, E. A., Caldwell, P. A. and Farooq, N. S., (2003) Thermosensory intensity and affect throughout the perceptible range, Somatosensory & motor research, 20, pp. 19-26.

Grimes, R., Walsh, E. and Walsh, P., (2010) Active cooling of a mobile phone handset, Applied Thermal Engineering, 30, pp. 2363-2369.

Groulx, D., White, M. A. and Joseph, A., (2014) PCM-Based Thermal Storage System Research at Dalhousie University: A Review, Eurotherm Seminar #99 Advances in Thermal Energy Storage.

Gurrum, S. P., Edwards, D. R., Marchand-Golder, T., Akiyama, J., Yokoya, S., Drouard, J. and Dahan, F. (2012). Generic thermal analysis for phone and tablet systems. Electronic Components and Technology Conference (ECTC), 2012 IEEE 62nd.

Haghighi, E., (2012) ICI 7640 Infrared Camera User Manual v 1.0.

Haiyan LI, J. L., (2011) Revolutionizing heat transport enhancement with liquid metals: Proposal of a new industry of water-free heat exchangers, Front. Energy, 5, pp. 20-42.

Hale, D., Hoover, J. and O'neill, M., (1971) Phase change materials handbook.

Hawes, D. W., Feldman, D. and Banu, D., (1993) Latent heat storage in building materials, Energy and Buildings, 20, pp. 77-86.

Hodes, M., Weinstein, R. D., Pence, S. J., Piccini, J. M., Manzione, L. and Chen, C., (2002) Transient Thermal Management of a Handset Using Phase Change Material (PCM), Journal of Electronic Packaging, 124, pp. 419-426.

Jam-Software. (2014). "Information on HeavyLoad." Retrieved June 6, 2015, from https://www.jam-software.com/heavyload/.

James C. Mulligan, R. D. G. (2002) "Use of MicroPCM Fluids as Enhanced Liquid Coolants in Automotive and HEV Vehicles−Final Report,"

Jan Kosny, N. S., and Ali Fallahi (2013) "Cost Analysis of Simple Phase Change Material-Enhanced Building Envelopes in Southern U.S. Climates,"

Johnson, M. B. and White, M. A. (2014). Thermal Methods - Multi Length-Scale Characterisation, John Wiley & Sons, Ltd.

Kamimoto, M., Abe, Y., Sawata, S., Tani, T. and Ozawa, T., (1986) Latent Thermal Storage Unit Using Form-Stable High Density Polyethylene; Part I: Performance of the Storage Unit, Journal of Solar Energy Engineering, 108, pp. 282-289.

Kamkari, B., Shokouhmand, H. and Bruno, F., (2014) Experimental investigation of the effect of inclination angle on convection-driven melting of phase change material in a rectangular enclosure, International Journal of Heat and Mass Transfer, 72, pp. 186-200.

Kandasamy, R., Wang, X.-Q. and Mujumdar, A. S., (2007) Application of phase change materials in thermal management of electronics, Applied Thermal Engineering, 27, pp. 2822-2832.

Kandasamy, R., Wang, X.-Q. and Mujumdar, A. S., (2008) Transient cooling of electronics using phase change material (PCM)-based heat sinks, Applied Thermal Engineering, 28, pp. 1047-1057.

Kheirabadi, A. and Groulx, D., (2014) Design of an Automated Thermal Cycler for Long-term Phase Change Material Phase Transition Stability Studies, COMSOL Conference Boston 2014, 7 p.

Krishnan, S., Garimella, S. V. and Kang, S. S., (2005) A novel hybrid heat sink using phase change materials for transient thermal management of electronics, IEEE Transactions on Components and Packaging Technologies, 28, pp. 281-289.

Lane, G., (1985) PCM science and technology: the essential connection, ASHRAE Trans.;(United States), 91.

Lane, G. A., (1980) Low temperature heat storage with phase change materials, International Journal of Ambient Energy, 1, pp. 155-168.

Lane, G. A., Kott, A. C., Warner, G. L., Hartwick, P. B. and Rossow, H. E. (1978) "Macro-encapsulation of heat storage phase-change materials for use in residential buildings. Final report, September 29, 1976-September 6, 1978,"

Li, J.-H., Zhang, G.-e. and Wang, J.-Y., (1991) Investigation of a eutectic mixture of sodium acetate trihydrate and urea as latent heat storage, Solar Energy, 47, pp. 443-445.

Lin, C. C., Wu, H. C., Pan, J. P., Su, C. Y., Wang, T. H., Sheu, H. S. and Wu, N. L., (2013) Investigation on suppressed thermal runaway of Li-ion battery by hyper-branched polymer coated on cathode, Electrochimica Acta, 101, pp. 11-17.

Lin, S.-C. and Chou, C.-A., (2004) Blockage effect of axial-flow fans applied on heat sink assembly, Applied Thermal Engineering, 24, pp. 2375-2389.

Liu, C., Murray, R. E. and Groulx, D., (2012) Experimental Study of Cylindrical Latent Heat Energy Storage Systems Using Lauric Acid as the Phase Change Material, ASME 2012 Summer Heat Transfer Conference, 10 p.

Loh, C. K., Nelson, D. and Chou, D. J. (2001). Thermal characterization of fan-heat sink systems in miniature axial fan and micro blower airflow. Semiconductor Thermal Measurement and Management, 2001. Seventeenth Annual IEEE Symposium.

Lorsch, H. G., Kauffman, K. W. and Denton, J. C., (1975) Thermal energy storage for solar heating and off-peak air conditioning, Energy Conversion, 15, pp. 1-8.

Lu, J., Fan, L.-w., Zeng, Y., Xiao, Y.-q., Xu, X. and Yu, Z.-t., (2014) Effect of the inclination angle on the transient performance of a phase change material-based heat sink under pulsed heat loads, Journal of Zhejiang University SCIENCE A, 15, pp. 789-797.

Luo, Z., Cho, H., Luo, X. and Cho, K.-i., (2008) System thermal analysis for mobile phone, Applied Thermal Engineering, 28, pp. 1889-1895.

McPherson, J. W. (2010). Reliability physics and engineering, Springer.

Mithal, P., (1996) Design of experimental based evaluation of thermal performance of a flichip electronic assembly, ASME EEP Proceedings. New York: ASME, 18, pp. 109-115.

Moore, G. E., (1998) Cramming More Components Onto Integrated Circuits, Proceedings of the IEEE, 86, pp. 82-85.

Murray, R. E., Desgrosseilliers, L., Stewart, J., Osbourne, N., Marin, G., Safatli, A., Groulx, D. and White, M. A., (2011) Design of a Latent Heat Energy Storage System

Coupled with a Domestic Hot Water Solar Thermal System, World Renewable Energy Congress 2011, 8 p.

Novikov, A., Lexow, D. and Nowottnick, M. (2014). Cooling of electronic assemblies through PCM containing coatings. Electronics System-Integration Technology Conference (ESTC), 2014.

Oró, E., de Gracia, A., Castell, A., Farid, M. M. and Cabeza, L. F., (2012) Review on phase change materials (PCMs) for cold thermal energy storage applications, Applied Energy, 99, pp. 513-533.

Pals, C. R. and Newman, J., (1995) Thermal modeling of the lithium/polymer battery I. Discharge behavior of a single cell, Journal of the Electrochemical Society, 142, pp. 3274-3281.

Patapoutian, A., Peier, A. M., Story, G. M. and Viswanath, V., (2003) ThermoTRP channels and beyond: mechanisms of temperature sensation, Nature Reviews Neuroscience, 4, pp. 529-539.

recyclecartons.ca. (2011). "Why Cartons?" Retrieved November 30, 2011, 2011, from http://www.recyclecartons.ca/recycling.html.

Regin, A. F., Solanki, S. C. and Saini, J. S., (2008) Heat transfer characteristics of thermal energy storage system using PCM capsules: A review, Renewable and Sustainable Energy Reviews, 12, pp. 2438-2458.

Ruthven, D. M. (1984). Principles of adsorption and adsorption processes, John Wiley & Sons.

Saha, S. K. and Dutta, P., (2010) Cooling of Electronics with Phase Change Materials, International Conference on Modeling, Optimization, and Computing, pp. 7.

Saha, S. K. and Dutta, P., (2012) Thermal Management of Electronics Using PCM-Based Heat Sink Subjected to Cyclic Heat Load, IEEE Transactions on Components, Packaging and Manufacturing Technology, 2, pp. 464-473.

Sari, A., (2003a) Thermal characteristics of a eutectic mixture of myristic and palmitic acids as phase change material for heating applications, Applied Thermal Engineering, 23, pp. 1005-1017.

Sari, A., (2003b) Thermal reliability test of some fatty acids as PCMs used for solar thermal latent heat storage applications, Energy Conversion and Management, 44, pp. 2277-2287.

Sarı, A. and Karaipekli, A., (2007) Thermal conductivity and latent heat thermal energy storage characteristics of paraffin/expanded graphite composite as phase change material, Applied Thermal Engineering, 27, pp. 1271-1277.

Sarvar, F., Poole, N. J. and Witting, P. A., (1990) PCB glass-fibre laminates: Thermal conductivity measurements and their effect on simulation, Journal of Electronic Materials, 19, pp. 1345-1350.

Schroder, J. (1980). R and D systems for thermal energy storage in the temperature range from - 25ºC to 150 ºC. Proc. Seminar New Ways to Save Energy, Reidel, Dordrecht.

Schultz, F. a., (2007) State of development of the work with seasonal PCM heat storage at the Department of Civil Engineering, Technical University of Denmark (DTU)," in "A Report of IEA Solar Heating and Cooling programme - Task 32: Advanced storage concepts for solar and low energy buildings, STREICHER W. (Ed.), International Energy Agency.

Schweitzer, P. A. (2009). Fundamentals of corrosion: mechanisms, causes, and preventative methods, CRC Press.

Sharifi, N., Robak, C. W., Bergman, T. L. and Faghri, A., (2013) Three-dimensional PCM melting in a vertical cylindrical enclosure including the effects of tilting, International Journal of Heat and Mass Transfer, 65, pp. 798-806.

Sharma, A., Sharma, S. D. and Buddhi, D., (2002) Accelerated thermal cycle test of acetamide, stearic acid and paraffin wax for solar thermal latent heat storage applications, Energy Conversion and Management, 43, pp. 1923-1930.

Sharma, A., Tyagi, V. V., Chen, C. R. and Buddhi, D., (2009) Review on thermal energy storage with phase change materials and applications, Renewable and Sustainable Energy Reviews, 13, pp. 318-345.

Sharma, S. D., Buddhi, D. and Sawhney, R. L., (1999) Accelerated thermal cycle test of latent heat-storage materials, Solar Energy, 66, pp. 483-490.

Shokouhmand, H. and Kamkari, B., (2013) Experimental investigation on melting heat transfer characteristics of lauric acid in a rectangular thermal storage unit, Experimental Thermal and Fluid Science, 50, pp. 201-212.

Siddiqui, A. (2015). "Processor Temperature Results for Tens of SoCs — How Hot is Your Chip?", from http://www.xda-developers.com/processor-temperature-results-for-tens-of-socs-how-hot-is-your-chip/.

Socaciu, L., Giurgiu, O., Banyai, D. and Simion, M., (2016) PCM Selection Using AHP Method to Maintain Thermal Comfort of the Vehicle Occupants, Energy Procedia, 85, pp. 489-497.

Sponagle, B. and Groulx, D., (2015) Thermal Modeling of Tablets: Temperature Management using Phase Change Materials, 1st Thermal and Fluid Engineering Summer Conference, TFESC, 14 p.

Statista.com. (2012). "Share of population that owned and used tablet computers in 2012, by country " Retrieved January 15, 2016, from http://www.statista.com/statistics/256277/ownership-and-personal-use-of-tablet-computers-by-country/.

Statista.com. (2016). "Shipment forecast of tablets, laptops and desktop PCs worldwide from 2010 to 2019 (in million units)." Retrieved January 15, 2016, from http://www.statista.com/statistics/272595/global-shipments-forecast-for-tablets-laptops-and-desktop-pcs/.

Stessel, R. I. (1996). Disposable Product Design and Recycling. Proceedgins of the 17th Bienneial Waste Processing Conference, ASME.

Story, G. M., (2006) The emerging role of TRP channels in mechanisms of temperature and pain sensation, Current neuropharmacology, 4, pp. 183.

Sutterlin, W. R. (2014) "A brief comparison of ice packs, salts, paraffins and vegetable-derived phase change materials,"

Tan, F. and Tso, C. P., (2004) Cooling of mobile electronic devices using phase change materials, Applied Thermal Engineering, 24, pp. 159-169.

Tan, F. L., Shen, W., Jony and Fok, S. C. (2009). Thermal performance of PCM-cooled mobile phone. Electronics Packaging Technology Conference, 2009. EPTC '09. 11th.

Taylor, B. (2015). "The Average Lifespan of 7 Popular Tech Products." Retrieved June 30, 2016, from http://smartphones.specout.com/stories/9635/average-lifespan-tech-products.

Telkes, M., (1947) Solar house heating - A problem of heat storage, Heating and Ventilating, 44, pp. 68-75.

Telkes, M., (1952) Nucleation of Supersaturated Inorganic Salt Solutions, Industrial & Engineering Chemistry, 44, pp. 1308-1310.

TetraPak (2011) "Mission Possible: sustainability update 2011," Pully, Switzerland.

Tian, T. (2010) "CPU Monitoring With DTS/PECI,"

Tomizawa, Y., Sasaki, K., Kuroda, A., Takeda, R. and Kaito, Y., (2016) Experimental and numerical study on phase change material (PCM) for thermal management of mobile devices, Applied Thermal Engineering, 98, pp. 320-329.

van Miltenburg, J. C. and Oonk, H. A. J., (2005) Thermal Properties of Ethyl Undecanoate and Ethyl Tridecanoate by Adiabatic Calorimetry, Journal of Chemical & Engineering Data, 50, pp. 1348-1352.

Wada, T., Yamamoto, R. and Matsuo, Y., (1984) Heat storage capacity of sodium acetate trihydrate during thermal cycling, Solar Energy, 33, pp. 373-375.

Wang, Y.-H. and Yang, Y.-T., (2011) Three-dimensional transient cooling simulations of a portable electronic device using PCM (phase change materials) in multi-fin heat sink, Energy, 36, pp. 5214-5224.

Webb, B. W. and Viskanta, R., (1986) Natural-convection-dominated melting heat transfer in an inclined rectangular enclosure, International Journal of Heat and Mass Transfer, 29, pp. 183-192.

Wee, A. G., Schneider, R. L. and Aquilino, S. A., (1998) Use of low fusing alloy in dentistry, The Journal of Prosthetic Dentistry, 80, pp. 540-545.

Werner, R., (1987) Compatibility of organic latent heat storage materials and plastic container materials, Heat Recovery Systems and CHP, 7, pp. 383-388.

Wise, D. (2015). "Stability Test – An Effective Stress Testing Tool For Your Android." from https://www.oneclickroot.com/how-to/stability-test-an-effective-stress-testing-tool-for-your-android/.

Xie, Q., Dousti, M. J. and Pedram, M., (2014) Therminator: a thermal simulator for smartphones producing accurate chip and skin temperature maps, Proceedings of the 2014 international symposium on Low power electronics and design, 117-122.

Yeh, L., (1995) Review of heat transfer technologies in electronic equipment, Journal of electronic packaging, 117, pp. 333-339.

Yeung, P. H., Said, N. M. and Rasiah, I. J. (2003). Stencil printable phase change material [heatsink applications]. Electronics Packaging Technology, 2003 5th Conference (EPTC 2003).

Zalba, B., Marín, J. M., Cabeza, L. F. and Mehling, H., (2003) Review on thermal energy storage with phase change: materials, heat transfer analysis and applications, Applied Thermal Engineering, 23, pp. 251-283.

Zhang, H., Wang, X. and Wu, D., (2010) Silica encapsulation of n-octadecane via sol–gel process: A novel microencapsulated phase-change material with enhanced thermal conductivity and performance, Journal of Colloid and Interface Science, 343, pp. 246-255.

Zhang, Y. P., Lin, K. P., Yang, R., Di, H. F. and Jiang, Y., (2006) Preparation, thermal performance and application of shape-stabilized PCM in energy efficient buildings, Energy and Buildings, 38, pp. 1262-1269.

Zhao, C. Y. and Zhang, G. H., (2011) Review on microencapsulated phase change materials (MEPCMs): Fabrication, characterization and applications, Renewable and Sustainable Energy Reviews, 15, pp. 3813-3832.

Appendix A

Additional Thermal Analysis Data of Tablet PCs

Graphics intense gaming

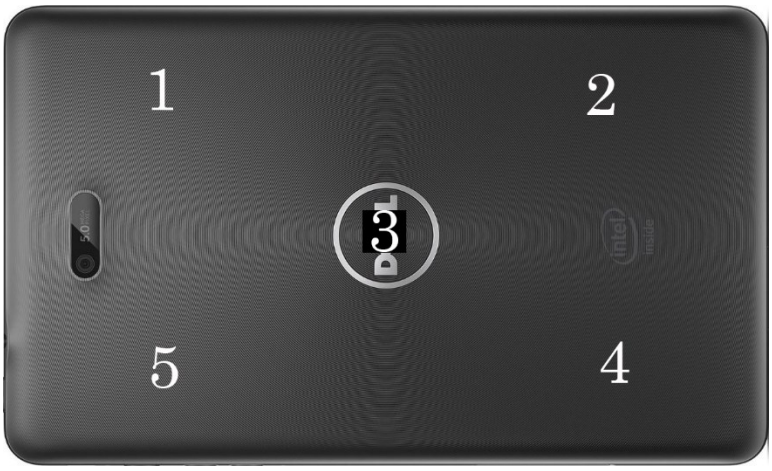

Figure A-1 Position of the five thermocouples attached on the back cover of the Dell tablet PC for thermal analysis.

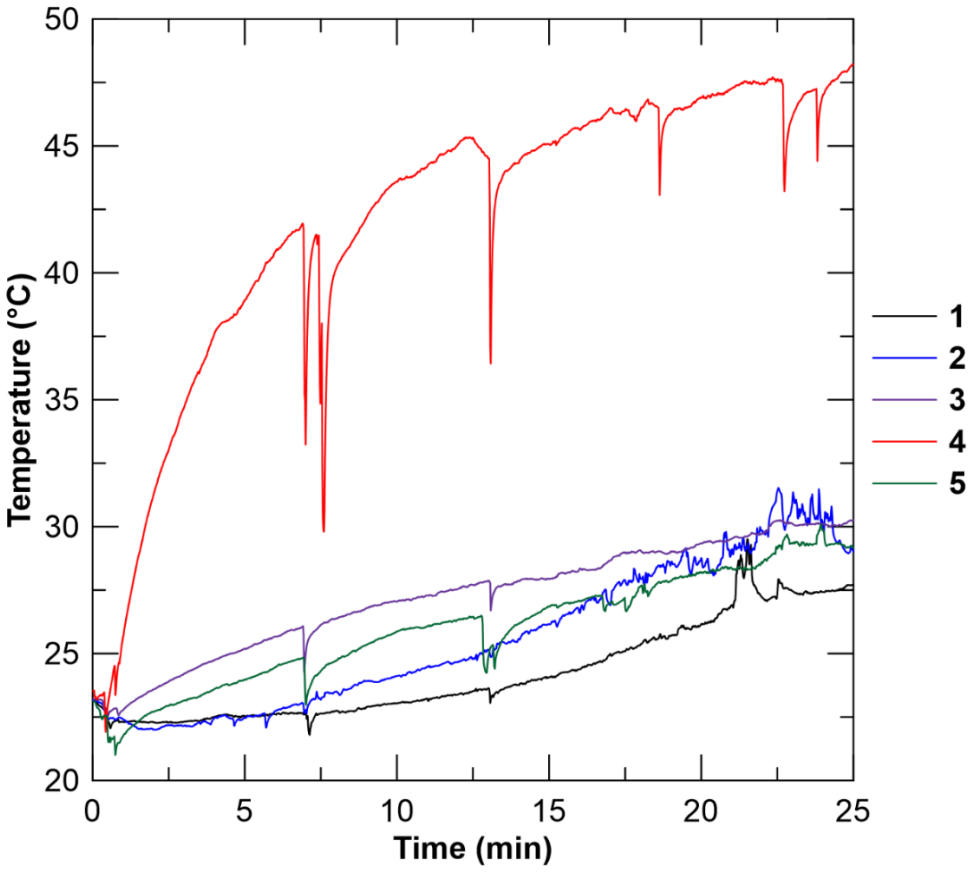

Figure A-2 Rapid increase in the back cover temperature of the Dell tablet PC while playing games for 25 minutes.

Thermal analysis of internal components (front side of the PCB)

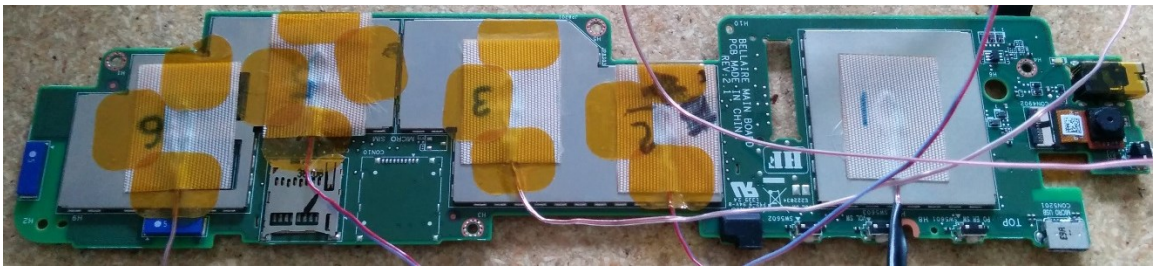

Figure A-3 Position of the five thermocouples attached on the front-side PCB of the Dell tablet PC for thermal analysis.

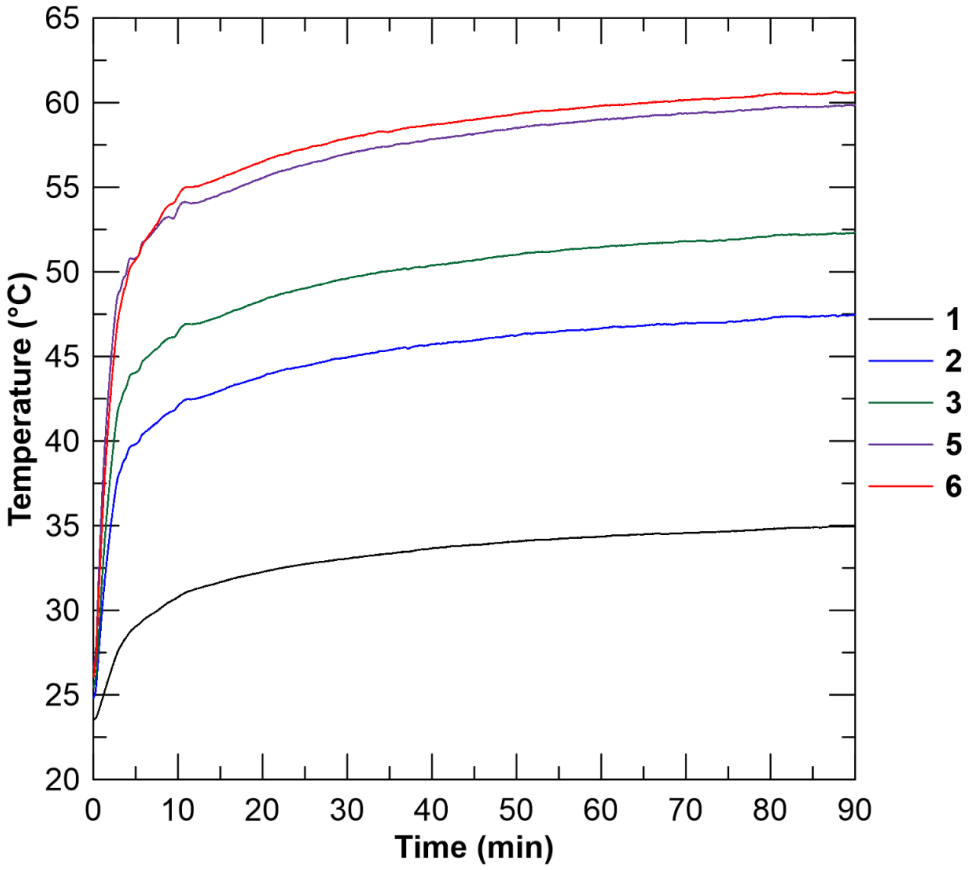

Figure A-4 Thermal response of internal components of the Dell tablet PC for the stress test (front-side).

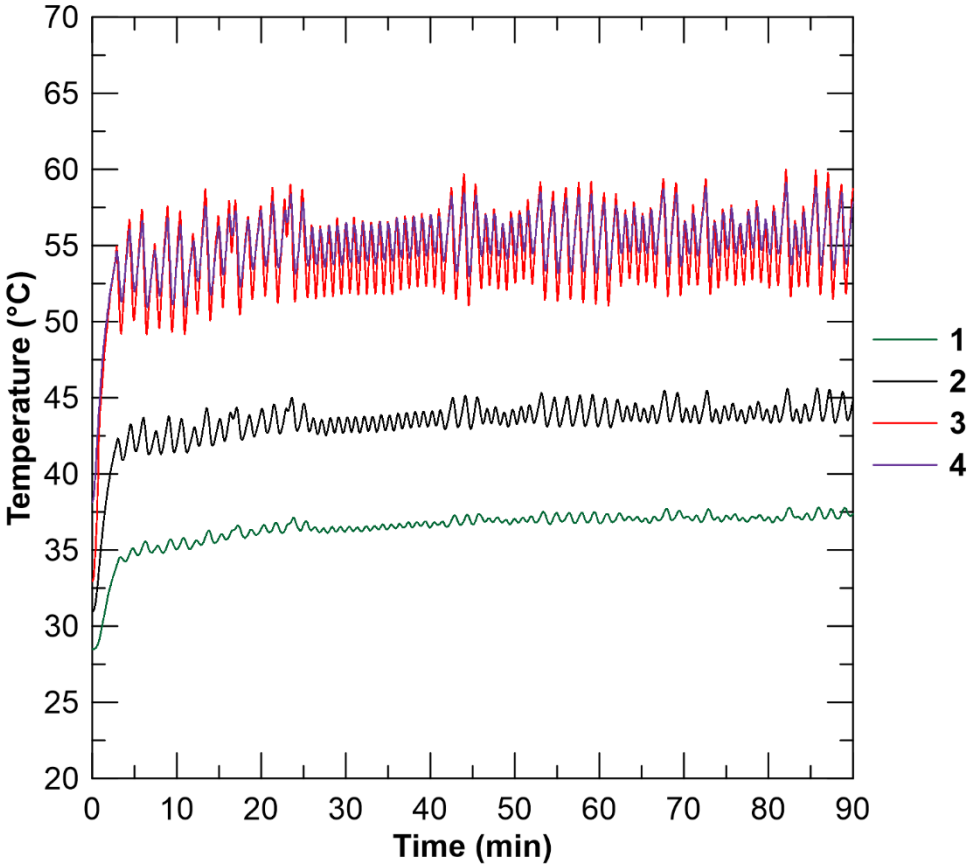

Figure A-5 Thermal response of internal components of the Samsung tablet PC for the stress test (front-side).

Thermal analysis of internal components (back side of the PCB)

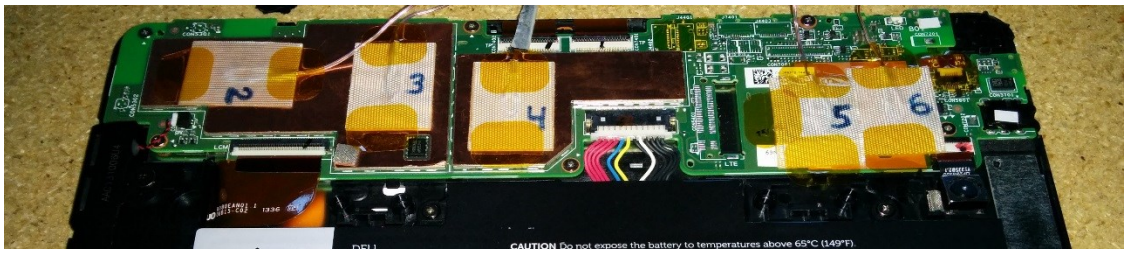

Figure A-6 Position of the five thermocouples attached on the back-side PCB of Dell Tablet PC for thermal analysis.

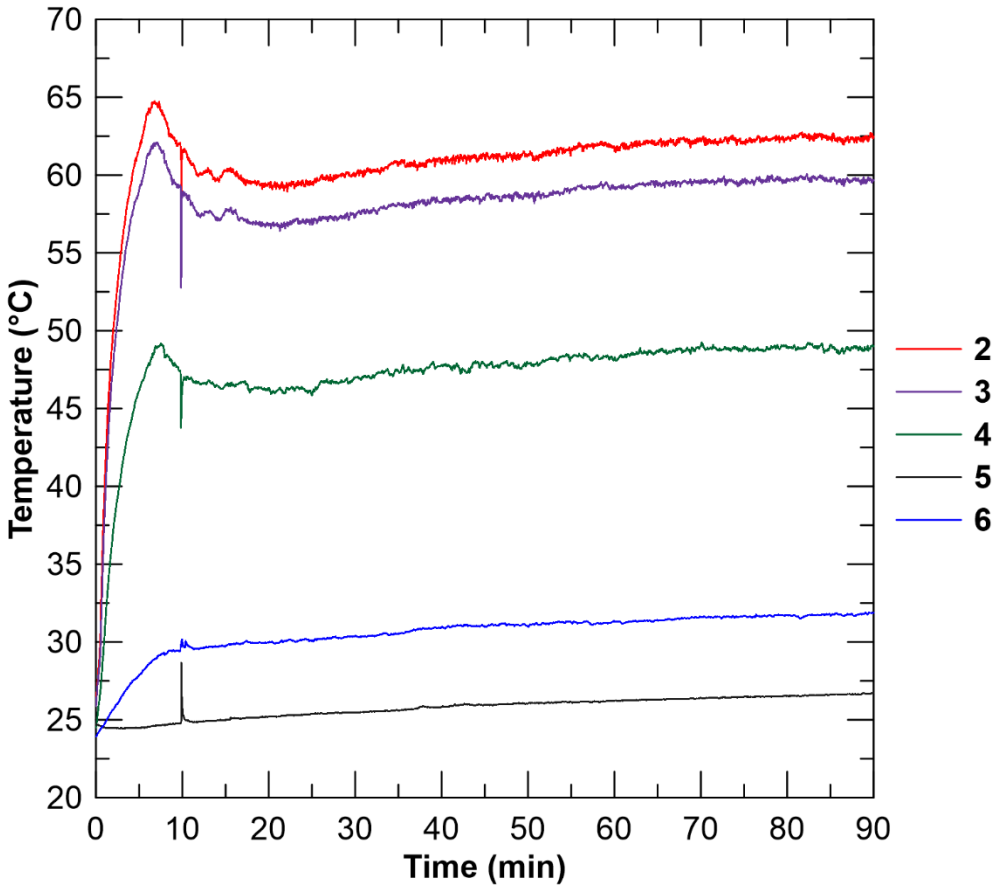

Figure A-7 Thermal response of internal components of the Dell tablet PC for the stress test (back-side).

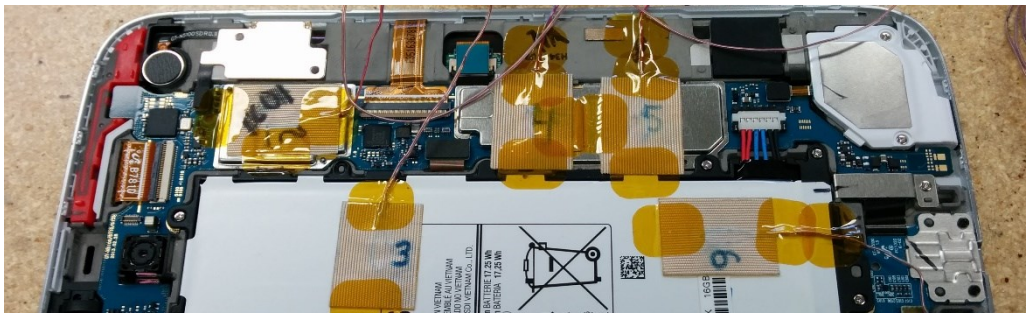

Figure A-8 Position of the five thermocouples attached on the back-side PCB of Samsung tablet PC for thermal analysis.

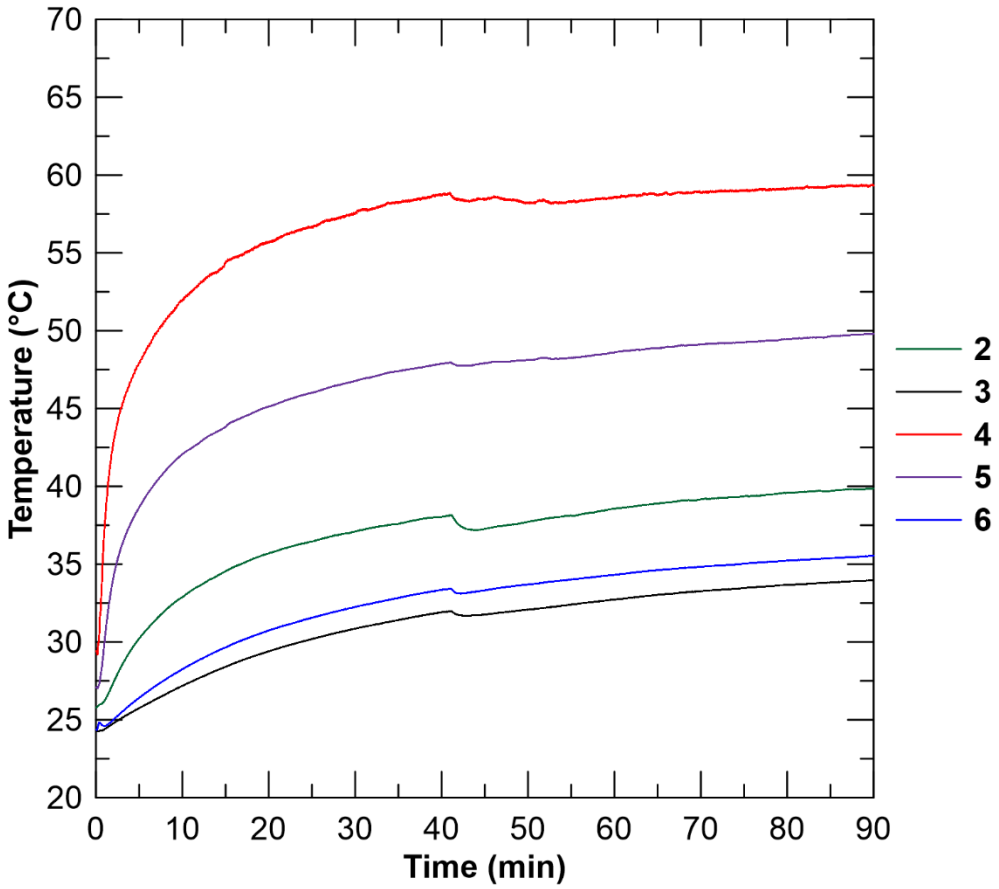

Figure A-9 Thermal response of internal components of the Samsung tablet PC for the stress test (back-side).

Appendix B

Technical Drawings

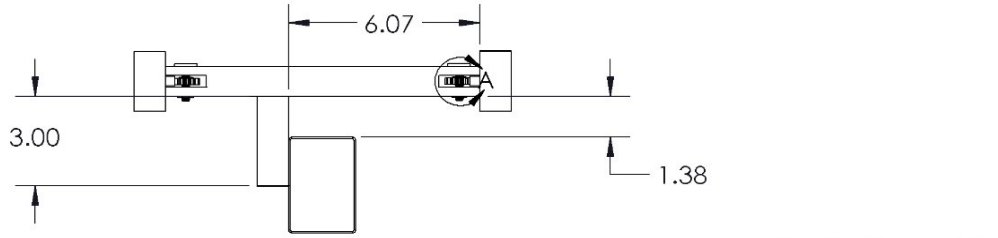

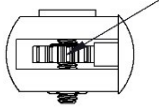

Plastic Gear - 14 - 1/2 Degree Pressure Angle, Press-Fit Mount, 16 Pitch, 12 Teeth

DETAIL A
SCALE 1 : 2

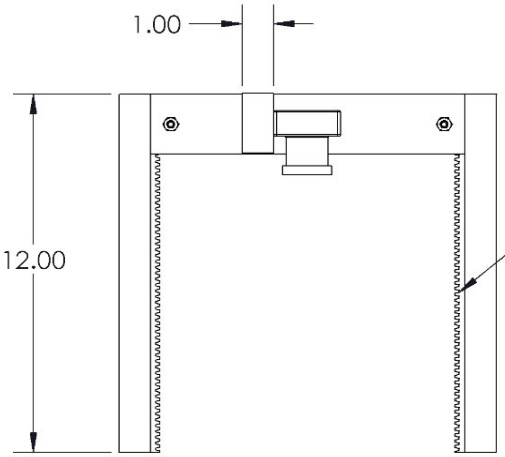

16 Pitch Rack for Plastic Gear - 14 - 1/2 Degree Pressure Angle

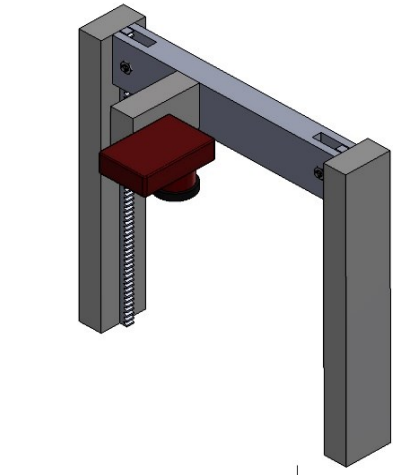

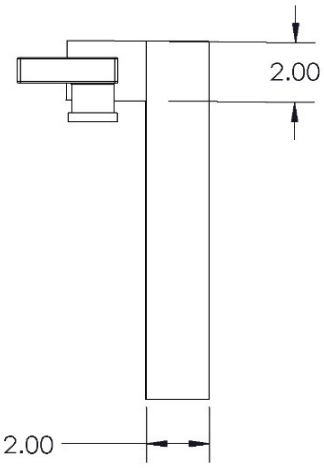

Dalhousie University	PROJECT: EXPERIMENTAL SETUP EXTENSION		DRAWING: IR CAMERA CARRIAGE ASSEMBLY	B00#: 00683325
	UNLESS OTHERWISE NOTED: SURFACE 1.6 µm; UNITS: mm X.XX +/- .10, X.X +/- .20, X +/- .50; UNITS: in X.XXX +/- .005, X.XX +/- .01, X.X +/- .02; ANGLES +/- 0.5°		DWN BY: TOUSIF AHMED	SIZE A / REV
			MATERIAL: HDPE	QTY: 1
			DATE: 31-OCT-2015	UNITS: inch / SCALE: 1:5 / SHEET 1 OF 1

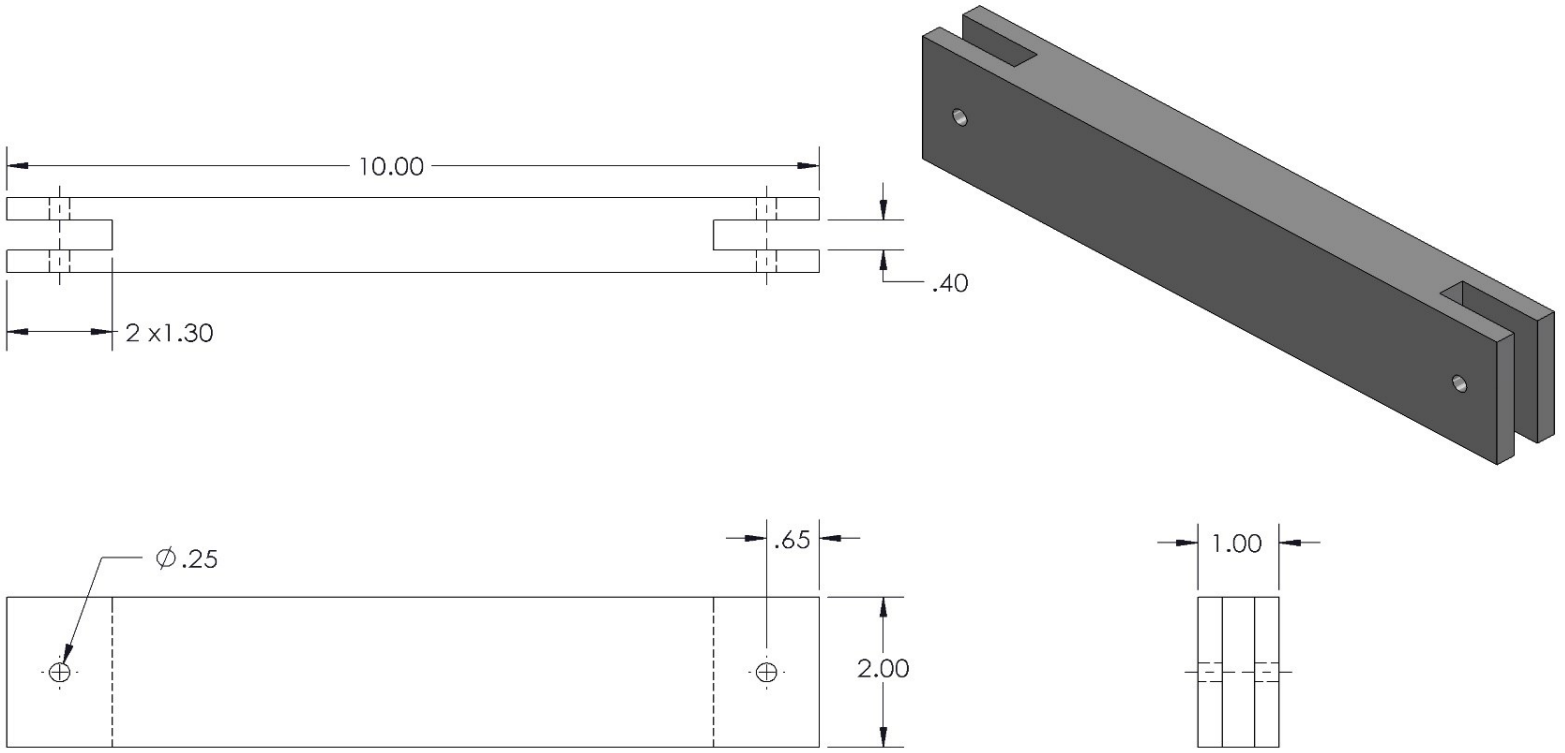

Dalhousie University	PROJECT: IR CAMERA HOLDER		DRAWING: SLIDER		B00#: 683325
	UNLESS OTHERWISE NOTED:		DWN BY: TOUSIF AHMED		SIZE: A / REV
	SURFACE: 1.6 µm	UNITS: mm: X.XX +/- .10, X.X +/- .20, X +/- .50	MATERIAL: HDPE	QTY: 1	
		UNITS: in: X.XXX +/- .005, X.XX +/- .01, X.X +/- .02	DATE:	UNITS: in	SCALE: 1:1
		ANGLES: +/- 0.5°			SHEET 1 OF 1

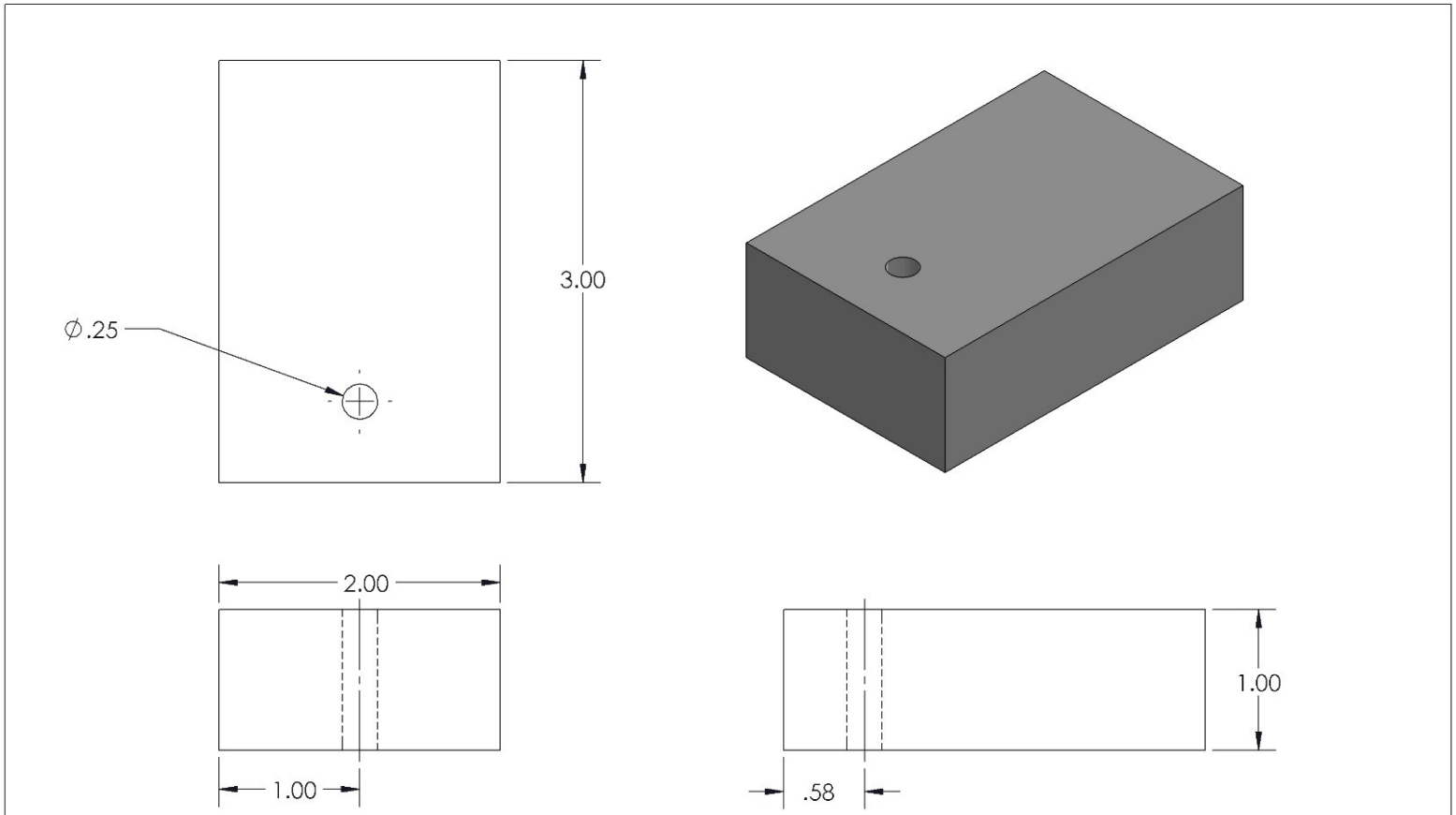

Dalhousie University	PROJECT: EXPERIMENTAL SETUP EXTENSION		DRAWING: IR CAMERA HOLDER		B00#: 00683325
	UNLESS OTHERWISE NOTED: SURFACE 1.6/ µm; UNITS: mm X.XX +/- .10, X.X +/- .20, X +/- .50; UNITS: in X.XXX +/- .005, X.XX +/- .01, X.X +/- .02; ANGLES +/- 0.5°		DWN BY: TOUSIF AHMED		SIZE A / REV
			MATERIAL: HDPE	QTY: 1	
			DATE: 31-OCT-2015	UNITS: inch / SCALE: 1:1	SHEET 1 OF 1

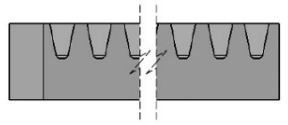

Pitch: 16

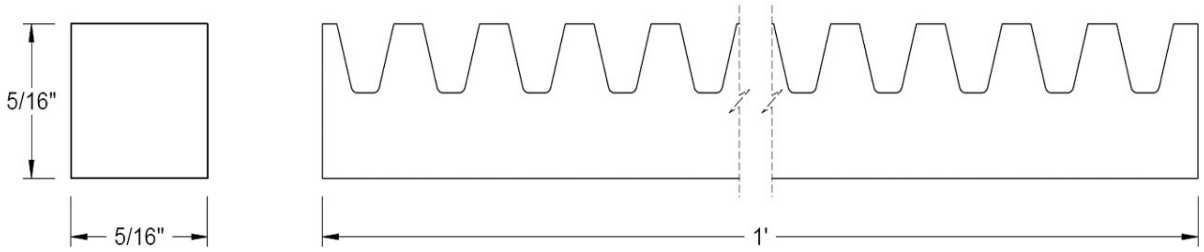

Dalhousie University	PROJECT: IR CAMERA HOLDER		DRAWING: PLASTIC RACK		B00#: 683325
	UNLESS OTHERWISE NOTED:		DWN BY: TOUSIF AHMED		SIZE: A / REV:
	SURFACE: 1.6 µm	UNITS: mm: X.XX +/- .10, X.X +/- .20, X +/- .50	MATERIAL: HDPE	QTY: 1	
	ANGLES: +/- 0.5°	UNITS: in: X.XXX +/- .005, X.XX +/- .01, X.X +/- .02	DATE:	UNITS: in / SCALE: 1:1	SHEET 1 OF 1

Pitch: 16
Number of Teeth: 12

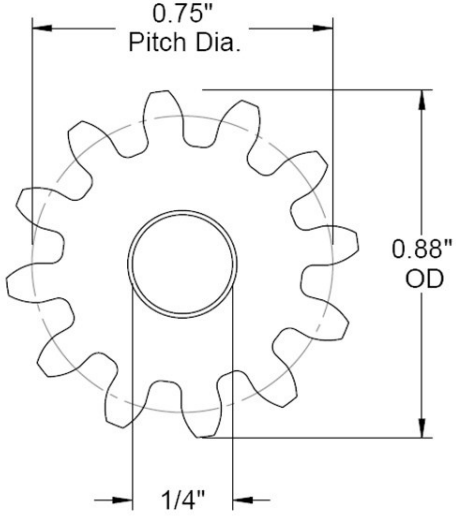

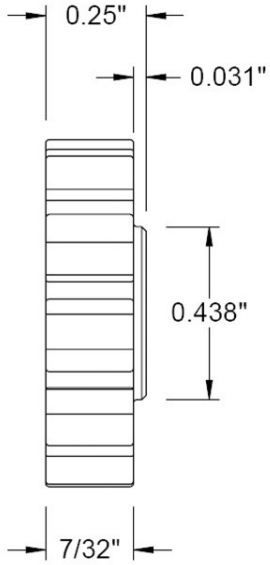

Dalhousie University	PROJECT: IR CAMERA HOLDER		DRAWING: PLASTIC PINION		B00#: 683325
	UNLESS OTHERWISE NOTED: SURFACE 1.6/ µm; UNITS: mm X.XX +/- .10, X.X +/- .20, X +/- .50; UNITS: in X.XXX +/- .005, X.XX +/- .01, X.X +/- .02; ANGLES +/- 0.5°		DWN BY: TOUSIF AHMED		SIZE A / REV
			MATERIAL: HDPE	QTY: 1	
			DATE:	UNITS: in / SCALE: 1:1	SHEET 1 OF 1

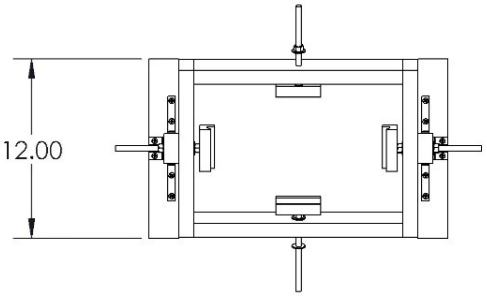

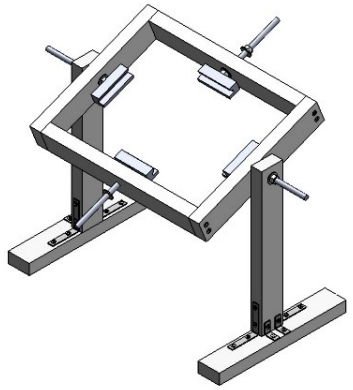

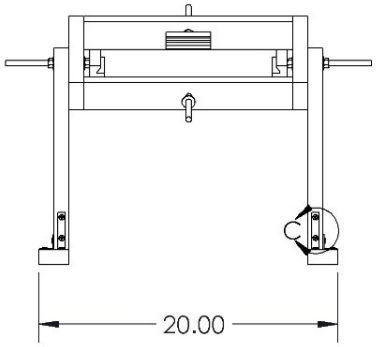

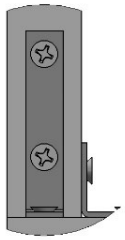

Bracket 1
SCALE 1 : 2

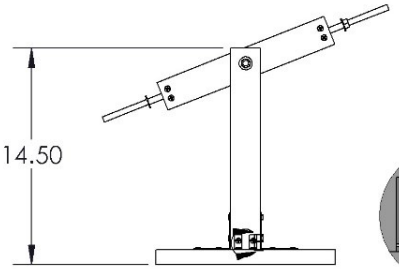

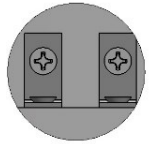

Bracket 2
SCALE 1 : 2

Dalhousie University	PROJECT: TEST STAND		DRAWING: THE TEST STAND		B00#: 683325
	UNLESS OTHERWISE NOTED: SURFACE 1.6 µm; UNITS: mm X.XX +/- .10, X.X +/- .20, X +/- .50; UNITS: in X.XXX +/- .005, X.XX +/- .01, X.X +/- .02; ANGLES +/- 0.5°		DWN BY: TOUSIF AHMED		SIZE A / REV
			MATERIAL: HDPE	QTY: 1	
			DATE: 7-JUL-2016	UNITS: in / SCALE: 1:10	SHEET 1 OF 1

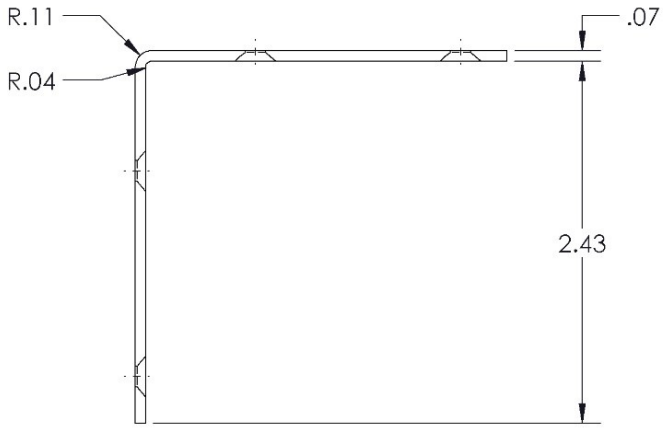

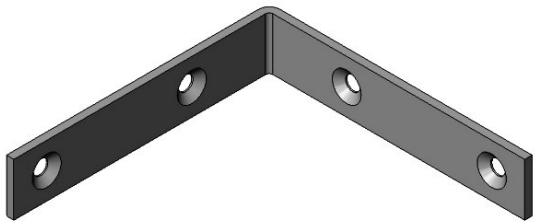

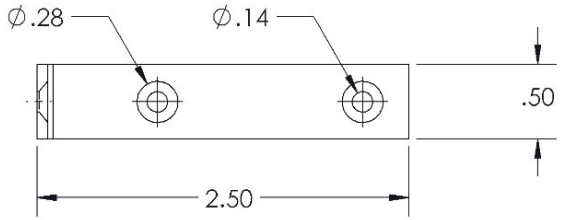

Dalhousie University	PROJECT: TEST STAND		DRAWING: BRACKET 1		B00#: 683325
	UNLESS OTHERWISE NOTED: SURFACE 1.6 µm; UNITS: mm X.XX +/- .10, X.X +/- .20, X +/- .50; UNITS: in X.XXX +/- .005, X.XX +/- .01, X.X +/- .02; ANGLES +/- 0.5°		DWN BY: TOUSIF AHMED		SIZE A / REV
			MATERIAL: CAST IRON	QTY:	
			DATE: 7-JUL-2016	UNITS: in / SCALE: 1:1	SHEET 1 OF 1

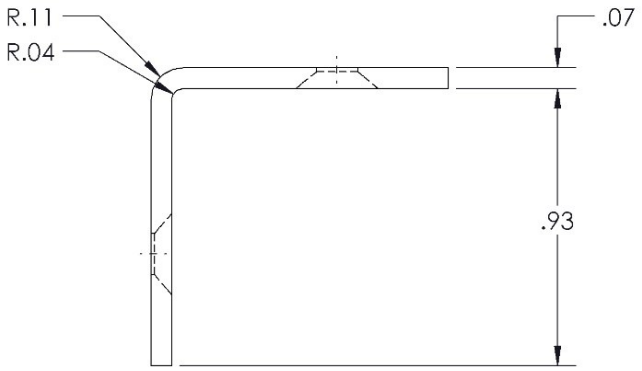

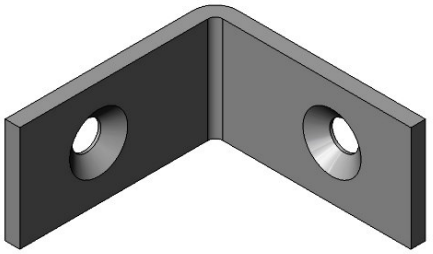

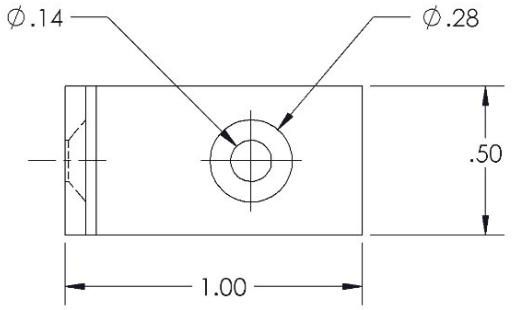

Dalhousie University	PROJECT: TEST STAND		DRAWING: BRACKET 2		B00#: 683325
	UNLESS OTHERWISE NOTED: SURFACE 1.6/ µm; UNITS: mm X.XX +/- .10, X.X +/- .20, X +/- .50; UNITS: in X.XXX +/- .005, X.XX +/- .01, X.X +/- .02; ANGLES +/- 0.5°		DWN BY: TOUSIF AHMED		SIZE A / REV
			MATERIAL: CAST IRON	QTY:	
			DATE: 07-JUL-2016	UNITS: in / SCALE: 2:1	SHEET 1 OF 1

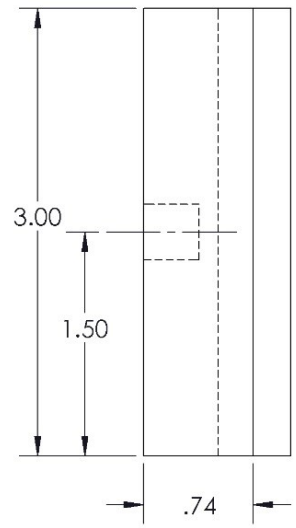

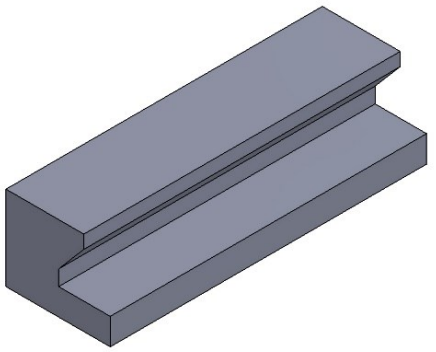

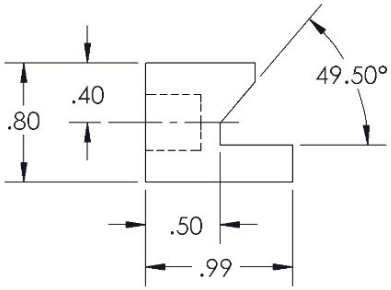

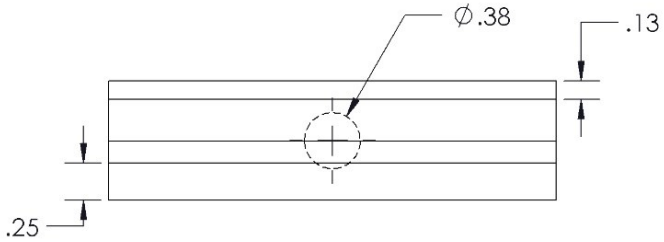

Dalhousie University	PROJECT: TEST STAND		DRAWING: 3D PRINTED CLAMP		B00#: 683325
	UNLESS OTHERWISE NOTED: SURFACE 1.6 µm; UNITS: mm X.XX +/- .10, X.X +/- .20, X +/- .50; UNITS: in X.XXX +/- .005, X.XX +/- .01, X.X +/- .02; ANGLES +/- 0.5°		DWN BY: TOUSIF AHMED		SIZE A / REV
			MATERIAL: PLA	QTY: 1	
			DATE: 07-Jul-2016	UNITS: in / SCALE: 1:1	SHEET 1 OF 1

Appendix C

Additional Melting-Solidification Data of PCMs

Effect of inclination with Size 2 PCM TES unit

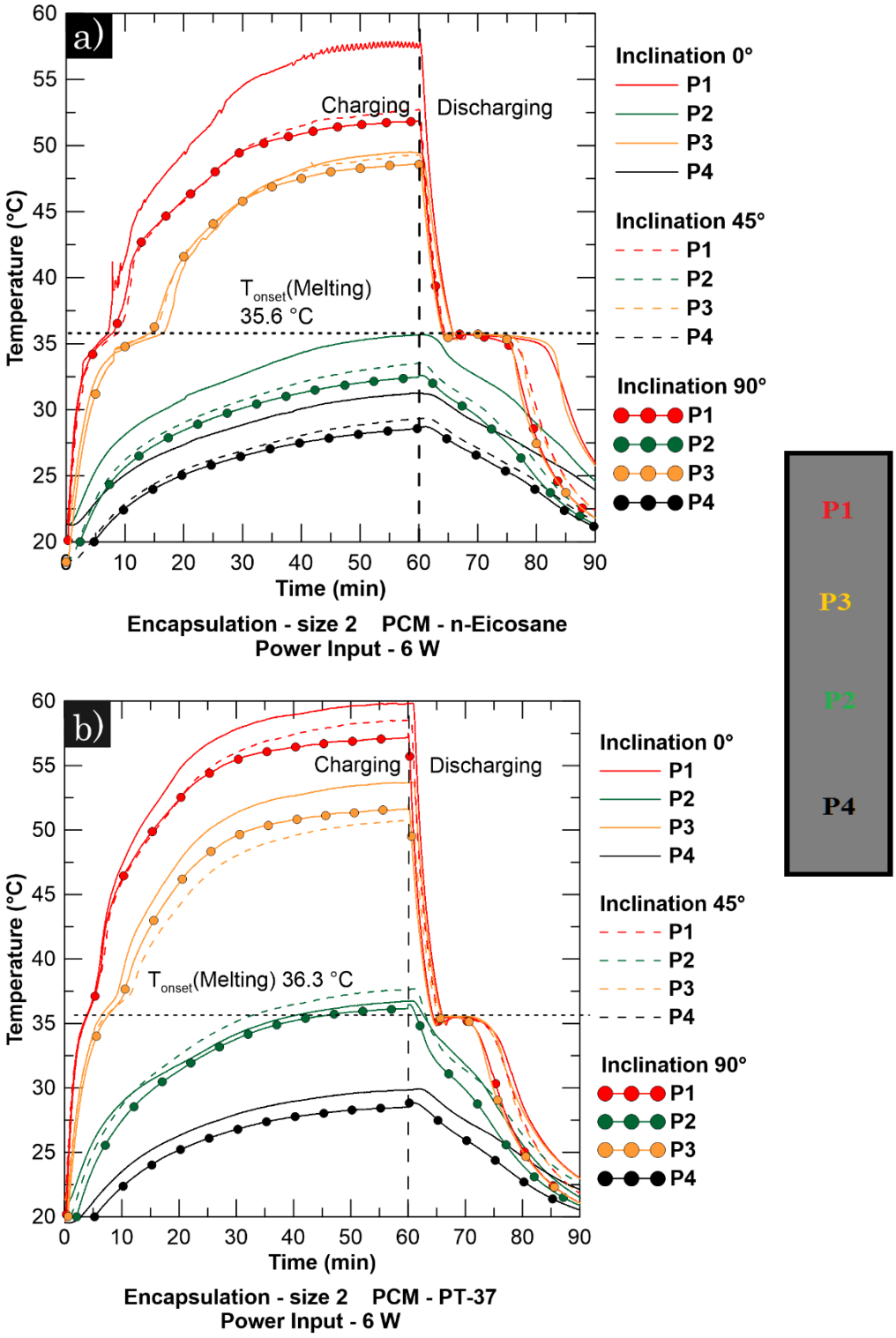

Figure C-1 Effect of inclination on PCM melting for continuous operation at 6 W power input with size 2 PCM TES Unit: a) n-eicosane b) PT-37.

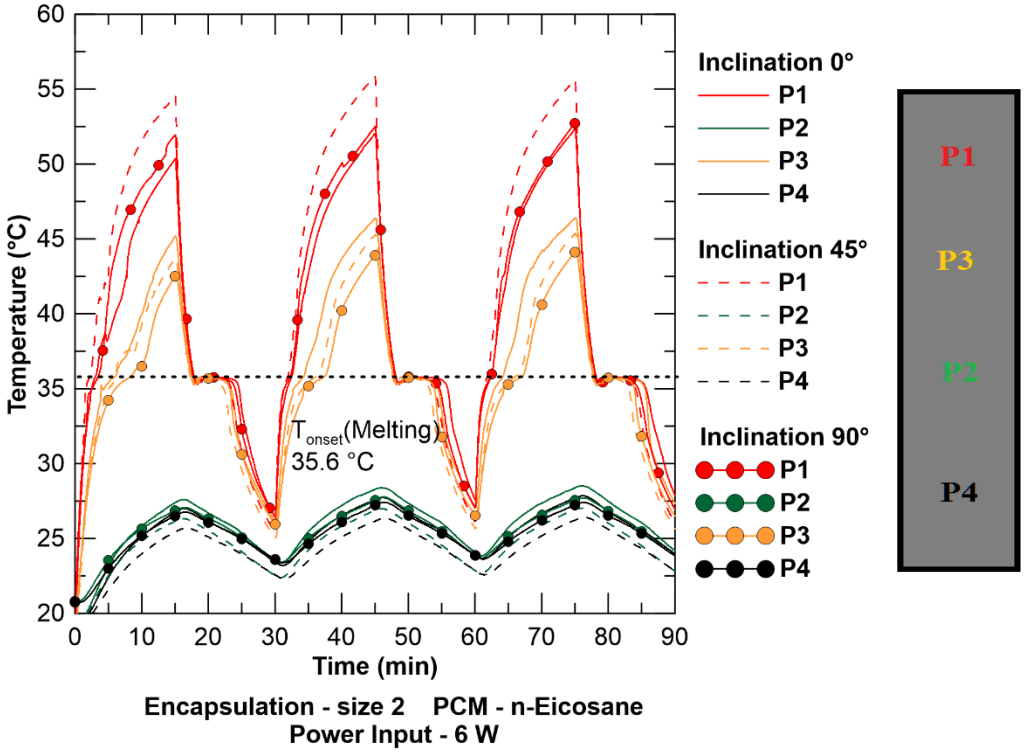

Figure C-2 Effect of inclination on PCM melting for intermittent operation at 6 W power input with size 2 PCM TES Unit (n-eicosane).

Effect of power input levels with Size 2 PCM TES unit

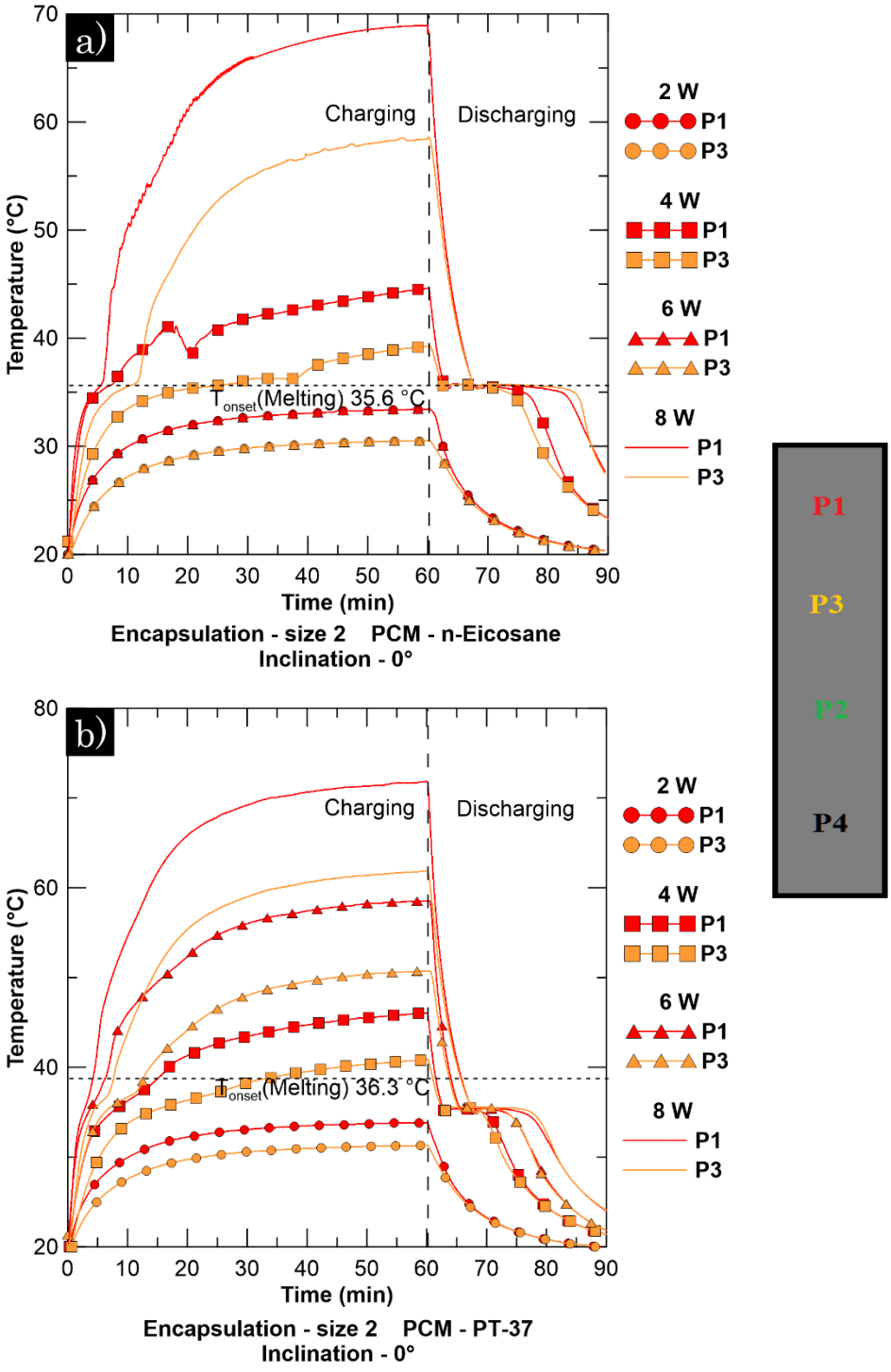

Figure C-3 Effect of power input levels on PCM melting for continuous operation at 0° inclination with size 2 PCM TES Unit: a) n-eicosane b) PT-37.

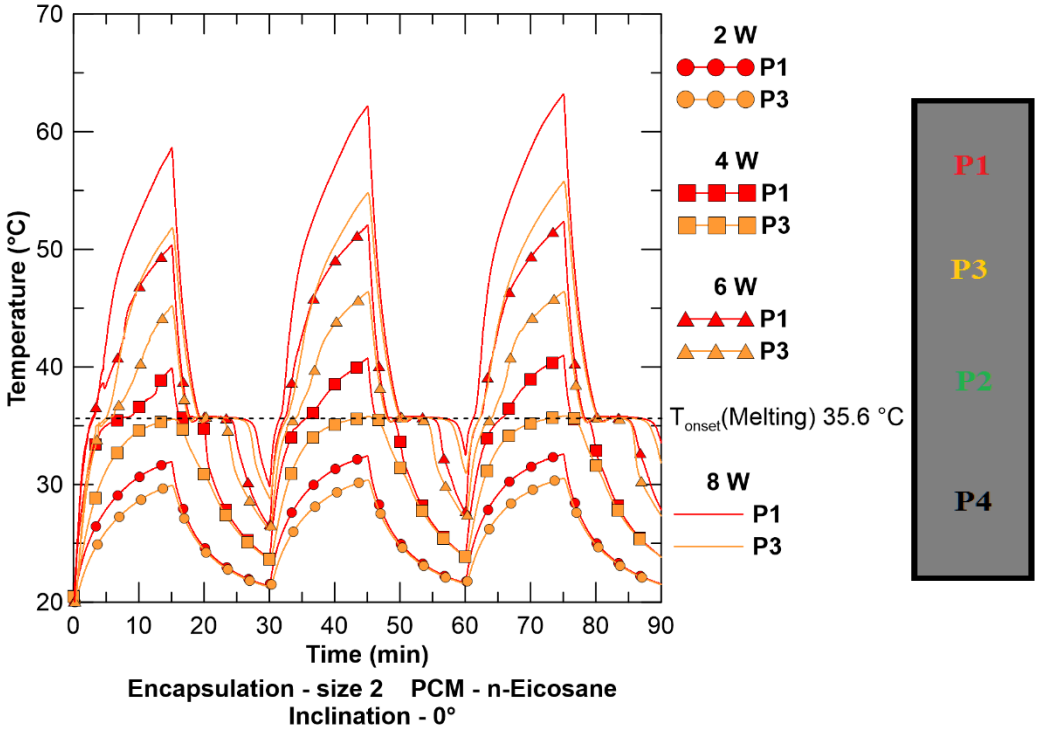

Figure C-4 Effect of power input levels on PCM melting for intermittent operation at 0° inclination with size 2 PCM TES Unit (n-eicosane).

Appendix D

Additional Thermal Performance Data of the Tablet PC

Effect of inclination with size 2 PCM TES unit

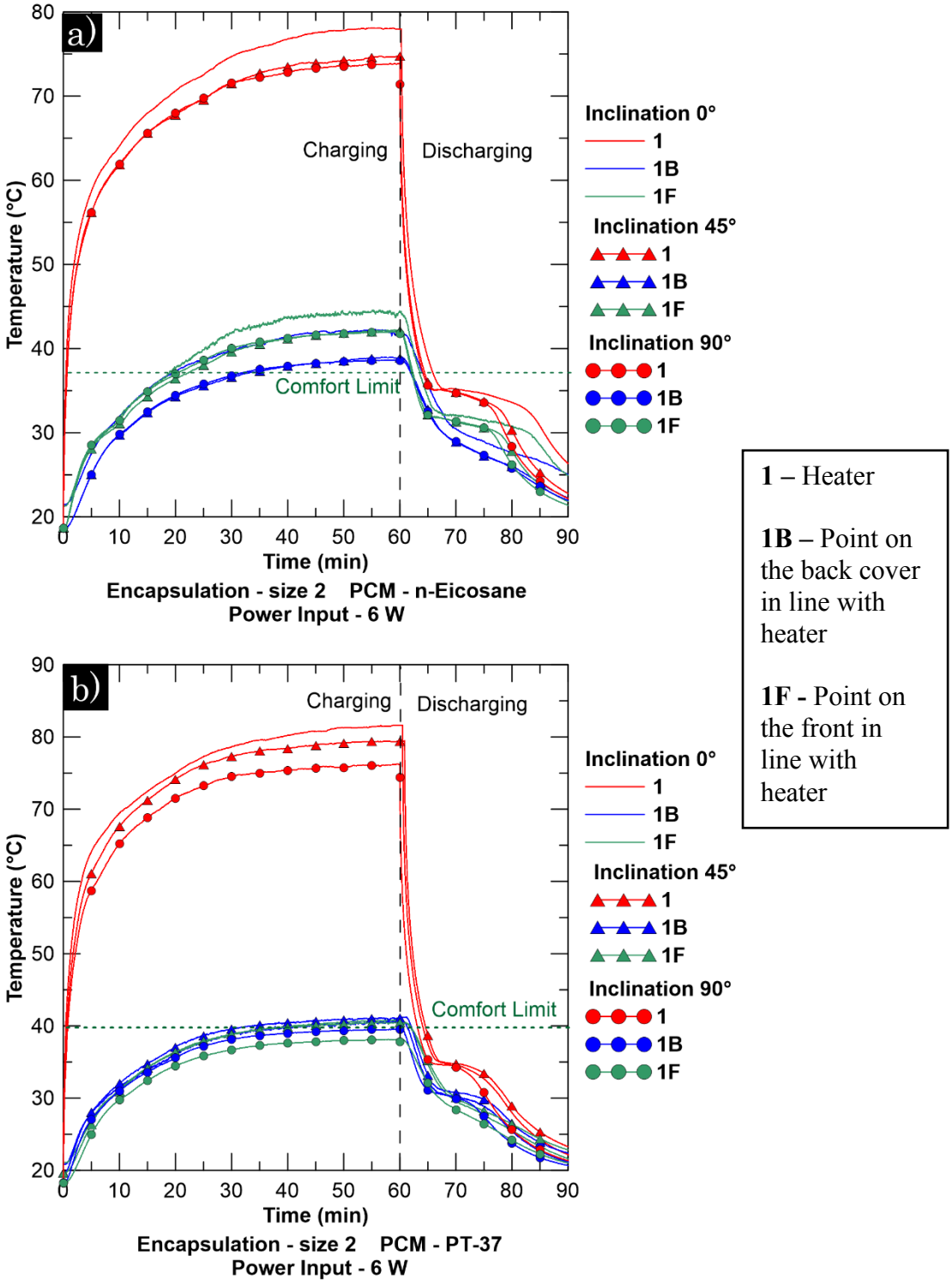

Figure D-1 Effect of inclination on the thermal response of the experimental tablet PC for continuous operation at 6 W power input with size 2 PCM TES Unit: a) n-eicosane b) PT-37.

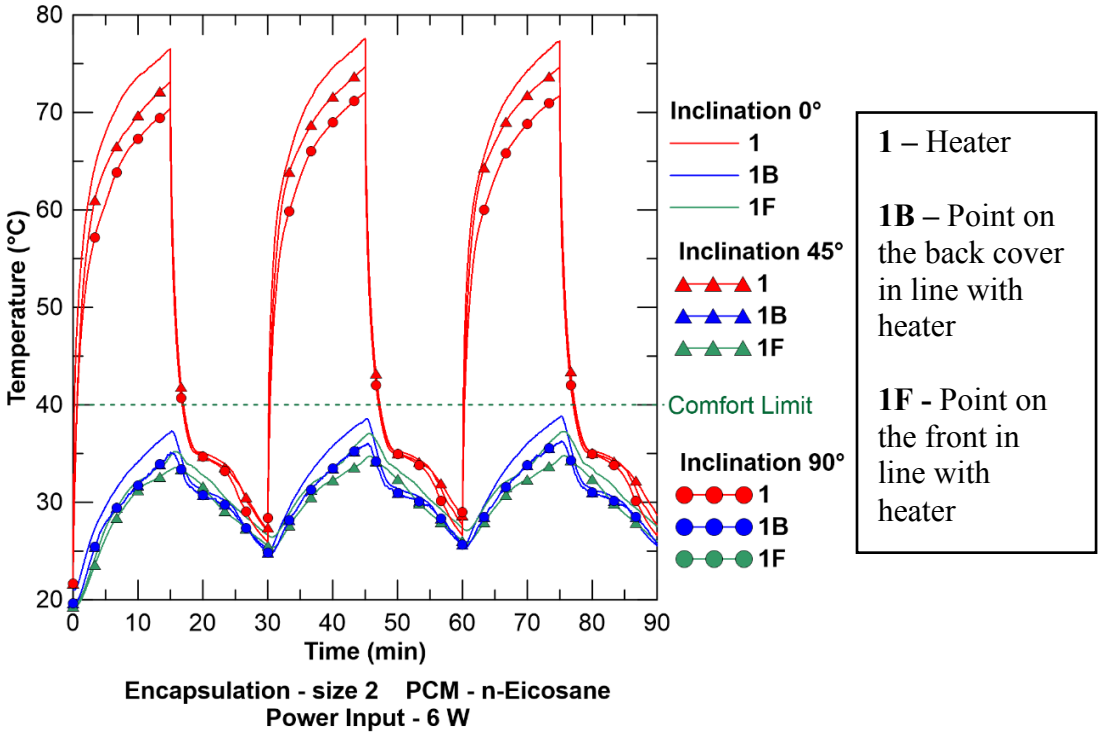

Figure D-2 Effect of inclination on the thermal response of the experimental tablet PC for intermittent operation at 6 W power input with size 2 PCM TES Unit (n-eicosane).

Effect of power input levels with size 2 PCM TES unit

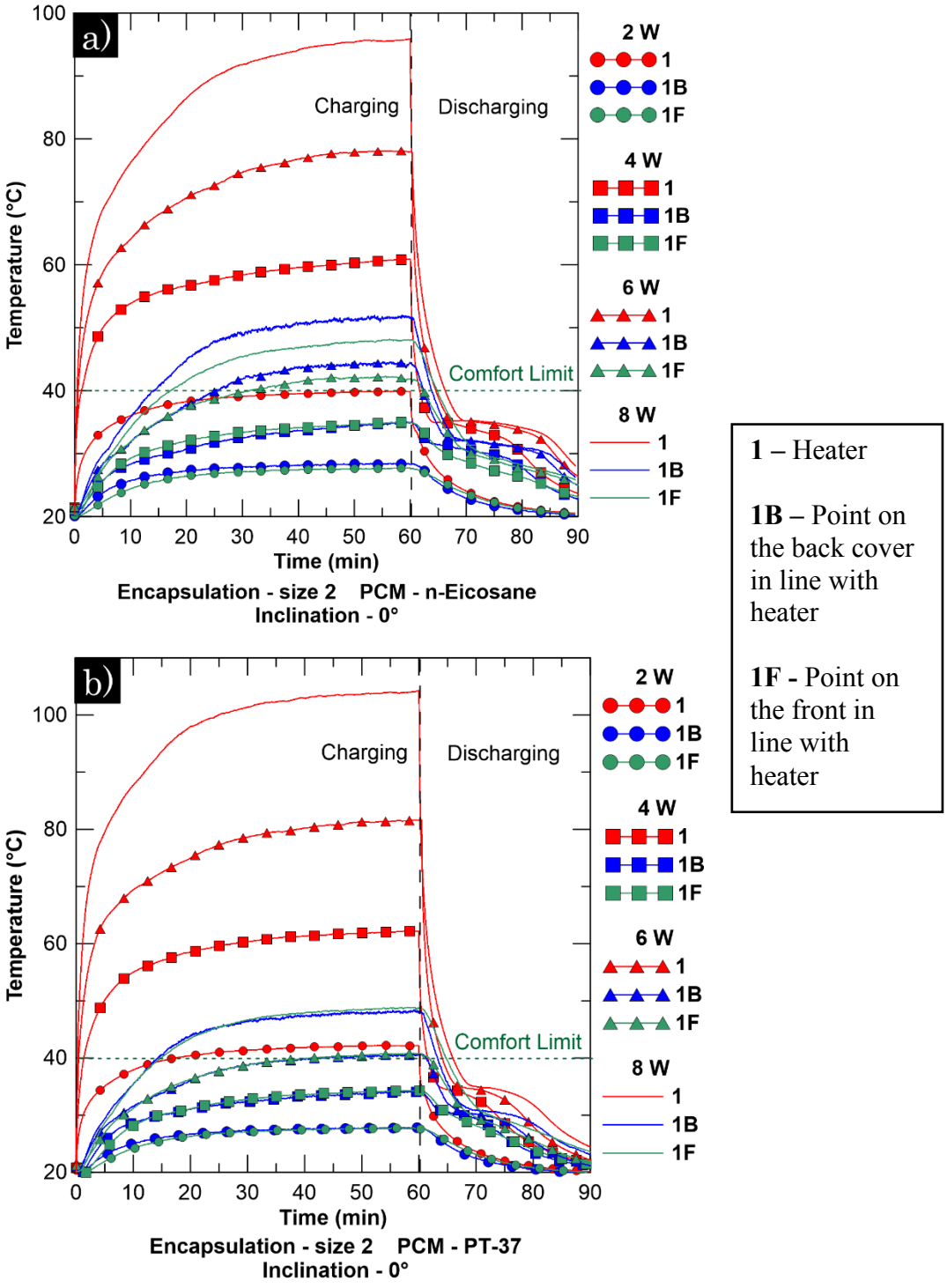

Figure D-3 Effect of power input levels on the thermal response of the experimental tablet PC for continuous operation at 0° inclination with size 2 PCM TES unit: a) n-eicosane b) PT-37.

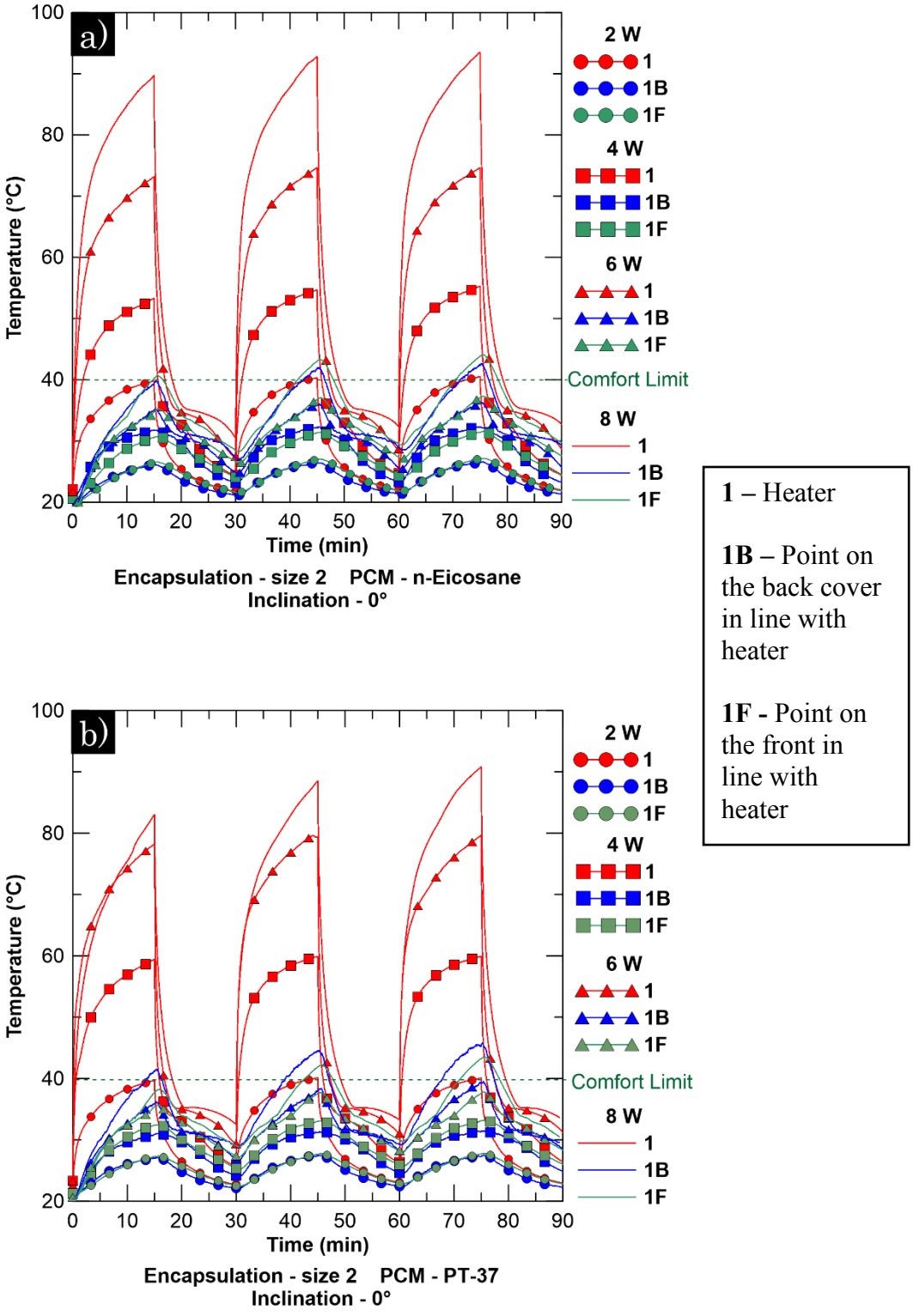

Figure D-4 Effect of power input levels on the thermal response of the experimental tablet PC for intermittent operation at 0° inclination with size 2 PCM TES unit: a) n-eicosane b) PT-37.

Effect of inclination with Size 3 PCM TES unit

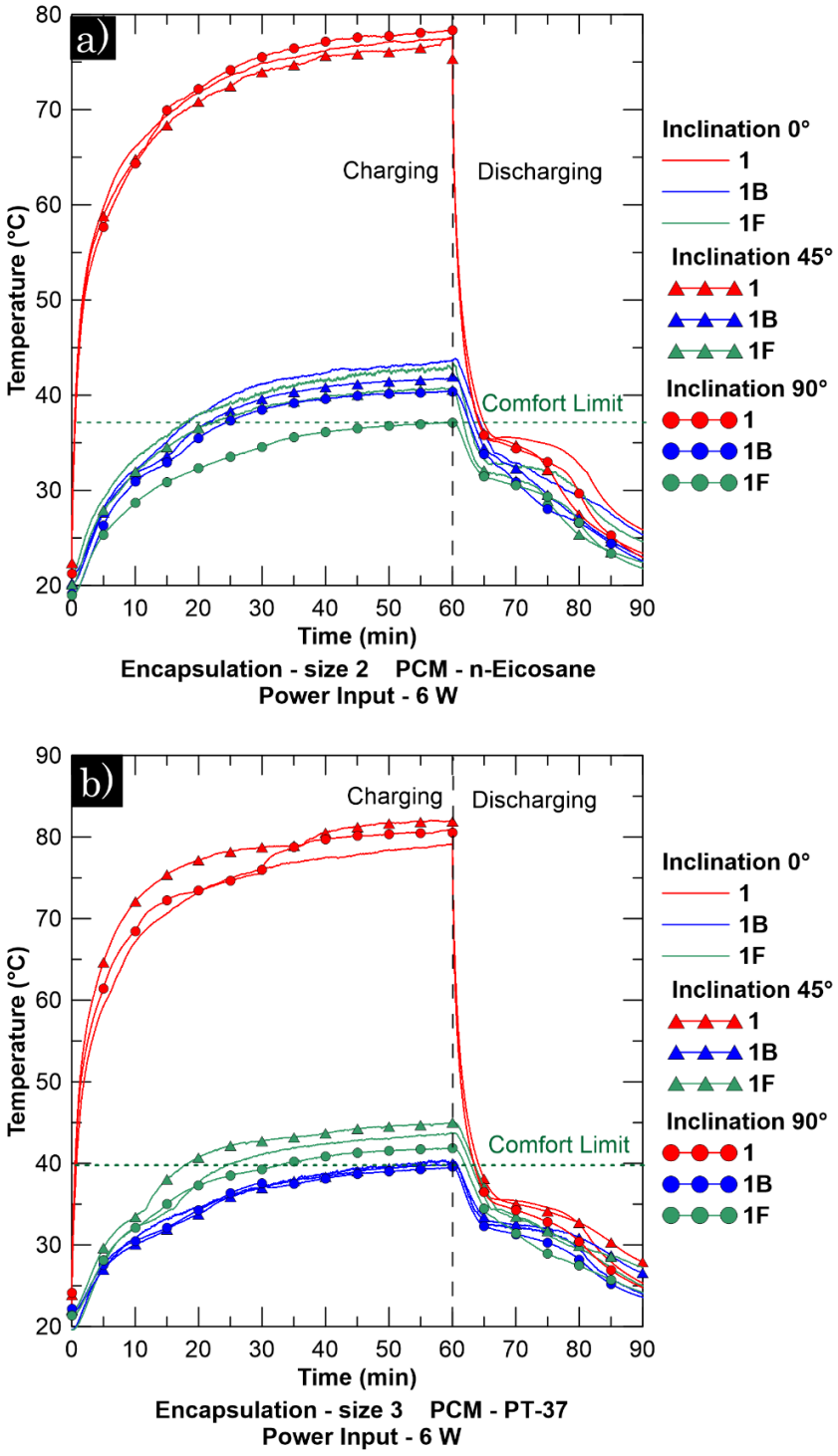

1 – Heater

1B – Point on the back cover in line with heater

1F - Point on the front in line with heater

Figure D-5 Effect of inclination on the thermal response of the experimental tablet PC for continuous operation at 6 W power input with size 3 PCM TES Unit: a) n-eicosane b) PT-37.

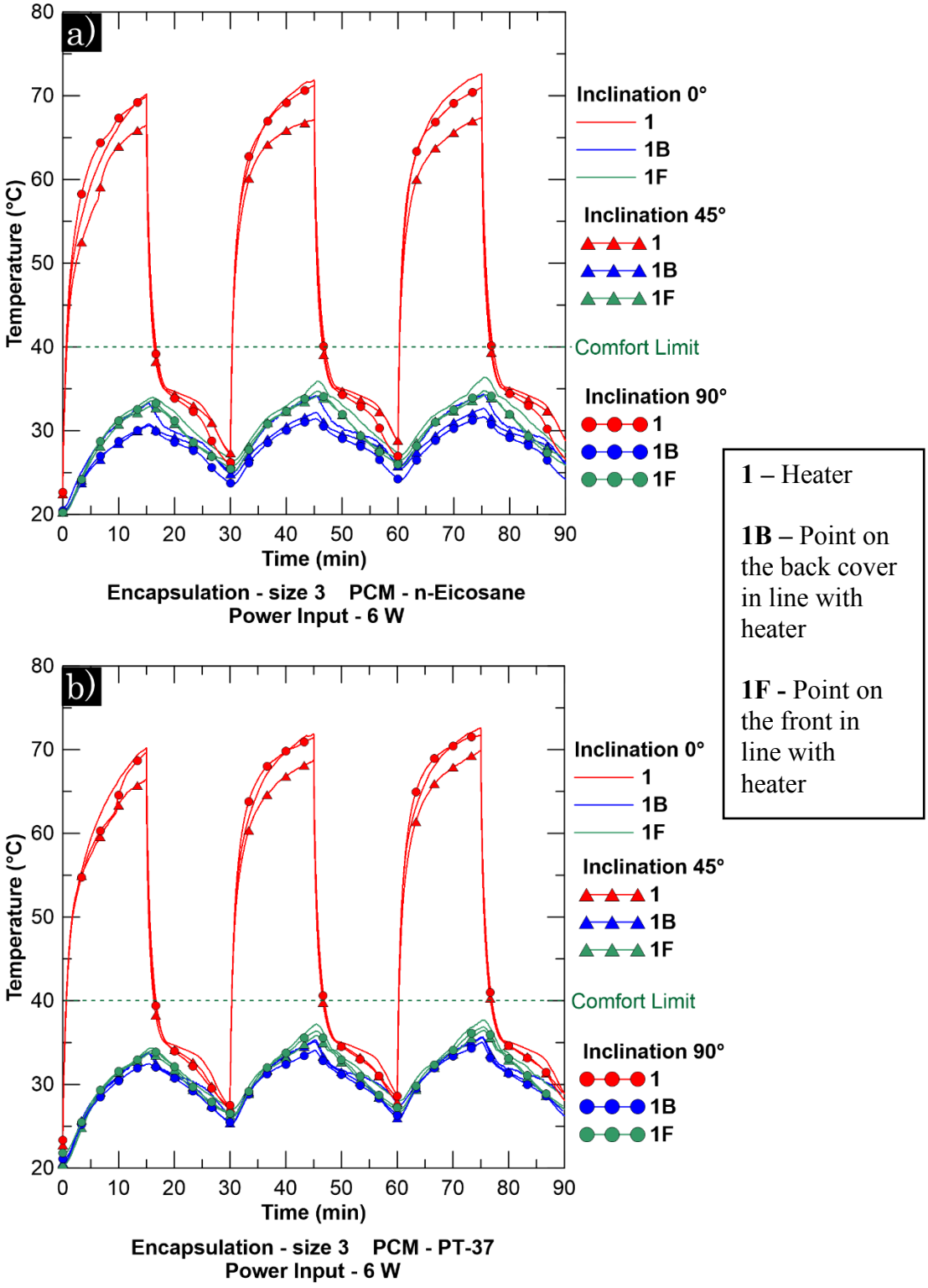

Figure D-6 Effect of inclination on the thermal response of the experimental tablet PC for intermittent operation at 6 W power input with size 3 PCM TES Unit: a) n-eicosane b) PT-37.

Effect of power input levels with Size 3 PCM TES unit

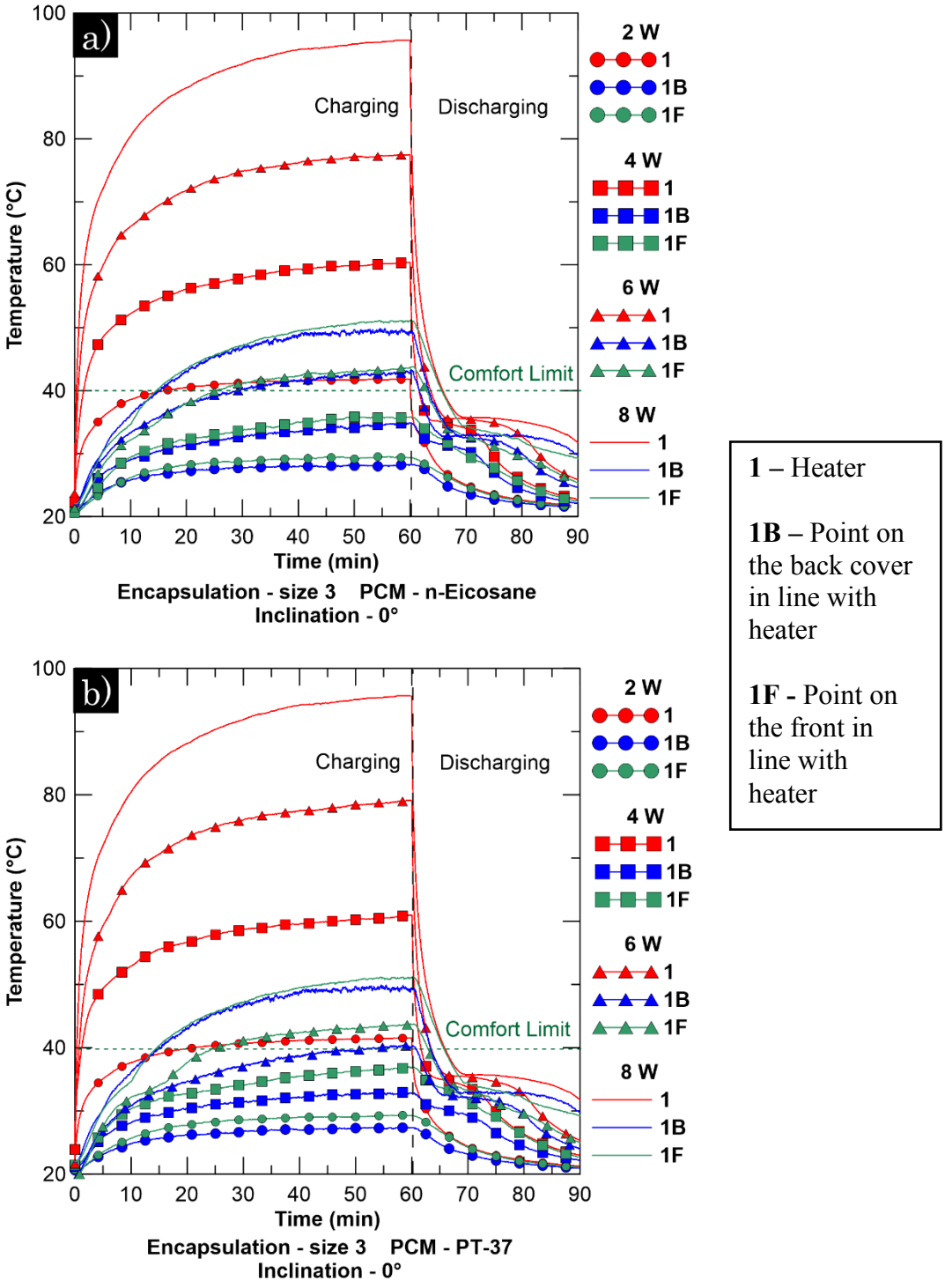

Figure D-7 Effect of power input levels on the thermal response of the experimental tablet PC for continuous operation at 0° inclination with size 3 PCM TES unit: a) n-eicosane b) PT-37.

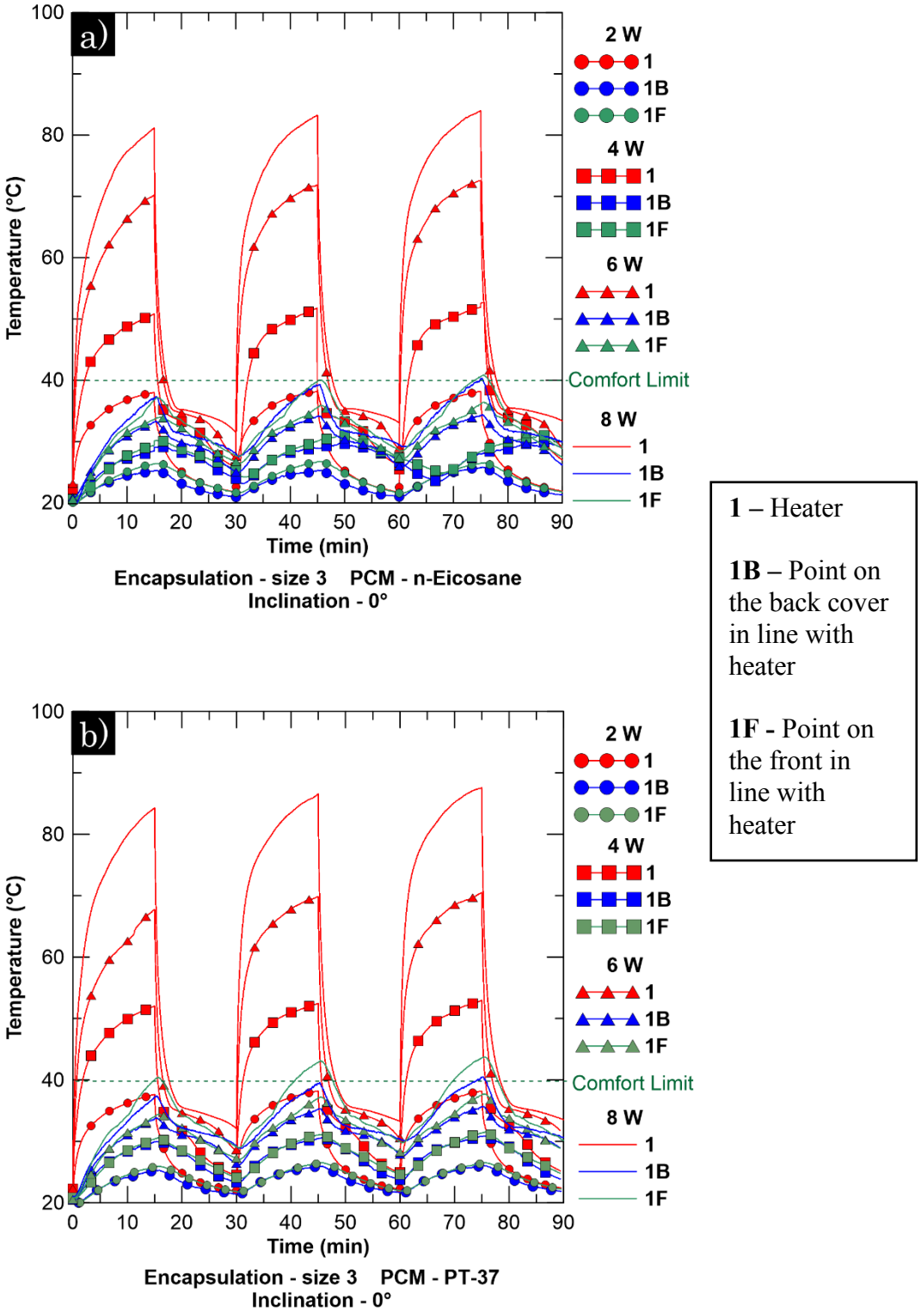

Figure D-8 Effect of power input levels on the thermal response of the experimental tablet PC for intermittent operation at 0° inclination with size 3 PCM TES unit: a) n-eicosane b) PT-37.

Appendix E

Additional IR Images of the Back Cover of the Experimental Tablet PC

Effect of TES Unit Size during Intermittent Operation

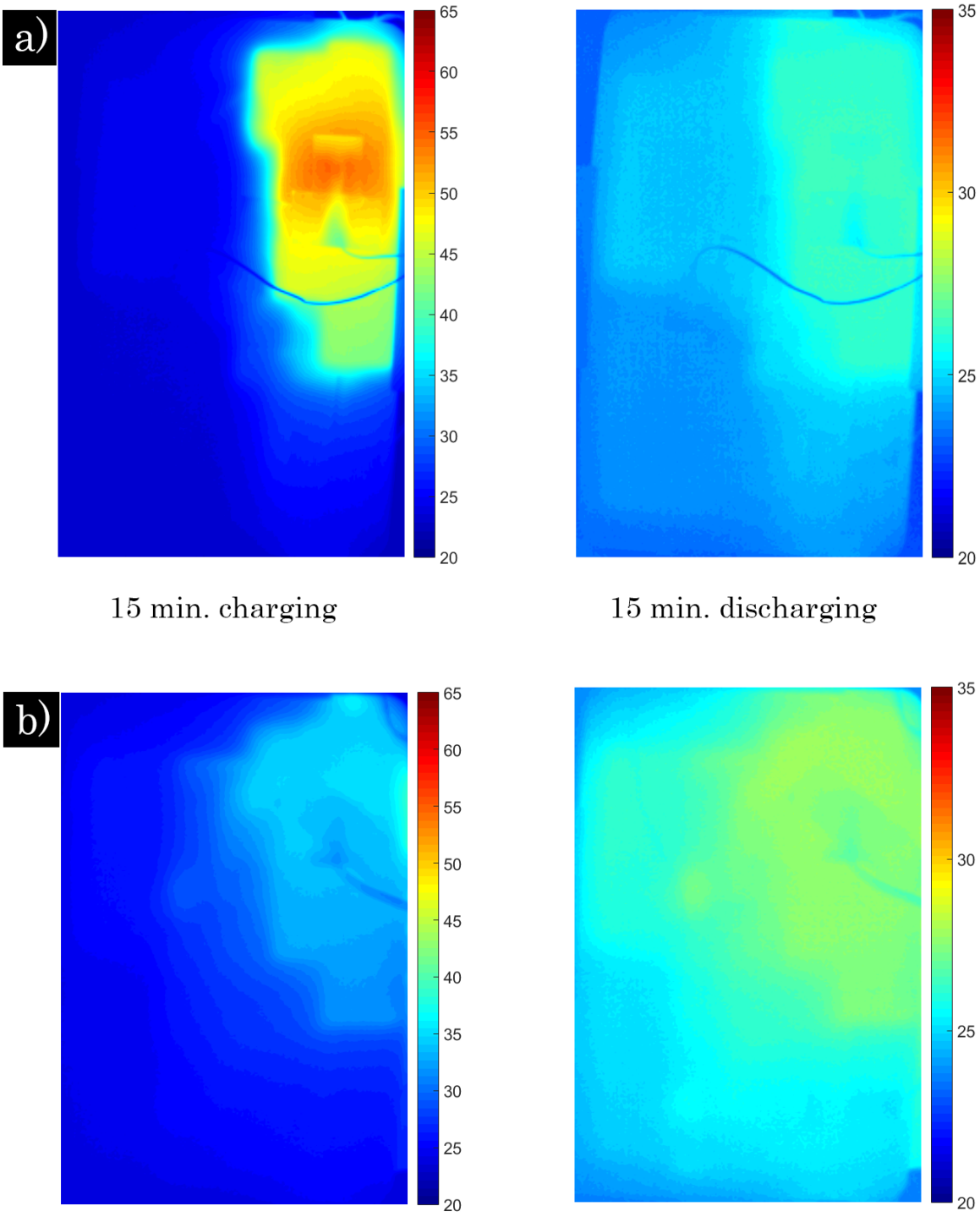

Figure E-1 Thermal images showing the effect of PCM TES size on the thermal performance of the experimental tablet PC at 6 W power input and 0° inclination during intermittent operation: a) Baseline b) Size 1 PT-37 TES Unit.

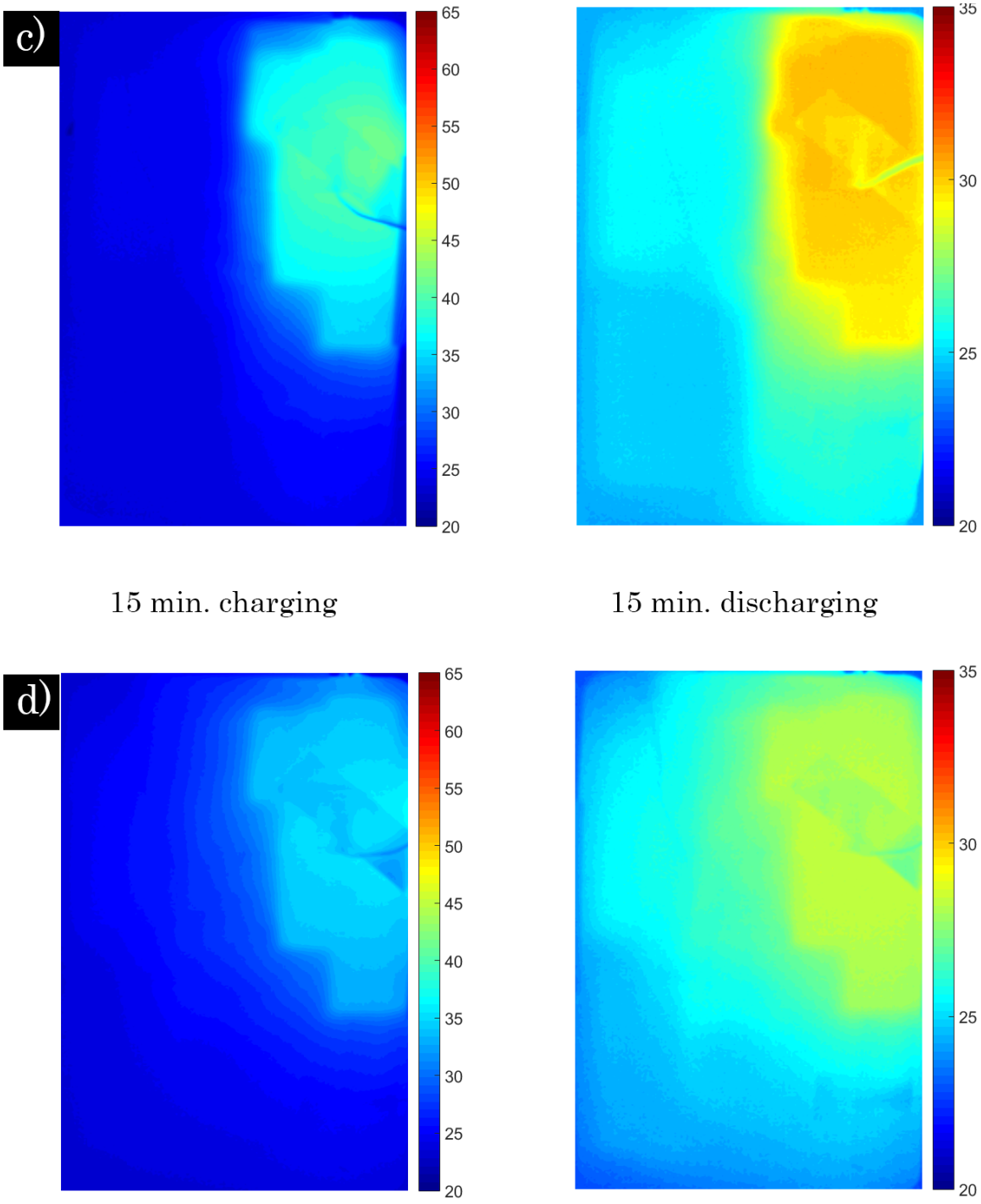

Figure E-1 Thermal images showing the effect of PCM TES size on the thermal performance of the experimental tablet PC at 6 W power input and 0° inclination during intermittent operation: c) Size 2 PT-37 TES Unit d) Size 3 PT-37 TES Unit.

Effect of Varying Latent Heat during Intermittent Operation

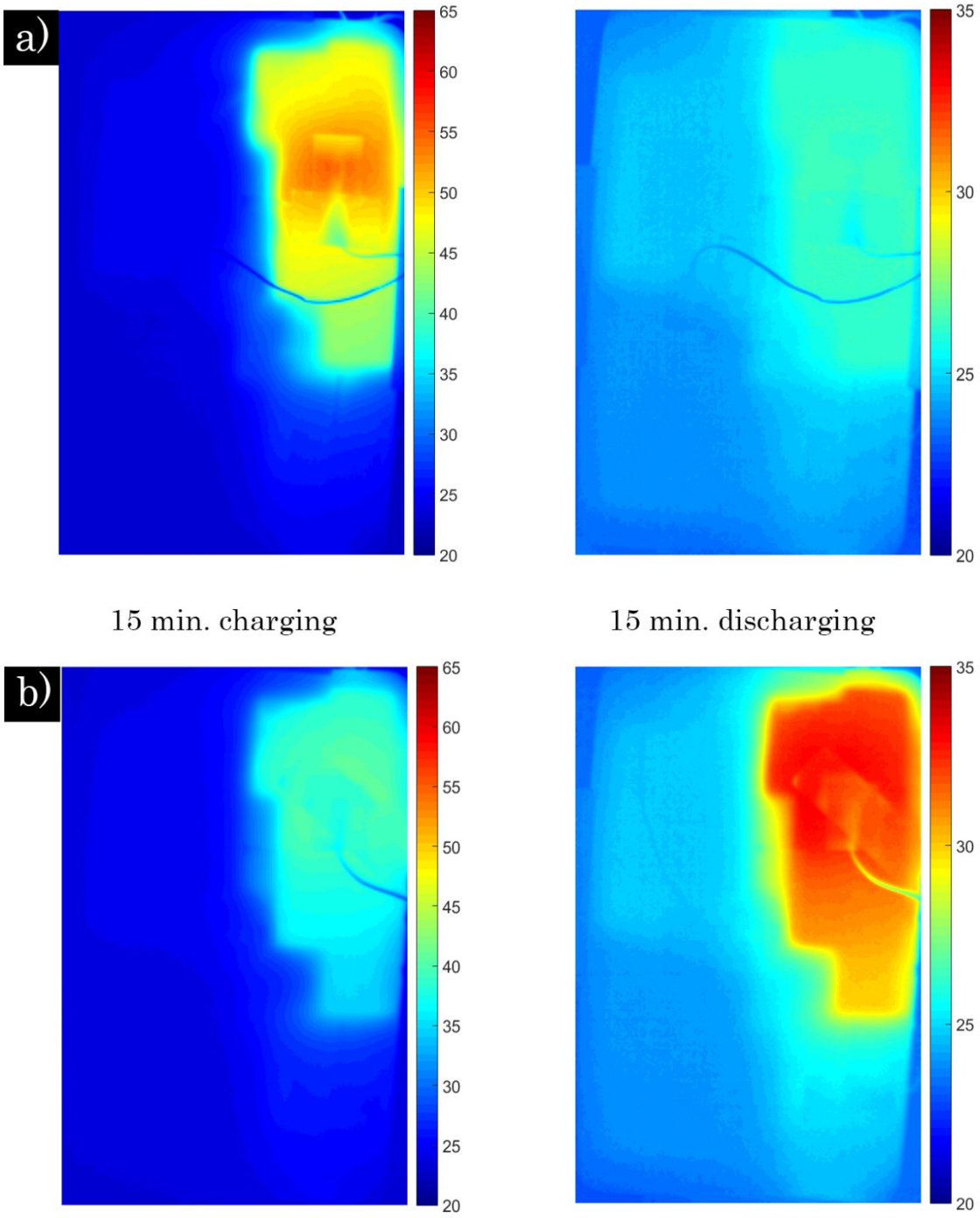

Figure E-2 Thermal images showing the effect of latent heat on the thermal performance of the experimental tablet PC at 6 W power input and 45° inclination during intermittent operation: a) Baseline b) 6g PT-37 (1.23 kJ).

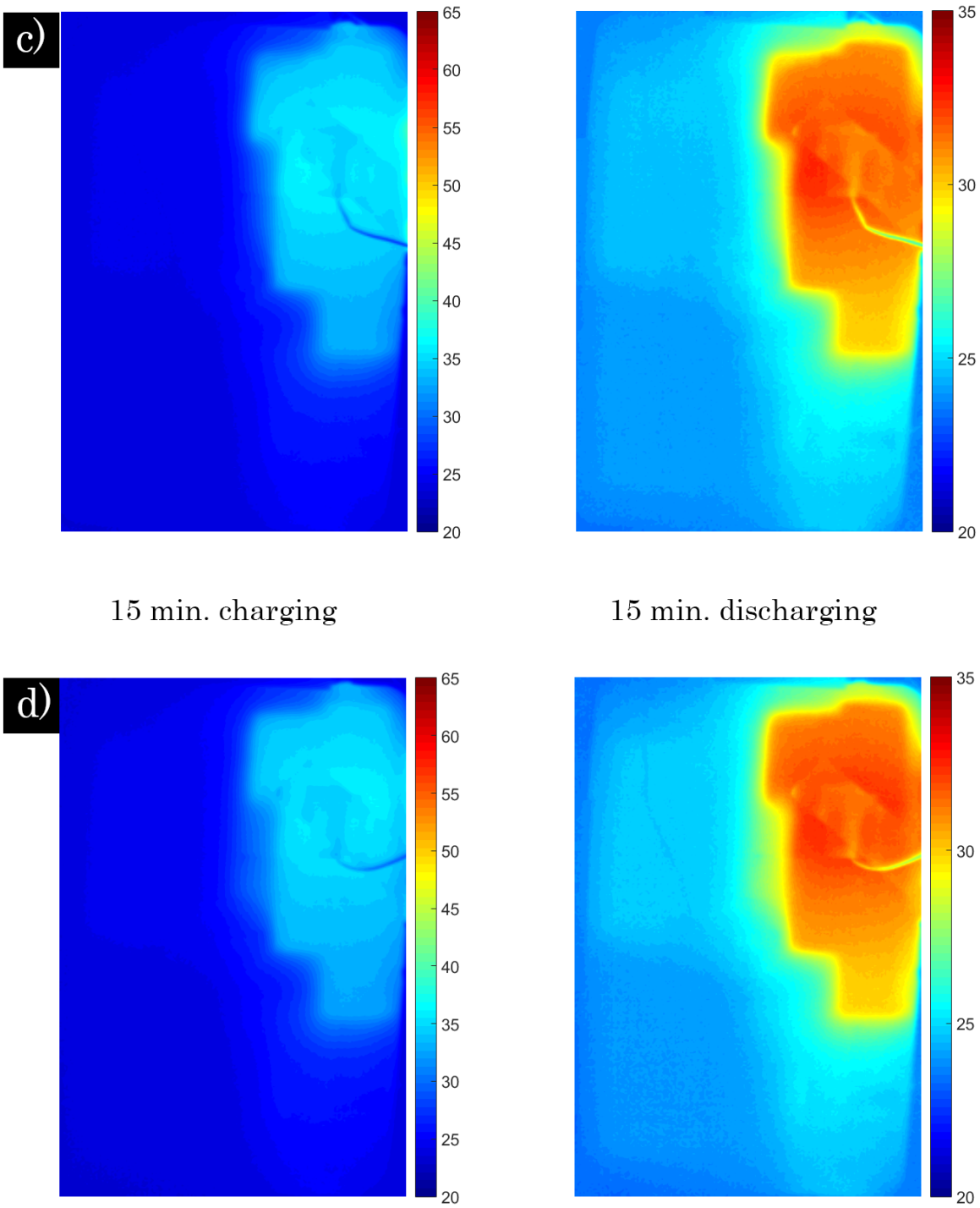

Figure E-2 Thermal images showing the effect of latent heat on the thermal performance of the experimental tablet PC at 6 W power input and 45° inclination during intermittent operation: c) 8g PT-37 (1.64 kJ) d) 10g PT-37 (2.05 kJ).

Appendix F

Copyright Permissions